

Bayerische Julius-Maximilians-Universität Würzburg

**MODULATION OF THE B-CELL REPERTOIRE
IN RHEUMATOID ARTHRITIS
BY TRANSIENT B-CELL DEPLETION**

**Dissertation zur Erlangung des
naturwissenschaftlichen Doktorgrades
der Bayerischen Julius-Maximilians-Universität Würzburg**

**vorgelegt von
Anne-Sophie Rouzière
(Laval, France)**

Würzburg, 2004

Eingereicht am:

Betreuer der Promotion: 7. April 2004

Medizinische Poliklinik: Prof. Dr. Hans-Peter Tony

Fakultät für Biologie: Prof. Dr. Erich Buchner

Mitglieder der Promotionskommission:

Vorsitzender: Prof. Dr. U. Scheer

Gutachter: Prof. Dr. Hans-Peter Tony

Gutachter: Prof. Dr. Erich Buchner

Tag des Promotionskolloquiums: 23. Juni 2004

Doktorurkunde ausgehändigt am:

CONTENT

INTRODUCTION.....	1
1. Immunoglobulin loci.....	1
1.1. Human IgH locus.....	1
1.2. Human IgL loci.....	3
1.2.1. Human Ig κ locus.....	3
1.2.2. Human Ig λ locus.....	5
2. Antibody diversity.....	7
3. V(D)J recombination.....	7
3.1. Recombination process.....	7
3.2. Orderly occurrence of V(D)J recombination during B-cell differentiation.....	8
3.3. Receptor editing.....	9
3.4. Receptor revision.....	11
4. Antibody maturation.....	12
4.1. Somatic hypermutation.....	12
4.2. Class-switch recombination.....	12
4.3. SHM and CSR share a common mechanism.....	13
5. Peripheral B-cell pool.....	14
6. IgV gene usage by B-cells from healthy individuals.....	15
7. IgV gene usage in autoimmune diseases.....	17
8. Rheumatoid arthritis.....	19
9. B-cell depletive therapy in RA.....	19
9.1. Rituximab.....	20
9.2. CD20.....	20
9.3. Rituximab and B-cell depletion.....	21
9.4. Rituximab therapy and RA.....	21
AIMS OF THE PROJECT.....	23
MATERIAL AND METHODS.....	24
1. Patients.....	24
2. Sample preparation.....	25

2.1. Genomic DNA extraction.....	25
2.2. RNA extraction.....	25
2.3. Determination of the concentration of nucleic acids.....	26
2.4. Single cell sorting.....	26
2.4.1. Cell preparation.....	26
2.4.2. Cell sorting.....	27
3. Amplification of V(D)J rearrangements.....	28
3.1. Oligonucleotides.....	28
3.1.1. Heavy chains - V _H DJ _H rearrangements.....	28
3.1.2. Light chains.....	29
3.1.2.1. V _κ J _κ rearrangements.....	29
3.1.2.2. V _λ J _λ rearrangements.....	30
3.2. Amplification of VDJ rearrangements by PCR - Heavy chains.....	31
3.2.1. Nested-PCR on bulk DNA.....	31
3.2.1.1. External amplification round.....	31
3.2.1.2. Internal amplification round.....	31
3.2.2. Single-cell PCR.....	32
3.2.2.1. Preamplification PCR step.....	32
3.2.2.2. External amplification round.....	33
3.2.2.3. Internal amplification round.....	34
3.3. Amplification of V(D)J rearrangements by RT-PCR - Heavy chains and light chains... 35	
3.3.1. RT-PCR on total RNA - Heavy chains.....	35
3.3.1.1. cDNA synthesis.....	35
3.3.1.2. External amplification round.....	35
3.3.1.3. Internal amplification round.....	36
3.3.2. RT-PCR on single cell - Light chains.....	37
3.3.2.1. External amplification round.....	37
3.3.2.1.1. External amplification for Kappa rearrangements.....	37
3.3.2.1.2. External amplification for Lambda rearrangements.....	38
3.3.2.2. Internal amplification round.....	39
3.3.2.2.1. Internal amplification for Kappa rearrangements.....	39

3.3.2.2.2. Internal amplification for Lambda rearrangements.....	40
4. Visualisation of PCR products and DNA recovery from agarose gel.....	41
5. Polishing.....	41
6. Subcloning and transformation.....	41
6.1. Ligation into pCR-Blunt vector.....	42
6.2. Transformation into One Shot TOP 10 competent cells.....	43
7. Analysis of the transformants.....	43
7.1. Restriction digest.....	44
7.2. PCR on plasmid or on bacteria.....	44
8. Sequencing.....	45
8.1. Reaction components.....	45
8.2. Cycling parameters.....	45
8.3. Purification and precipitation of the PCR products.....	46
9. Analysis of the sequences.....	46
9.1. Databases.....	46
9.2. Sequence analysis.....	47
10. Statistical analyses.....	49
11. Materials.....	49
11.1. Buffers.....	49
11.2. Agarose gel.....	50
11.3. Media.....	50
RESULTS.....	51
1. Heavy chains.....	51
1.1. Clinical data.....	51
1.2. Detection of peripheral B-cells by PCR.....	52
1.3. Distribution of V_H genes.....	52
1.4. Use of D segments.....	60
1.5. Distribution of J_H gene segments.....	61
1.6. CDR3 length.....	62
1.7. Mutational frequencies in V_H rearrangements.....	63

1.7.1. Overall mutational frequencies of V _H rearrangements amplified by PCR from bulk DNA.....	63
1.7.2. Overall mutational frequencies of V _H rearrangements amplified by PCR from single CD19 ⁺ cells.....	67
1.7.3. Overall mutational frequencies of V _H rearrangements amplified by RT-PCR on total RNA at the time point 7 months.....	68
2. Light chains.....	69
2.1. Clinical data.....	69
2.2. Amplification of light chain genes from individual B-cells.....	70
2.3. Ratio κ to λ.....	72
2.4. V _L family distribution before and after therapy in naive and memory B-cells.....	73
2.4.1. V _κ family distribution.....	73
2.4.2. V _λ family distribution.....	74
2.5. V _L gene distribution before and after therapy in naive and memory B-cells.....	75
2.5.1. V _κ rearrangements.....	75
2.5.1.1. Distribution of individual V _κ genes.....	75
2.5.1.2. Comparison of the usage of the J _κ proximal and J _κ distal cassettes.....	76
2.5.2. V _λ gene distribution.....	77
2.6. Mutational frequencies in V _L rearrangements.....	79
2.7. J _L gene distribution before and after therapy in naive and memory B-cells.....	80
2.7.1. J _κ gene distribution.....	80
2.7.2. J _λ gene distribution.....	81
2.8. CDR3 lengths, N nucleotides and exonuclease activity.....	82
2.8.1. V _κ J _κ rearrangements.....	82
2.8.2. V _λ J _λ rearrangements.....	83
DISCUSSION.....	85
REFERENCES.....	94
SUMMARY.....	103
ZUSAMMENFASSUNG.....	105
ABBREVIATIONS.....	108

ACKNOWLEDGEMENTS.....	111
CURRICULUM VITAE.....	112
PUBLICATIONS.....	113
EIDESSTATTLICHE ERKLÄRUNGEN.....	115

INTRODUCTION

The B-cell repertoire corresponds to the multiple antigen specificities carried by B lymphocytes and is the basis of the immunoglobulin variation. Antigen diversity is generated by somatic recombination of variable (V), joining (J) and, in the case of heavy chains, diversity (D) gene segments. There is some evidence that the B-cell repertoire is changed in autoimmune diseases. Studying the distribution of the genes used in heavy and light chain rearrangements can be an indication of changes in the immune repertoire in healthy individuals or in patients suffering from autoimmune diseases.

1. Immunoglobulin loci

1.1. Human IgH locus

The human immunoglobulin heavy chain (IgH) locus is located on chromosome 14 at band 14q32.33, at the telomeric extremity of the long arm. The chromosomal orientation of elements in the V_H locus is: telomere, 5' V_H -D-J_H-C_H 3', centromere. The V_H locus spans 1250 kilobases and comprises 123 to 129 V_H genes, among them 38 to 50 are functional. By sequence homology of at least 80%, the V_H segments are classified into seven families, as shown in Table 1 (Suzuki, 1995; Matsuda, 1998; Tomlinson, 1999; Lefranc, 2001c). Figure 1 represents the localisation of the different Ig- V_H genes along the chromosome 14. The first figure corresponds to the family, whereas the second one determines the gene.

Table 1. Repartition of the different V_H genes into V_H families

V_H families	Number of members	Genes with Open Reading Frame
V_H1	14	9 (11)*
V_H2	4	3
V_H3	65	22
V_H4	32	7 (11)*
V_H5	2	2
V_H6	1	1
V_H7	5	1

Adapted from Matsuda, 1998 and (*) from Tomlinson, 1999

V_H - Physical map

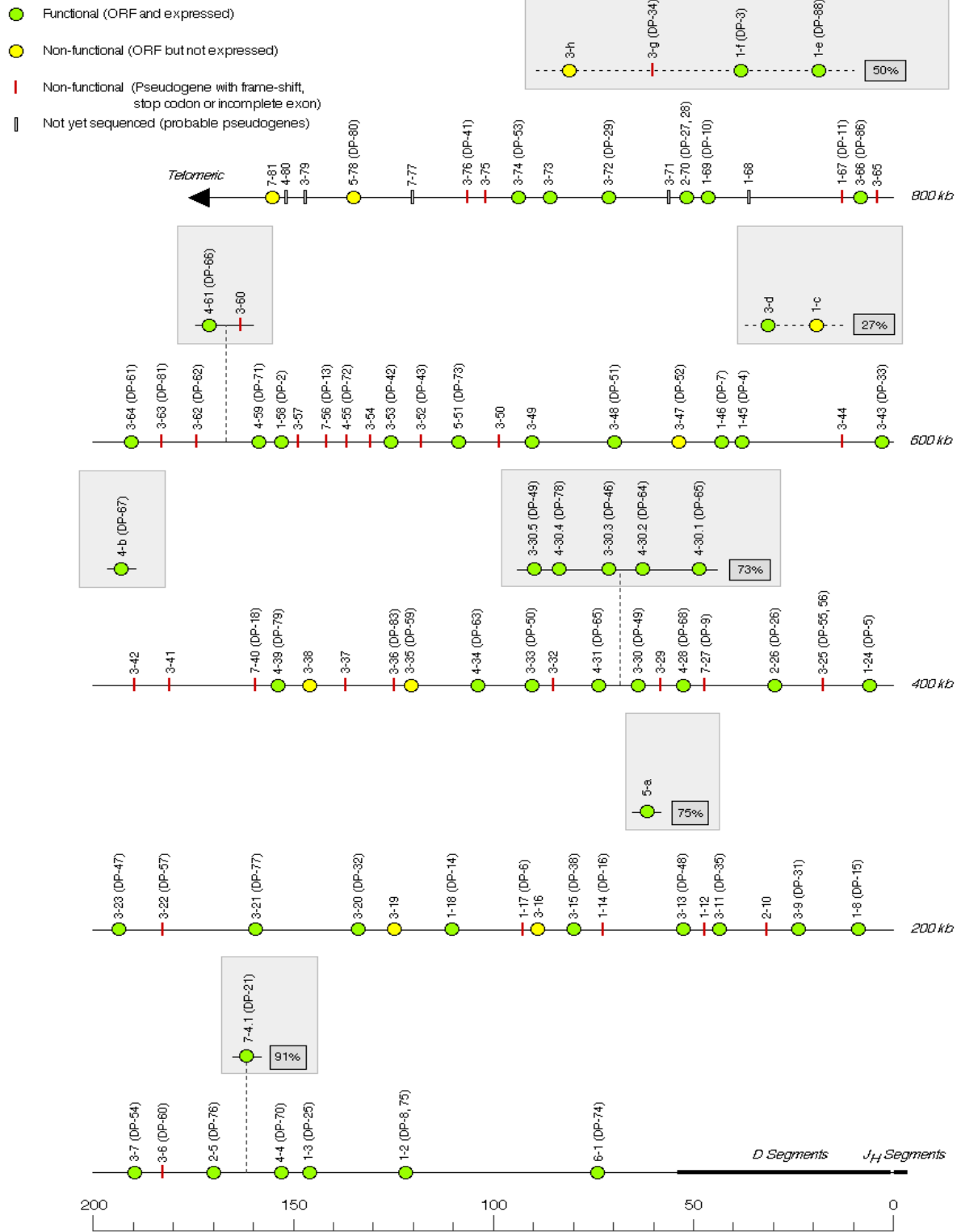


Fig. 1. Human V_H locus on chromosome 14 (adapted from Lefranc, 2001c)

The human Ig heavy chain locus also contains 25 to 27 diverse (D) genes that are subdivided into seven families (Fig. 2), six functional joining (J_H) genes and, in the most frequent haplotype, nine constant (C_H) genes.

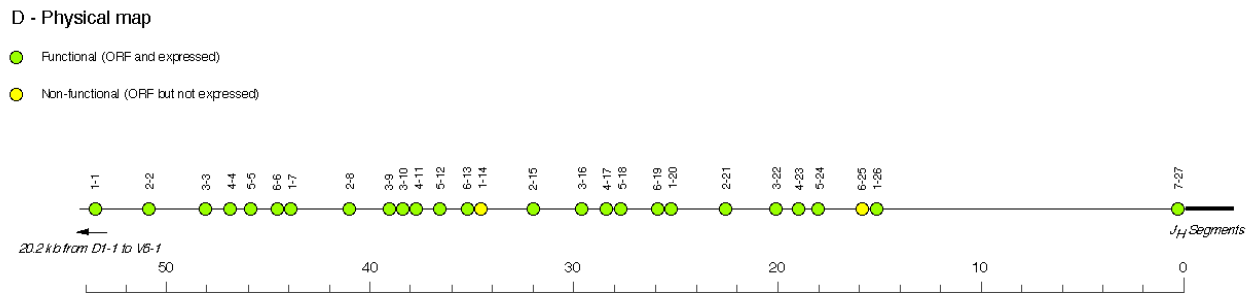


Fig. 2. Human D locus on chromosome 14 (adapted from Lefranc, 2001c)

1.2. Human IgL loci

1.2.1. Human Ig κ locus

The human $V\kappa$ locus (Fig. 3) is located at band 2p11.2 of the short arm of chromosome 2. It spans 1820 kilobases and consists of approximately 40 functional V gene segments that are organised into two cassettes (one J-proximal and the other J-distal) separated by 800 kb (Schäble, 1993). $V\kappa$ genes are classified into seven families based on sequence similarity. Six of these families contain functional genes (Table 2). The $V\kappa 7$ is made up of a single member that is thought to be a pseudogene (Foster, 1997). The $Ig\kappa$ locus also contains 5 $J\kappa$ genes and a unique $C\kappa$ gene (Schaeble, 1993; Tomlinson, 1999; Lefranc, 2001b).

Table 2. Distribution of $V\kappa$ families (adapted from Foster, 1997)

$V\kappa$ family	$V\kappa 1$	$V\kappa 2$	$V\kappa 3$	$V\kappa 4$	$V\kappa 5$	$V\kappa 6$
Known functional genes	19	9	7	1	1	3

V_k - Physical map

- Functional (ORF and expressed)
- Non-functional (ORF but not expressed)
- | Non-functional (Pseudogene with frame-shift, stop codon or incomplete exon)

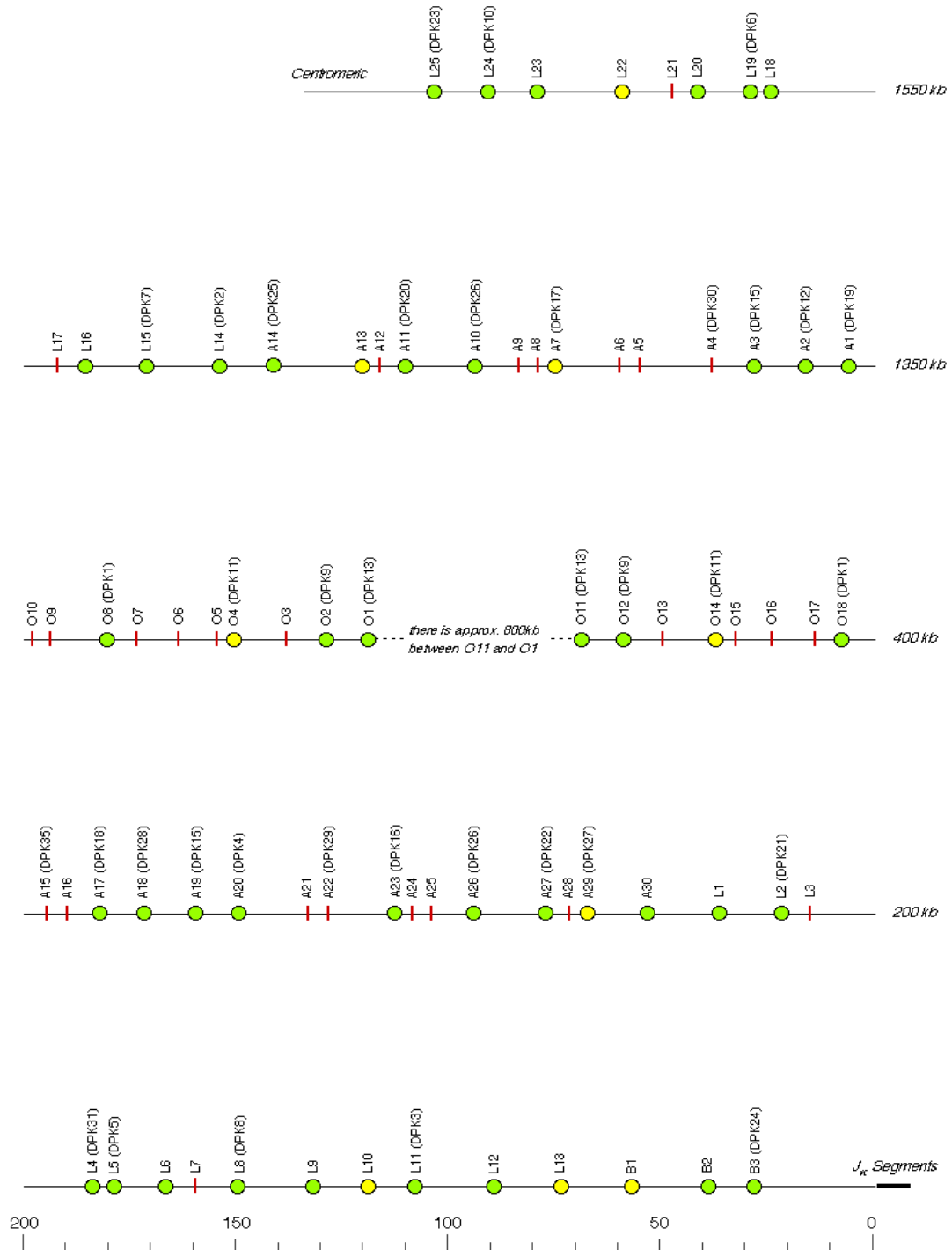


Fig. 3. Human V_k locus on chromosome 2 (adapted from Lefranc, 2001b)

1.2.2. Human Ig λ locus

The human V λ locus (Fig. 4) is located at band 22q11.2 on the long arm of chromosome 22. It spans 1050 kilobases and is arranged so that J λ /C λ pairs are downstream of the V λ genes (Frippiat, 1995). The locus comprises 51 V λ genes, among them 30 are functional. According to sequence homology, the V λ genes are classified into 10 families that are themselves divided into three clusters (Table 3). Cluster A, which is J λ -proximal, contains the V λ 2 and V λ 3 families and the 4c gene from the V λ 4 family; cluster B contains the V λ 1, V λ 5, V λ 7 and V λ 9 families, and cluster C, which is J λ -distal, contains the V λ 6, V λ 8 and V λ 10 families, as well as the genes 4a and 4b from V λ 4 family (Frippiat, 1995; Farner, 1999; Tomlinson, 1999; Lefranc, 2001a).

Table 3. Distribution of V λ families (adapted from Farner, 1999)

V λ family	V λ 1	V λ 2	V λ 3	V λ 4	V λ 5	V λ 6	V λ 7	V λ 8	V λ 9	V λ 10
Known functional genes	5	5	8	3	3	1	2	1	1	1
Cluster	B	A	A	A-C	B	C	B	C	B	C

There are seven J λ segments, of which four (J λ 1, J λ 2, J λ 3 and J λ 7) are considered functional. J λ 4, J λ 5 and J λ 6 are not considered functional because the GT dinucleotide sequence in the 5' splice donor site of these three J segments has been deleted (Vasicek, 1990). The J λ segments are arranged so that one of the seven C λ segments is located between each J λ segments. This is in contrast to the heavy and κ gene loci, in which all J segments are grouped together followed by the C segment(s).

V λ - Physical map

- Functional (ORF and expressed)
- Non-functional (ORF but not expressed)
- | Non-functional (Pseudogene with frame-shift, stop codon or incomplete exon)

Note: Nomenclature is from Williams *et al.*, 1996 except for segment 2-19 and 4-6 which come from Kawasaki *et al.*, 1997

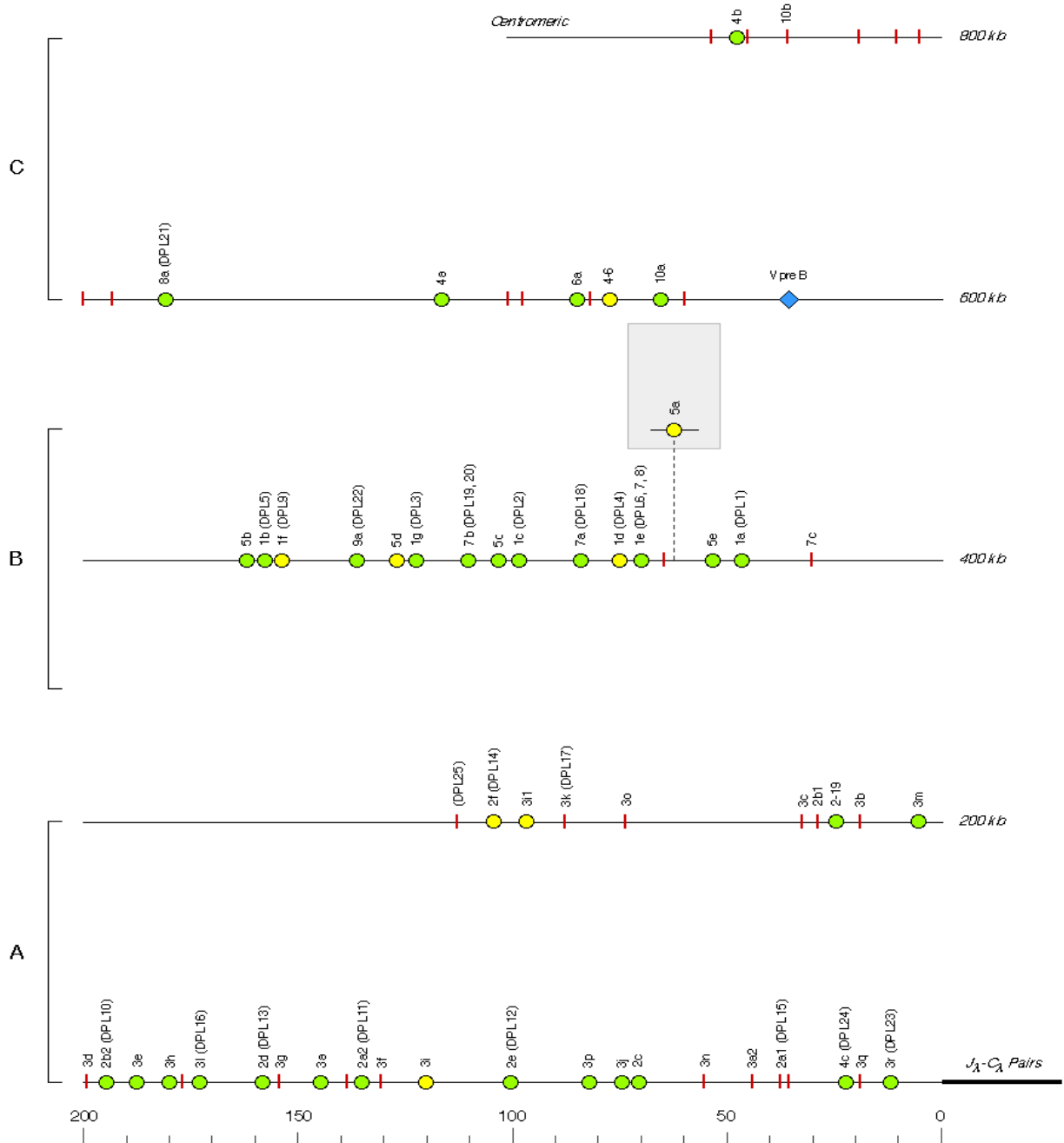


Fig. 4. Human V λ locus on chromosome 22 (adapted from Lefranc, 2001a)

2. Antibody diversity

Antibody diversity is generated by a number of lymphocyte-specific molecular mechanisms that include recombination of one of a number of variable (V), joining (J) and, in the case of heavy chains, diversity (D) genetic elements (Tonegawa, 1983); additions and deletions of nucleotides at the junctions between the different gene segments during VDJ recombination and random pairing of heavy (H) and light (L) chains. These processes occur at the early stages in B-cell development in the bone marrow. Additional diversity is created by somatic hypermutation, which introduces point mutations to change amino acid codons (Berek, 1988). This event takes place in germinal center when B-cells encounter antigens.

3. V(D)J recombination

3.1. Recombination process

Every V, D and J gene segment is flanked on its recombining side(s) by a recombination signal sequence (RSS), which consists of a highly conserved heptamer (5'-CACAGTG-3') and a slightly less conserved nonamer (5'-ACAAAACC-3'), separated by a non-conserved spacer region of either 12 or 23 nucleotides (± 1 nucleotide) in length (Feeney, 2000a-b; Schlissel, 2003; de Villartay, 2003; Zhang, 2004). Gene segments of a particular type are all flanked by RSSs with the same spacer length (23 nucleotides in the case of V_H gene segments, for example). Only gene segments that are flanked by RSSs with dissimilar spacer lengths can recombine with one another due to the 12/23 rule. Twelve base pairs is the approximate length of one turn of the DNA double helix and 23 bp encompasses two turns, suggesting that the 12/23 recombination restriction reflects a DNA structural requirement (Zhang, 2004).

The V(D)J recombination process requires different proteins and is represented in figure 5. It is initiated by two recombinases, RAG1 and RAG2 (which stand for recombination-activating gene-1 and -2). RAG1 and RAG2 form a heterodimer that recognises and binds the RSSs that flank the gene segments to be rearranged, and generates double-stranded DNA breaks at the junction between the heptamer and the coding sequence (de Villartay, 2003). The resolution of DNA damage is then carried out by the general DNA-repair machinery of the cell,

specifically by the DNA-dependent protein kinase (DNA-PK) complex, formed by the Ku70 and Ku80 heterodimer and the DNA-PK catalytic subunit (DNA-PKcs). Ligation of the joints is performed by the DNA ligase IV. Coding joints are imprecise; their diversity is generated by short deletion, palindromic duplications (p nucleotides) or non-templated nucleotide addition (N nucleotides) that is introduced by the terminal deoxynucleotidyl transferase (TdT).

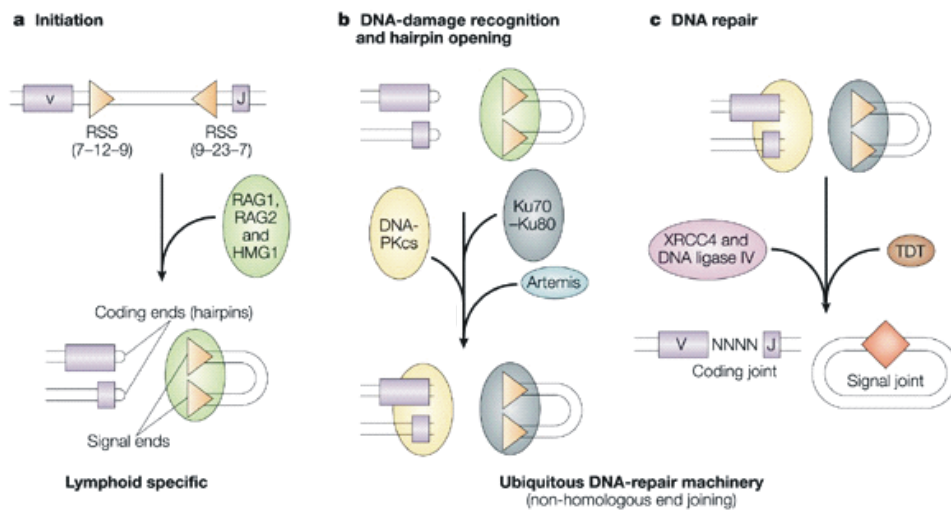


Fig. 5. V(D)J recombination process (adapted from de Villartay, 2003)

3.2. Orderly occurrence of V(D)J recombination during B-cell differentiation

Immunoglobulin gene rearrangement proceeds in a stepwise manner during early B-lineage development. The $D \rightarrow J_H$ rearrangement occurs first, beginning when RAG expression is initiated at the early common lymphoid progenitor cell stage. This step is not restricted to B-lineage cells and DJ_H can be easily detected in thymocytes. The next step of $V_H \rightarrow DJ_H$ rearrangement is B-cell specific. The successful accomplishment of a productive $V_H DJ_H$ rearrangement leads to the expression of $Ig\mu$ heavy chain, which is a prerequisite for a further development along the B-lineage pathway. Once the μ heavy-chain is produced, it associates with the surrogate light chain elements ($\lambda 5$ and $VpreB$) and with the transmembrane signalling chains $Ig\alpha$ and $Ig\beta$ to form the pre B-cell receptor (pre-BCR). The deposition of the pre-BCR on the cell

surface initiates the signalling and results in the proliferation of the pre-B-cells, until its expression is extinguished by silencing of surrogate light chain genes to allow exit from the cell cycle and light chain rearrangement. During the proliferation process, RAG gene expression is downregulated. RAG genes must then be reexpressed at the pre-B-cell stage to promote light chain gene rearrangement. Light chain rearrangement normally begins in one of the κ loci. If the first $V\kappa J\kappa$ rearrangement is not productive, rearrangement can occur on the second κ allele, and on the λ loci in the case the second rearrangement is still not productive. If the newly formed light chain (κ or λ) can pair with the μ heavy chain, the B-cell receptor (BCR) can appear on the cell surface. BCR expression is a critical developmental checkpoint for B-cells, as it delivers signals for cell survival and maturation. As the B-cells mature, they usually extinguish the expression of many genes that were important for the early stages of B-cell development: $VpreB$, $\lambda 5$, RAG1, RAG2 and TdT.

As the coding joint formation during V(D)J recombination is imprecise, two-thirds of the $V_H \rightarrow DJ_H$ and $V_L \rightarrow J_L$ joints are out of frame and thus unable to encode Ig chains (Zhang, 2004). Cells with non functional IgH or IgL rearrangements cannot survive, unless they are rescued by a subsequent functional rearrangement or by abnormal expression of an oncogene. Another feature of the non random nature of the antibody diversification process is the generation of cells with self-reactive receptors. About 60% of early immature B-cells are autoreactive (Wardemann, 2003). Because of their harmful potential, these self-reactive B-cells have to be removed or rendered anergic before entry into peripheral pool of B-cells. As a consequence of the negative selection, only about 10% of newly regenerated B-cells are apparently released into periphery.

3.3. Receptor editing

B-cells producing antibody molecules that recognise self-antigens are subjected to inactivation through various mechanisms of tolerance. The B-cell might undergo clonal deletion or become anergic. A further possibility is that the B-cell receptor is edited by a continuing or secondary rearrangement of Ig genes (Klonowski, 2001). Receptor editing can rescue autoreactive B-cells by changing their antibody specificity (Zhang, 2004). Immature B-cells have the capability to generate a new variable region. Most studies of receptor editing have focused on

the light chain genes. The organisation of the V_L and J_L gene segments within the $Ig\kappa$ and λ loci allows secondary rearrangements to occur by joining of an upstream V_L and a downstream J_L gene segment to delete the primary $V_L \rightarrow J_L$ rearrangement. Because the remaining germline V_L and J_L gene segments are flanked by compatible RSS sites, the secondary rearrangement of light chain genes can occur in the same way as the primary rearrangement, as long as the recombination machinery is operative (Zhang, 2004). Secondary light chain rearrangement is a frequent consequence of stimulation of immature B-cells in the bone marrow, after ligation of their BCRs. The capacity to edit light chains is limited to early immature B-cells, when they are resistant to apoptosis. The immature B-cells then become more sensitive to apoptosis, presumably to allow clonal deletion.

Light chain gene editing is an efficient process that plays an important role in shaping the primary B-cell repertoire (Seagal, 2002). Using genetically engineered mice carrying human and mouse $C\kappa$ genes, it was shown that receptor editing has major contribution to the antibody repertoire, and about 25% of the B-cells undergo secondary rearrangement (Casellas, 2001).

Secondary recombination can also occur at the heavy chain locus, but through a different mechanism. Whereas V_L recombination replaces the entire preexisting $V_L J_L$ rearrangement, a new V_H gene rearranges into the preexisting $V_H D J_H$ rearrangement, using a cryptic recombination signal sequence (cRSS), to produce hybrid V_H genes. The majority of the functional V_H germline genes contain heptameric cRSS motifs (5'-TACTGT-3') embedded at the end of the third framework region (Seagal, 2002; Zhang, 2004) and potentially could participate in V_H replacement (Radic, 1996). V_H replacement normally occurs primarily at the immature B-cell stage and may also occur at lower frequency in the pro-B- and pre-B-cell stages. The serial V_H replacement not only rescues pro-B-cells carrying a non-functional $V_H D J_H$ rearrangement but also creates intraclonal diversity. With each round of V_H replacement, the resulting IgH gene renews the entire V_H -coding region, except for a short stretch of 3' nucleotides from the replaced V_H gene that is retained in the V_H -D joint as a V_H replacement footprint (Zhang, 2004). This generates charged amino acids into the CDR3 region and results in the increase of its length.

3.4. Receptor revision

It was surprising to find that peripheral B-cells can undergo further rounds of Ig gene rearrangements. Receptor revision occurs in germinal center (GC) B-cells that reexpress RAG, sometimes after the initiation of somatic hypermutation, and contributes in the generation of high affinity antibodies during affinity maturation. DNA recombination and receptor revision are reactivated in GC B-cells exposed to antigens to which their receptor binds at low affinity. The formation of GC requires B-cell activation with appropriate T-cell help. The GC is an anatomical site where activated B-cells proliferate and differentiate to antibody-producing cells, undergo heavy chain isotype switch, and form immunological memory (Seagal, 2002). It is also the site where somatic hypermutation and affinity maturation take place. The GC cell subset that expresses most RAG activity appears to be the non-cycling centrocytes cells. Unlike other peripheral B-cells, these cells express many markers shared by immature bone marrow B-cells, including surrogate light chain components, IL-7 receptor and TdT (Nemazee, 2000; Seagal, 2002). The similarities between RAG-expressing bone marrow and germinal center raise the possibility that receptor editing is going on in immature B-cells that have migrated to the periphery and have been recruited into spleen and lymph node. Several studies confirm this theory (Kuwata, 1999; Monroe, 1999; Yu, 1999). However, other studies contradict it, showing that receptor revision occurs in cells undergoing somatic hypermutation in GC (Brard, 1999; de Wildt, 1999; Wilson, 2000).

Despite many similarities, receptor editing and receptor revision are distinct (Nemazee, 2000; Seagal, 2002). Editing occurs in immature bone marrow B-cells as a mechanism of negative selection, whereas cells undergoing revision are found in the periphery. Revision may be a rare event and apparent only in specific circumstances such as chronic antigen drive or autoimmunity. Editing minimizes autoreactivity in immature, preimmune cells by specifically replacing autoreactive receptors, whereas revision occurs during antigen-driven immune responses and is suppressed, rather than induced, by sIg cross-linking. Therefore, revision, unlike editing, should complicate immune tolerance by generating new, often reactive receptors in activated, mature B-cells.

4. Antibody maturation

The maturation of the antibody repertoire is mediated by two different mechanisms: somatic hypermutation (SHM) and class-switch recombination (CSR). These two processes are T-cell dependent and occur in the germinal centers of secondary lymphoid organs. SHM leads to the selection of B-cells expressing a BCR with high affinity for the antigen. CSR leads to the production of antibody of different isotypes.

4.1. Somatic hypermutation

Somatic hypermutation introduces mutations in the V region and its flanking region on both H and L chain genes with high frequency (1.10^{-3} bases per generation) (Neuberger, 1995 and 2003; Honjo, 2002; Durandy, 2003; de Villartay, 2003). The majority (> 90%) of somatic mutations in Ig genes are point mutations, the rest are small deletions and duplications (Bross, 2002). Tetramers with a RGYW motif (purine, G, pyrimidine, A/T) and its inverse complement WRCY are intrinsic mutational hotspots where about 50 to 60% of all mutations are found (Neuberger, 1995). Targeting to RGYW is dependent on T-cells, and especially on CD40/CD154 interaction (Dörner, 2001; Monson, 2001a). SHM is normally followed by the positive selection of B-cells that express a BCR with high affinity for the antigen, whereas B-cells with low affinity are deleted by apoptosis. This selection process occurs in close contact with follicular dendritic cells (FDC) in germinal centers and may be mediated by competition for limited amounts of antigen on the surface of FDC (Honjo, 2002).

4.2. Class-switch recombination

Class-switch recombination involves recombination between two different switch (S) regions that are located upstream from each C region of IgH with deletion of the intervening DNA. Replacement of the C μ region by a C region of another class of Ig (C γ 1-4, C α 1-2 or C ϵ) results in the production of different isotypes (IgG1-4, IgA1-2 or IgE, respectively) with the same V region, and therefore, the same specificity and affinity for the antigen. The nature of the produced isotype determines its activity (half-life, ability to bind Fc receptors or to activate

complement) and the location to which it is delivered (such as IgA in the mucosa) (Neuberger, 2003; de Villartay, 2003).

4.3. SHM and CSR share a common mechanism

SHM and CSR occur simultaneously, in germinal center, but neither is a prerequisite for the other. Not all IgA or IgG carry somatic hypermutation, whereas IgM can be mutated. These processes share common features (Fig. 6). Both require close cooperation between T and B-cells. Both processes require transcription of the targeted (S or V) DNA. Both processes require DNA alterations. DNA cleavages are produced by activation-induced cytidine deaminase (AID). This enzyme is only expressed in germinal center B-cells and is the only B-cell specific factor required for SHM and CSR.

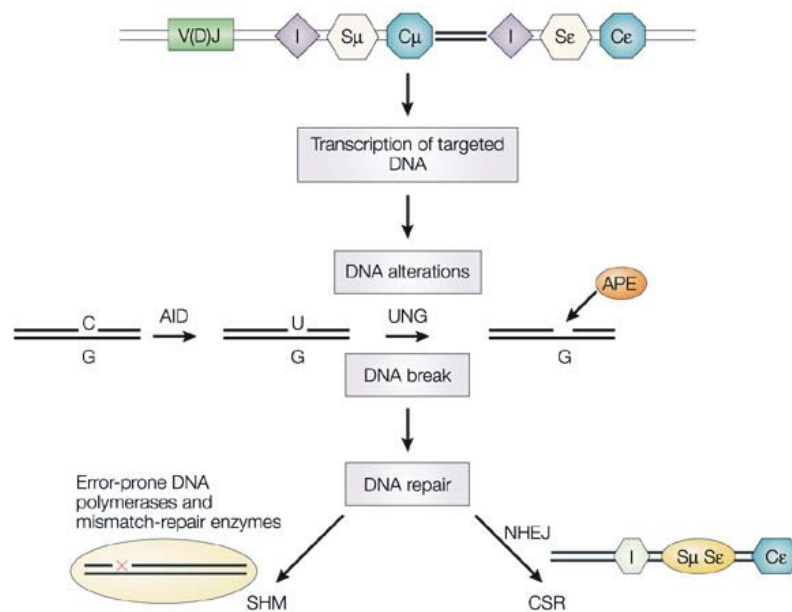


Fig. 6. Mechanisms of somatic hypermutation (SHM) and class switch recombination (CSR) (adapted from de Villartay, 2003)

5. Peripheral B-cell pool

The differentiation of naive B-cells into memory cells occurs within the GC in secondary lymphoid organs, where activated naive B-cells undergo vigorous proliferation, interaction with Ag, Ag-driven selection, somatic hypermutation of the IgV genes, isotype switching and differentiation into memory B-cells and plasma cells (Agematsu, 2001). CD27 represents a key marker for memory cells and interaction of CD27 with its ligand on T-cells, CD70, serves as an important signal for B-cell differentiation into plasma cells (Klein, 1998; Tangye, 1998).

B-cells with unmutated V genes are IgM⁺ IgD⁺ CD27⁻ and comprise about 60% of peripheral blood (PB) B-cells. IgM⁺ IgD⁺ CD27⁻ cells can be further distinguished into CD5⁻ and CD5⁺ B-cells. CD5⁺ B-cells represent a small subset of B-cells (10-20% of B-cells in adult PB). These cells are thought to derive from a separate B-cell lineage and may not participate in T-cell dependent immune responses (Klein, 1998). CD5⁻ B-cells are the naive B-cells that form the precursors of GC B-cells in T-cell dependent immune responses. They represent 40 to 50% of PB B lymphocytes (Fig. 7).

Somatically mutated CD27⁺ memory B-cells represent about 40% of PB B-cells (Fig. 7). They can be divided into: class-switched cells that represent 15% of PB B-cells, IgM⁺ IgD⁺ (15% of PB B-cells), IgM-only (10% of PB B-cells) and IgD-only (<1% of PB B-cells).

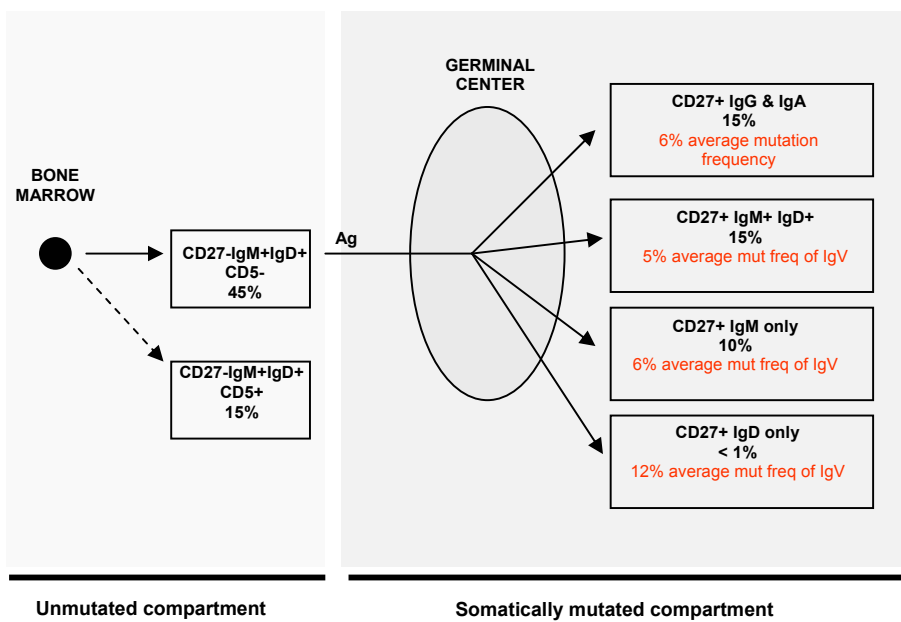


Fig. 7. Peripheral blood B-cell pool (adapted from Klein, 1998)

6. IgV gene usage by B-cells from healthy individuals

The distribution of V, D and J gene segments in the productive and non productive repertoires in both heavy and light chains has been studied in healthy donors (Brezinschek, 1995 and 1997; Foster, 1997; Farner, 1999). The non productive repertoire is not influenced by selection, since it does not encode expressed Ig molecules. It assesses the impact of molecular processes, such as recombination and somatic hypermutation. In contrast, the distribution of B-cells and their productive IgV gene rearrangements can be influenced by a variety of selective events during development and subsequent antigenic stimulation.

A number of specific V_H and V_K genes are positively and negatively selected in the normal repertoire. In contrast, there is no positive selection in V_L genes.

Only about 25% of the functional V_H repertoire is utilised in the formation of the diverse B-cell repertoire (Rao, 1999). In general, the distribution of Ig- V_H gene families reflects their germline complexity: V_{H3} , the largest family, is found most often, followed by V_{H4} and V_{H1} (Gallo, 2000). However, not all V_H gene segments within a family are represented equally.

At the pro-B-cell stage, the genes V_{H3-23} and 3-30 for the V_{H3} family, and 4-34, 4-39 and 4-59 for the V_{H4} family are the most frequently used during the recombination processes (Rao, 1999). In peripheral blood of healthy donors, 10 V_H genes (V_{H3-23} , 4-59, 4-39, 3-07, 3-30, 1-18, 3-30.3, DP58, 4-34 and 3-09) are employed by about 60% of normal B-cells (Brezinschek, 1995 and 1997). One particular gene, V_{H3-23} , is used by approximately 13% of unselected B-cells. Selection of V_{H3-23} is independent of the D and J_H gene segments used, the length and characteristics of CDR3, and the pairing with V_L chains. Concerning the J_H segments, J_{H4} and J_{H6} are preferentially used, compared with the other J_H genes.

The molecular mechanisms that result in the preferential rearrangements of particular V_H elements during gene assembly are still unclear. Some explanations have been proposed (Rao, 1999), such as the accessibility of the DNA to the recombination machinery, a more favourable spacer in recombinase sequence signal (RSS), a more efficient cleavage in RSS, promoter and enhancer efficiencies or unknown factors outside the V_H locus. In more recent studies, Feeney et al. (2000a-b) show that, in many cases, the RSS can account for the differences in recombination frequencies and that the sequence of the spacer of the RSS can play an important role. The position of the genes within the V_H locus has also been suggested to contribute to the preferential

rearrangement of some genes. In mice, the most D-proximal V_H gene segment, V_H81X , a member of V_H7183 predominates early in ontogeny (Rao, 1999). In humans, however, proximity to J_H does not appear to influence the rearrangement frequency of V_H genes in early or later stages of ontogeny. The efficient pairing with surrogate light chain or light chain may also account for the difference of representation in B-cell repertoire (Rao, 1999). This is seen as the reason for the high frequency of the gene V_H4-31 in pro-B-cells, which is not observed anymore in mature B-cells.

In the case of V_K genes, the V_K1 and V_K3 families are the most frequently expressed and some specific gene segments are overrepresented: A27 that is one of the eight members of the V_K3 family, O8/O18 and O2/O12 that belong to the V_K1 family, A19/A3 and A17 that belong to the V_K2 family and B3 that is the single V_K4 family member. Concerning the J_K segments, J_K1 and J_K2 are preferentially used compared with the other J_K gene segments (Foster, 1997).

In the cases of V_L genes, the V_L1 and V_L2 families are found the most often in the productive repertoire. One gene segment is predominately used, the gene 2a2 that belongs to V_L2 family. Farner et al. (1999) have shown that six genes account for 60% of the productive repertoire: 2a2, 3h, 2b2, 1c, 1g and 1b.

Importantly, the distribution of particular V_H and V_L minigenes appears to be an intrinsic feature of human B-cells and does not vary between individuals of different ethnic background or age. Moreover, the general distribution of the V_H gene family repertoire has been reported to be stable for a time period up to 9 years (Dijk-Hård, 2002).

7. IgV gene usage in autoimmune diseases

In some autoimmune diseases, such as Sjögren's syndrome (SS) or systemic lupus erythematosus (SLE), minimal abnormalities in the non-productive V_H , V_K and V_L gene repertoires have been described (Dörner, 1999, 2001 and 2002; Heimbächer, 2001; Kaschner, 2001), suggesting that the basic process of IgV recombination is largely normal in patients with these diseases. However, there are major distortions of the repertoire that result from the impact of selection and somatic hypermutation.

There are few examples of an association between particular V_H genes and autoimmune disorders. One example is the almost exclusive usage of V_H4-34 in cold agglutinin disease (Dörner, 2001 and 2002). Antibodies using the V_H4-34 gene segment also recognise different autoantigens, such as rheumatoid factors, anti-DNA antibodies and anti-D antibodies. This gene is normally negatively selected in healthy subjects. Its overrepresentation in autoantibodies may reflect an abnormality in negative selection, or alternatively a positive selection by antigen in some autoimmune diseases, like SLE. Another example is the gene V_H3-23 that encodes the 16/6 idiotype expressed by some anti-DNA antibodies. Autoantibodies often employ V_H genes that are frequent in the normal repertoire, such as V_H3-23 , 1-69, 4-34, 4-39 and 3-07. However, anti-DNA antibodies can also use uncommon V_H genes, such as V_H1-46 , 3-64 and 3-74. There is no typical pattern of autoimmune V genes.

V_L genes are also broadly distributed in human monoclonal antibodies. The V_K1-3 family members are used more frequently than the V_L genes. They comprise about 40% of the overall repertoire in anti-DNA antibodies and are characteristic of cold agglutinins (Dörner, 2002). V_L genes have also been shown to be critical part of a number of autoantibodies, including antibodies to double-stranded DNA, rheumatoid factors, antibodies to lamin B (Kaschner, 2001). In this regard, frequent use of V_L3 family members by antibodies with RF activity has been reported (Elagib, 1999).

More than in the VDJ recombination process, abnormalities in the selection of B-cells have been observed in autoimmune disorders. For example, mutational frequencies are frequently disturbed in autoimmune diseases. Potentially pathogenic autoantibodies may arise via somatic hypermutation during the immune response to foreign antigen from antibodies that have no reactivity to autoantigen in their germline configuration. Most pathogenic anti-DNA antibodies

are heavily mutated (Dörner, 2001). In SLE (Dörner, 2001) and rheumatoid arthritis (RA) (Huang, 1998), a marked increase in the overall mutational frequency is observed. On the other hand, this is not the case in SS (Dörner, 2001).

The role of receptor editing in shaping the B-cell repertoire in autoimmunity is controversial. Because receptor editing is thought to have a major role in rescuing autoreactive B-cells from deletion, defects in receptor editing could have a role in the aetiology of some autoimmune diseases. Patients with SLE (Dörner, 2001) and RA (Itoh, 2000) show an enhanced receptor editing/revision, in contrast to patients with SS where receptor editing is decreased (Dörner, 2001).

Clonal expansion is another characteristic feature of B-cell repertoires in autoimmune diseases. Clonally expanded B-cells have been described in various autoimmune disorders, such as SLE (Dörner, 2001), SS (Dörner, 2001; Stott, 1998), RA (Itoh, 1999), myasthenia gravis (Sims, 2001).

The analysis of the B-cell subsets also shows some disturbances in patients with autoimmune diseases when compared with healthy controls. The phenotype and Ig-V_H gene usage has been examined in 13 patients with SLE (Odendhal, 2000). There is a marked reduction of CD19⁺ CD27⁻ naive B-cells, retention of CD19⁺ CD27⁺ memory cells and increased numbers of CD19^{low}CD27^{high} plasma cells. These B-cell subpopulations differ in their V_H gene usage: in naive and memory B-cells, the gene V_H3-23 is found the most often, whereas in plasma cells, V_H4-34 and 4-59 are frequently used. In RA also, patients manifest a normal frequency of CD27⁻ naive B-cells, an increased frequency of CD27⁺ memory B-cells and a substantial population of CD27^{high} plasma cells (Lindenau, 2003). In SS, the distribution of B-cell subsets in peripheral blood is different, with a clear predominance of naive B-cells (Dörner, 2001).

8. Rheumatoid arthritis

Rheumatoid arthritis (RA) is one of the most common inflammatory autoimmune disorders, with a high incidence (1% throughout Europe). It is a debilitating disease that affects three times more women than men. Onset of the disease in adults is usually between the ages of 30 to 45 years, although it can occur at any age. RA is a progressive disease with radiographic evidence of joint damage, declines in functional status and premature mortality (Lee, 2001).

Little is known about the pathogenesis of RA and its aetiology remains unclear. RA is characterised by the development of an inflammation in the synovial tissue and by the infiltration of mononuclear cells in the joint, consisting of macrophages, T lymphocytes and plasma cells. Although there is considerable controversy regarding the relative importance of the various cell types and their products in the inflammatory reactions of RA, it seems likely that all cell lineages participate in the disease pathogenesis. B lymphocytes may not be necessary to initiate the inflammatory reactions, but B-cells and their products can perpetuate and potentiate these responses, via their functions of presentation of antigen to T-cells and elaboration of the antibodies (Itoh, 2000).

There are indications that B-cell activity is enhanced (Kim, 2000; Dörner, 2003). B-cells are found in the synovium, where they form aggregates with T-cells and develop tertiary lymphoid tissue structures (Kim, 2000). The mutational activity of these B-cells is markedly enhanced and abnormalities in positive and negative selection are found (Dörner, 2003). Furthermore, elimination of B-cells by anti-CD20 antibodies from the synovial tissue provokes a disruption of T-cell activation and production of proinflammatory monokines (Takemura, 2001), proving the important role of B-cells in the pathogenesis of RA.

9. B-cell depletive therapy in RA

B-cell depletive therapies have been shown to have beneficial effects on patients suffering from autoimmune diseases and especially from rheumatoid arthritis. B-cell depletion using rituximab, a monoclonal antibody directed against the CD20 surface molecule, has attracted intensive attention since good clinical responses have been observed.

9.1. Rituximab

Rituximab is a genetically engineered chimeric antibody that consists of human IgG1 and kappa constant regions, and of mouse variable regions from a hybridoma directed at human CD20 (Silverman, 2003a). Rituximab has a binding affinity for human CD20 of approximately 8 nM.

9.2. CD20

CD20 is a specific B-cell marker present in most of the stages of B-cell development (Fig. 8). It appears at the pre-B-cell stage and remains highly expressed on the surface of on both resting and activated mature B-cells. It is not expressed by haematopoietic stem cells, pro-B-cells or plasma cells or in other normal tissues. Its level of expression on memory B-cells has not yet been determined (Silverman, 2003a).

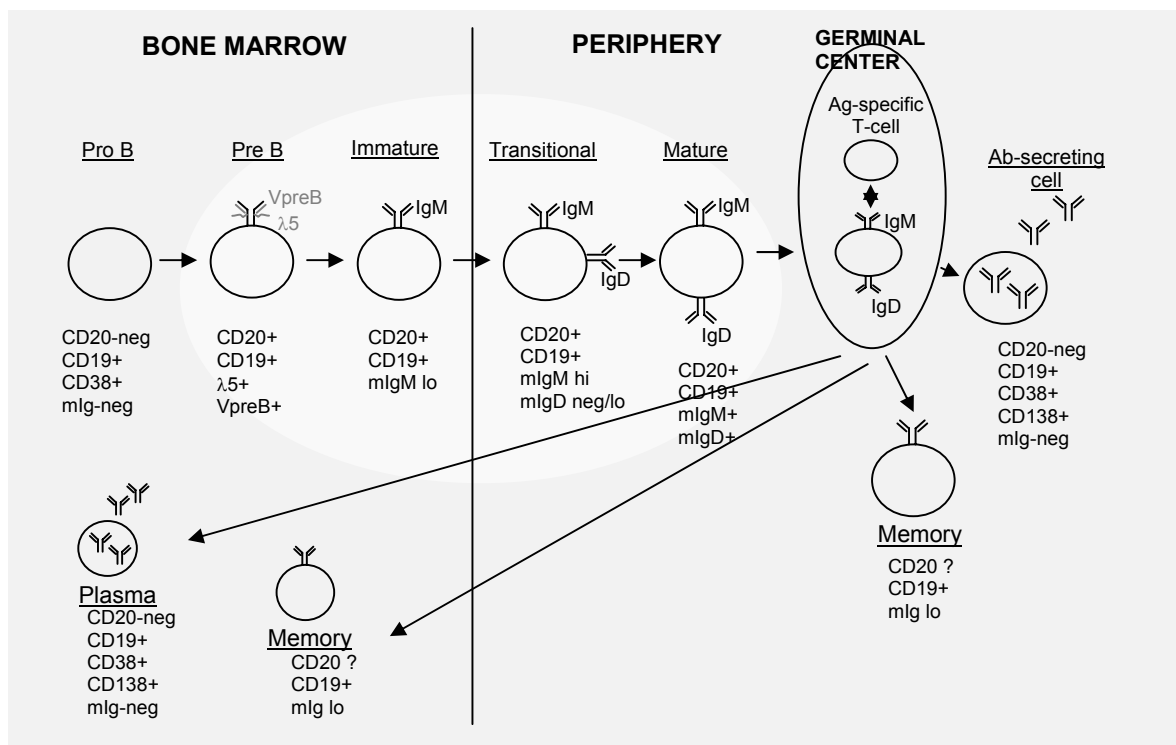


Fig. 8. Surface phenotype of B lymphocytes undergoing differentiation (adapted from Silverman, 2003a)

The role of CD20 in B-cell physiology remains unknown; there is no known natural ligand and CD20-knockout mice have no obvious B-cell deficits (O’Keefe, 1998). Based on structural homologies, CD20 has been speculated to function as a calcium channel subunit. Its ligation can affect B-cell activation, differentiation and cell cycle progression from the G1 to the S phase (Silverman, 2003a).

The use of CD20 as therapeutic target is supported by several observations. It is expressed at high levels on the membrane of B-cells and does not exist in a soluble form. Its binding does not modulate its expression and result in endocytosis. It does not shed and there is no other known membrane or secreted analogs to interfere with its use for B-cell targeting (Silverman, 2003a; Gorman, 2003)

9.3. Rituximab and B-cell depletion

Rituximab is administrated as intravenous infusion. It selectively depletes B-cells from the peripheral blood completely for 6 months and more, well beyond the persistence of rituximab itself (Eisenberg, 2003). B-cells are also removed in the spleen and the bone marrow for several months. Due to the absence of CD20 on the surface of plasma cells, serum immunoglobulins do not fall substantially during treatment, explaining the lack of infections in the patients. Since CD20 is not expressed on early B-cell precursors, the bone marrow is able to repopulate with B lymphocytes after treatment.

The mechanism of cytotoxicity of rituximab is not clear, but may involve a combination of effects, including complement-mediated lysis and antibody-dependent cell-mediated cytotoxicity, induction of apoptosis and/or recruitment of effector cells (Cerny, 2002; Cheson, 2002; Maloney, 2002; Silverman 2003a).

9.4. Rituximab therapy and RA

Different independent studies have shown clinical efficacy (Edwards, 2002; Patel, 2002; Kneitz 2002 and 2004; Gorman, 2003; Hainsworth, 2003; Silverman, 2003a-b; Kneitz, 2004). Edwards and Cambridge (2001) studied 5 patients with refractory RA. They were treated with a

regimen of rituximab in conjunction with intravenous cyclophosphamide and high dose steroids. All patients achieved responses meeting the American College of Rheumatology 70% improvement criteria (ACR70) after the first or the second treatment cycle. This early open label study was extended to include 22 patients treated with five different protocols to assess a possible dose-response relationship with rituximab and whether the inclusion and omission of cyclophosphamide was relevant. Major responses were associated with higher doses of rituximab (equal or greater than a total treatment dose of 600 mg/m²) in combination with cyclophosphamide. Clinical relapse was associated with rises in autoantibodies (rheumatoid factors, anti-cyclic citrullinated peptides) rather than only with return of B-cells (Gorman, 2003). Another study by De Vita et al (2002) also showed the beneficial effects of rituximab on patients with RA who were not responsive to combination therapy with methotrexate and cyclosporine A with or without anti-tumor necrosis α factor (anti-TNF α) therapy.

A double blind placebo controlled randomised study has shown that protocols based on rituximab are effective in treating patients with active RA. 161 patients were randomised into four groups and received methotrexate plus placebo infusion, rituximab alone, rituximab plus methotrexate, or rituximab plus cyclophosphamide. Combination treatments with rituximab plus methotrexate, and rituximab plus cyclophosphamide gave comparable results and were both superior to rituximab alone (Stahl, 2003).

Taken together, the studies on anti-CD20 therapy for RA provide evidence that B-cells may play an important role in RA pathogenesis.

AIMS OF THE PROJECT

Although the role of B-cells in autoimmunity is not completely understood, their importance in the pathogenesis of autoimmune diseases has been more appreciated in the past few years. It is now well known that they have additional roles than (auto) antibody production and are involved by different mechanisms in the regulation of T-cell mediated autoimmune disorders. The B-cell repertoire itself is influenced by these immune regulatory processes in the course of autoimmune diseases.

B-cell depletive therapies have beneficial effects in patients suffering from rheumatoid arthritis (RA), highlighting the central role of B-cells in the pathogenesis of this disease. Nevertheless, the mechanism of action is unclear. It has been hypothesised that B-cell depletion is able to reset humoral immunity. Therefore we wanted to investigate if transient B-cell depletion results in changes of the peripheral B-cell receptor repertoire.

To address this issue, the B-cell repertoire of two patients suffering from RA was analysed, one for the heavy chain repertoire (patient H), one for the light chain repertoire (patient L). Both patients were treated with rituximab, an anti-CD20 monoclonal antibody that selectively depletes peripheral CD20+ B-cells for several months. The B-cell repertoire was studied before therapy and at the earliest time point after B-cell regeneration in both patients. A longer follow-up (up to 27 months) was performed in patient H who was treated a second time with rituximab after 17 months.

With this study, we wanted to answer two questions:

- Is a temporary B-cell depletion able to modulate the preexisting repertoire?
- Is there a correlation between the changes in B-cell repertoire and the activity of the disease?

MATERIAL AND METHODS

1. Patients

Two patients were studied for the analysis of their B-cell repertoire: patient H for the heavy chain repertoire and patient L for the light chain repertoire. They were diagnosed rheumatoid arthritis using the American College of Rheumatology (ACR) criteria.

Patient H (male, 45 years) has been treated unsuccessfully with three disease-modifying antirheumatic drugs (DMARDs) regimen including methotrexate and also failed therapy with TNF α blockers. Except for 5 mg prednisolone equivalent daily, he received no other antiproliferative treatment during the whole study.

Patient L (female, 49 years) has been treated unsuccessfully with more than three DMARDs regimen. At the beginning of the study, she was receiving 5 mg prednisolone daily and 25 mg etanercept (recombinant soluble TNF α receptor) twice weekly. This treatment was kept constant during the whole study.

Before entering the study, both patients gave their informed consent and were treated in an open label protocol approved by the local ethics committee. Rituximab (Mabthera[®], Hoffmann La-Roche, Grenzach-Whylen, Germany) was administrated intravenously at a dose of 375mg/m² once a week for a total of four infusions (day 1, 8, 15 and 22).

Disease activity was regularly determined using the disease activity score 28 (DAS28) and by monitoring the C reactive protein (CRP) levels.

The analysis of lymphocyte subsets by immunofluorescence staining was performed by incubating peripheral blood mononuclear cells (PBMCs) with anti-CD19 and anti-CD3 antibodies (PE or FITC-labeled; all antibodies from Becton-Dickinson, Heidelberg, Germany) using a FACS Calibur (Becton-Dickinson, San Jose, CA). Frequencies of cell populations were calculated using CellQuest software.

2. Sample preparation

2.1. Genomic DNA extraction

Peripheral blood mononuclear cells (PBMCs) were prepared from 40 ml blood by Ficoll hypaque gradient centrifugation at 900g, without brake, at room temperature for 25 minutes and washed twice in HBSS medium containing 1% FCS, 1% penicillin-streptomycin and 1% L-glutamine.

Genomic DNA was isolated from 5.10^6 PBMCs using the QIAamp® DNA Blood Mini Kit (Qiagen), according to manufacturer's instructions.

Samples were stored at 4°C until further analysis.

2.2. RNA extraction

Total cellular RNA was extracted from 1.10^7 PBMCs, which were pelleted by centrifugation and lysed in 1.5 ml Trizol Reagent by repetitive pipetting.

The homogenized samples were incubated for 5 minutes at room temperature to permit the complete dissociation of nucleoprotein complexes. 0.3 ml chloroform was added and the tubes were shaken vigorously by hand for 15 seconds and incubated at room temperature for 2 to 3 minutes. Then samples were centrifuged at 12,000g at 4°C for 15 minutes. During centrifugation, the mixtures separated into a lower red phenol-chloroform phase, an interphase and a colourless upper aqueous phase. RNA remains exclusively in the aqueous phase.

The aqueous phase was transferred to a new tube and the RNA was precipitated by mixing with 0.75 ml isopropanol. Then samples were incubated for 10 minutes at room temperature and centrifuged at 12,000g at 4°C for 10 minutes. The RNA precipitate was visible as a gel-like pellet.

After removal of the supernatant, the pellet was washed once with 1.5 ml of 75% ethanol. The samples were mixed by vortexing and centrifuged at 7,500g at 4°C for 5 minutes.

After discarding the ethanol, the RNA pellet was air-dried for 5 to 10 minutes and dissolved in RNase-free water by passing the solution a few times through a pipette tip and incubating at 55°C for 10 minutes.

Samples were stored at -20°C until further analysis.

2.3. Determination of the concentration of nucleic acids

The concentration of nucleic acids was calculated using a spectrophotometer Ultraspec 1000 (Pharmacia Biotech) by measuring the absorbance of the sample at 260 nm wavelength. Absorbance at 280 nm wavelength was also measured to assess the purity of the sample. The purity of the sample was assessed by the ratio A_{260}/A_{280} that should range between 1.6 and 2.0. To determine the nucleic acid concentration (in $\mu\text{g/ml}$), the A_{260} reading was multiplied with a factor of 50 for double stranded DNA and 40 for RNA and with the dilution factor.

2.4. Single cell sorting

2.4.1. Cell preparation

PBMCs were prepared from 40 ml blood as described in section 2.1. After the second washing step, the cells were suspended in 2 ml RPMI rich medium containing 10% FCS, 1% penicillin-streptomycin and 1% L-glutamine and counted.

1.10^7 PBMCs were then labelled with different antibodies in order to be sorted into 96-well plates. The following antibodies were used:

- CD19 PE (phycoerythrin)
- CD27 Cy5
- IgD FITC (fluorescein isothiocyanate)

After 15 minutes-incubation at 4°C , the cells were washed again and suspended in 1 ml RPMI containing 10% FCS, 10% penicillin-streptomycin and 10% L-glutamine.

2.4.2. Cell sorting

Single CD19⁺ IgD⁺ CD27⁺ and CD19⁺ IgD⁺ CD27⁻ cells were sorted into 96-well PCR plates (ABgene) using a FACSDiVa outfitted with an automated cell deposition unit (Becton-Dickinson). Each well contained 5 µl or 30 µl of a lysis buffer *. Four wells on each plate received no cell and served as negative controls.

After sorting, an upper reaction buffer * was added to each well, followed by an incubation.

* Depending on the type of reaction, different buffers were used.

	PCR	RT-PCR
Lysis buffer	5 µl 200 mM KOH/ 50 mM DTT	30 µl 5 mM DTT/ 20 U RNase inhibitor/0.5 µg BSA/ 400 ng oligo dT/ 1% Triton X100
	incubation 65°C for 10 min = lysis of the cell	
Upper reaction buffer	5 µl Neutralising solution 900 mM Tris HCl pH 9.0/ 300 mM KCl/ 200 mM HCl	20 µl 1X RT-PCR buffer (with MgCl ₂)/ 0.2 mM dNTPs/ 20 U Reverse Transcriptase
	store at 4°C until the preamplification step	incubation 50°C for 40 min = cDNA synthesis
		store at 4°C until the nested PCRs

At the end of this step, the wells contained the material for further amplification of the V(D)J rearrangements: genomic DNA in the case of PCR and cDNA in the case of RT-PCR.

3. Amplification of V(D)J rearrangements

3.1. Oligonucleotides

The primers used to amplify the different V(D)J rearrangements have been described in previous publications (Brezinschek, 1995. Foster, 1997; Farner, 1999).

All the primers were synthesised by Gibco BRL. All the sequences are given 5' to 3'.

3.1.1. Heavy chains - V_HDJ_H rearrangements

External primers

M173-ExVH1L-17: CCA TGG ACT GGA CCT GG

M174-ExVH2L-20: ATG GAC ATA CTT TGT TCC AC

M175-ExVH3L-20: CCA TGG AGT TTG GGC TGA GC

M176-ExVH4L-20: ATG AAA CAC CTG TGG TTC TT

M177-ExVH5L-20: ATG GGG TCA ACC GCC ATC CT

M178-ExVH6L-20: ATG TCT GTC TCC TTC CTC AT

M179-ExJH1,2,4,5-21: TGA GGA GAC GGT GAC CAG GGT

M180-ExJH3-20: TAC CTG AAG AGA CGG TGA CC

M181-ExJH6-19: ACC TGA GGA GAC GGT GAC C

Primers for the constant region

M260-C μ -20: TCA GGA CTG ATG GGA AGC CC

M261-C γ -19: CAG GCC GCT GGT CAG AGC G

M262-C α -20: AGG CTC AGC GGG AAG ACC TT

Nested primers

M182-IntVH1FR-26: GGT GCA GCT GGT RCA GTC TGG GGC TG

M183-IntVH2FR-26: CAG RTC ACC TTG ARG GAG TCT GGT CC

M184-IntVH3FR-26: CAG GTK CAG CTG GTG GAG TCT GGG GG

M185-IntVH4FR-27: GGT GCA GCT GCA GGA GTS GGG CSC AGG

M186-IntVH5FR-24: AGC TGG TGC AGT CTG GAG CAG AGG

M187-IntVH6FR-27: TAC AGC TGC AGC AGT CAG GTC CAG GAC

M188-IntJH1,3,4,5-25: CGA CGG TGA CCA GGG TBC CYT GGC C

M189-IntJH2-25: CGA CAG TGA CCA GGG TGC CAC GGC C

M190-IntJH6-24: CGA CGG TGA CCG TGG TCC CTT GCC

External VHL primers and nested VHFR primers hybridise to the leader peptide sequence and to the framework region 1 respectively, of the respective family. The external and internal 3' primers were based on Küppers (1993).

3.1.2. Light chains

3.1.2.1. VκJκ rearrangements

External primers

M267-ExVκ1,2-17: GCT CAG CTC CTG GGG CT

M268-ExVκ3-17: GGA A(AG)C CCC AGC (AGT)CA GC

M269-ExVκ4,5-19: CT(GC) TT(GC) CT(CT) TGG ATC TCT G

M270-ExVκ6,7-17: CT(GC) CTG CTC TGG G(CT)T CC

M271-ExJκ2-19: ACG TTT GAT CTC CAG CTT G

M272-ExJκ5-2: CTT ACG TTT AAT CTC CAG TC

Nested primers

M273-IntVκ1-21: CAT CCA G(AT)T GAC CCA GTC TCC

M274-IntVκ2-23: TCC AGT GGG GAT ATT GTG ATG AC

M275-IntVκ3-23: GTC T(GT)T GTC TCC AGG GGA AAG AG

M276-IntVκ4-22: GAC ATC GTG ATG ACC CAG TCT C

M277-IntVκ5-22: GGG CAG AAA CGA CAC TCA CGC A

M278-IntVκ6-23: TCC AGG GGT GAA ATT GTG (AC)TG AC

M279-IntVκ7-22: GCT GCA ATG GGG ACA TTG TGC T

M280-IntJκ2-21: CAG CTT GGT CCC CTG GCC AAA

M281-IntJκ5-20: CCA GTC GTG TCC CTT GGC CG

All external primers bind in the leader sequence and all nested primers bind at the 5' end of framework region 1.

3.1.2.2. VλJλ rearrangements

External primers

M282-ExV11-17: CCT GGG CCC AGT CTG TG
M283-ExV12-18: CTC CTC A(GC)(CT) CTC CTC ACT
M284-ExV13-18: TC(CT) TAT G(AT)G CTG AC(AT) CAG
M285-ExV14-17: C(AT)G C(CT)T GTG CTG ACT CA
M286-ExV15,9-17: CCC TCT C(GC)C AG(GC) CTG TG
M287-ExV16-19: TCT TGG GCC AAT TTT ATG C
M288-ExV17,8-19: ATT C(CT)C AG(AG) CTG TGG TGA C
M289-ExV110-17: CAG TGG TCC AGG CAG GG

M290-ExJ1-17: AGG ACG GT(GC) A(GC)C T(GT)G GT

Nested primers

M291-IntV11-21: CCA GTC TGT G(CT)T GAC (GT)CA GCC
M292-IntV12.1-20: CAG TCT GCC CTG ACT CAG CC
M293-IntV12.2-21: GTG TC(CT) (AG)GG (GT)CT CCT GGA CAG
M294-IntV13.1-22: TGA CTC AGG ACC CTG CTG TGT C
M295-IntV13.2-22: TGA C(AT)C AGC CAC (CT)CT C(AG)G TGT C
M296-IntV14.1-20: TCT GCC TCT GC(CT) TCC CTG GG
M297-IntV14.2-20: TCT GCA TCT GCC TTG CTG GG
M298-IntV15,9-20 CAG (GC)CT GTG CTG ACT CAG CC
M299-IntV16-23: CCA ATT TTA TGC TGA CTC AGC CC
M300-IntV17,8-19: CTG TGG TGA C(CT)C AGG AGC C
M301-IntV110-19: CAG GCA GGG C(AT)G ACT CAG C

M302-IntJ11-21: GGT (GC)AC CTT GGT (GC)CC A(GC)T (GT)CC
M303-IntJ12,3-21: GGT CAG CT(GT) GGT (GC)CC TCC (GT)CC

External primers hybridise to the 5' leader sequences. Nested primers hybridise to the 5' end of framework region 1.

3.2. Amplification of VDJ rearrangements by PCR - Heavy chains

PCR reactions for individual gene families were performed by using a family specific 5' (VH) external primer in combination with a mixture of the 3' (JH) external primers.

3.2.1. Nested-PCR on bulk DNA

3.2.1.1. External amplification round

The 80 µl-reaction mix consisted of:

- 5 µl (250 ng) of template (genomic DNA)
- 1.6 µl of deoxynucleoside triphosphate (10 mM each, Peqlab)
- 5 µl of VH - family specific- 5' external primer (10 µM)
- 5 µl of JH - mixed - 3' external primer (10 µM)
- 8 µl of MgCl₂ (25mM)
- 8 µl of 10X buffer II w/o MgCl₂
- 0.5 µl of AmpliTaq DNA polymerase (5 U/µl)
- 46.9 µl of H₂O

The AmpliTaq polymerase, 10X buffer II and MgCl₂ were supplied by Applied Biosystems.

The PCR amplifications were performed on Gene Amp PCR System 2400 (Perkin Elmer).

The PCR reaction conditions consisted of:

- 1 cycle of denaturation at 95°C for 5 minutes,
 annealing at 50°C for 1 min
 extension at 72°C for 1 min, followed by
- 35 cycles of denaturation at 94°C for 1min,
 annealing at 50°C for 30 sec,
 extension at 72°C for 1 min,
- and a final extension of 5 min at 72°C.

3.2.1.2. Internal amplification round

The nested PCR was performed in an identical manner, except that internal primers were taken and 5µl of each reaction product from the external PCR were used as template.

The differences in the nested amplification program were an annealing temperature of 65°C (instead of 50°C) and the number of cycles decreased to 30 (instead of 35).

3.2.2. Single-cell PCR

3.2.2.1. Pre-amplification PCR step

A pre-amplification PCR step using a random primer (15N) was performed to amplify the whole genome in order to increase the starting material.

A reaction mix (for 1 plate) was prepared as followed:

- 3590 μ l of H₂O
- 600 μ l of MgCl₂ (25 mM)
- 60 μ l of dNTPs (10 mM each)
- 50 μ l of 15-base random oligonucleotide
- 600 μ l of a 10X specific buffer
- 100 μ l of AmpliTaq DNA polymerase (5 U/ μ l)

50 μ l of this reaction mix were added to each well containing the single cells in the buffers.

The 10X specific buffer was composed by:

- 180 μ l of 1% Triton X100 (Sigma)
- 1 ml of Tris-HCl 1.8 M – pH 9.0
- 16.82 ml of H₂O

Amplification for 60 cycles was performed in a Px2 thermal cycler (Thermo Hybaid) according to the following program:

- 1 cycle of initial denaturation for 12 min at 95°C,
 annealing for 2 min at 37°C,
 elongation for 4 min at 55°C, followed by
- 58 cycles of denaturation for 1 min at 94°C,
 annealing for 2 min at 37°C,
 elongation for 4 min at 55°C, followed by
- 1 cycle of denaturation for 1 min at 94°C,
 annealing for 2 min at 37°C,
 elongation for 10 min at 55°C.

All plates were stored at 4°C for further analysis by specific amplification.

3.2.2.2. External amplification round

The reaction mixes were prepared as followed:

Lower reaction mix (for 1 plate):

1036 μ l of H₂O

800 μ l of MgCl₂ (25 mM)

160 μ l of dNTPs (10 mM each)

56 μ l of each external VH primer (100 μ M)

56 μ l of each external JH primer (100 μ M)

Upper reaction mix (for 1 plate):

4150 μ l of H₂O

800 μ l of 10X buffer II w/o MgCl₂

50 μ l of AmpliTaq DNA polymerase (5 U/ μ l)

25 μ l of the lower reaction mix and 50 μ l of the upper one were pipetted into a new 96-well plate and 5 μ l of template generated in the preamplification step were added.

The amplification program consisted of:

- 1 cycle of denaturation at 95°C for 7 minutes,
 annealing at 50°C for 1 min
 extension at 72°C for 1 min 30, followed by
- 34 cycles of denaturation at 94°C for 1 min,
 annealing at 50°C for 30 sec,
 extension at 72°C for 1 min 30,
- 1 cycle of denaturation at 94°C for 1 min
 annealing at 50°C for 30 sec,
 extension at 72°C for 7 min

3.2.2.3. Internal amplification round

The nested PCR was performed in an identical manner, except that internal primers were taken and 5µl of each reaction product from the external PCR were used as template.

Lower reaction mix (for 1 plate): 25 µl in each well

1348 µl of H₂O

800 µl of MgCl₂ (25 mM)

160 µl of dNTPs (10 mM each)

48 µl of VH - family specific - internal primer (100 µM)

48 µl of each external JH primer (100 µM)

Upper reaction mix (for 1 plate): 50 µl in each well

4150 µl of H₂O

800 µl of 10X buffer II w/o MgCl₂

50 µl of AmpliTaq DNA polymerase (5 U/µl)

The only difference in the nested amplification program was an annealing temperature of 65°C (instead of 50°C).

3.3. Amplification of V(D)J rearrangements by RT-PCR - Heavy chains and light chains

3.3.1. RT-PCR on total RNA - Heavy chains

3.3.1.1. cDNA synthesis

The reaction was performed using Titan One Tube RT-PCR System (Roche).

All the reagents were provided by Roche, except the RNase inhibitor, RNAGuard™, which was purchased from Amersham Pharmacia.

The master mixes were prepared as followed:

Master mix 1: 25 µl

- 1 µl of dNTPs (10 mM each)
- 2.5 µl of DTT (100 mM)
- 0.25 µl of RNase inhibitor (32 U/µl)
- 2 µl of oligo dT (200 ng/µl)
- 1 µg of RNA
- up to 25 µl of H₂O

Master mix 2: 25 µl

- 10 µl of 5X RT-PCR
- 1 µl of enzyme mix
- 14 µl of H₂O

Master mixes were mixed gently and the reactants were incubated 60 minutes at 42°C.

3.3.1.2. External amplification round

The amplification of the VDJ rearrangements from cDNA was performed in a comparable manner as the one from genomic DNA, except for the difference of the template and that the 3' primers used in RT-PCR were specific of the constant regions.

The 80 µl-reaction mix consisted of:

- 5 µl of template (cDNA)
- 1.6 µl of dNTPs (10mM each)
- 5 µl of VH - family specific- 5' external primer (10 µM)
- 5 µl of CH - isotype specific - 3'external primer (10 µM)
- 8 µl of MgCl₂ (25 mM)
- 8 µl of 10X buffer II w/o MgCl₂
- 0.5 µl of AmpliTaq DNA polymerase (5 U/µl)
- 46.9 µl of H₂O

The AmpliTaq polymerase, 10X buffer II and MgCl₂ were supplied by Applied Biosystems.

The PCR reaction conditions consisted of:

1 cycle of denaturation at 95°C for 5 minutes,
 annealing at 50°C for 1 min
 extension at 72°C for 1 min, followed by
35 cycles of denaturation at 94°C for 1min,
 annealing at 50°C for 30 sec,
 extension at 72°C for 1 min,
and a final extension of 5 min at 72°C.

3.3.1.3. Internal amplification round

The nested PCR was performed in an identical manner, except that internal JH primers were taken and 5µl of each reaction product from the external PCR were used as template.

The differences in the nested amplification program were an annealing temperature of 65°C and the number of cycles decreased to 30.

3.3.2. RT-PCR on single cell - Light chains

The cDNA was synthesised as described in section 2.4.2.

3.3.2.1. External amplification round

3.3.2.1.1. External amplification for Kappa rearrangements

The reaction mixes were prepared as followed:

Lower reaction mix (for 1 plate):

- 1120 μ l of $MgCl_2$ (25 mM)
- 160 μ l of dNTPs (10 mM each)
- 40 μ l of each external V_{κ} primer (100 μ M)
- 40 μ l of each external J_{κ} primer (100 μ M)
- 980 μ l of H_2O

Upper reaction mix (for 1 plate):

- 4150 μ l of H_2O
- 800 μ l of 10X buffer II w/o $MgCl_2$
- 50 μ l of AmpliTaq DNA polymerase (5 U/ μ l)

25 μ l of the lower reaction mix and 50 μ l of the upper one were pipetted into a new 96-well plate and 5 μ l of cDNA were added to each well.

The amplification program consisted of:

- 1 cycle of denaturation at 95°C for 7 minutes,
 annealing at 56°C for 1 min
 extension at 72°C for 1 min 30, followed by
- 34 cycles of denaturation at 94°C for 1min,
 annealing at 56°C for 30 sec,
 extension at 72°C for 1 min 30,
- 1 cycle of denaturation at 94°C for 1 min
 annealing at 56°C for 30 sec,
 extension at 72°C for 5 min

3.3.2.1.2. External amplification for Lambda rearrangements

The reaction mixes were prepared as followed:

Lower reaction mix (for 1 plate):

- 640 μ l of $MgCl_2$ (25 mM)
- 160 μ l of dNTP (10 mM each)
- 40 μ l of each external $V\lambda$ primer (100 μ M)
- 40 μ l of external $J\lambda$ primer (100 μ M)
- 1340 μ l of H_2O

Upper reaction mix (for 1 plate):

- 4150 μ l of H_2O
- 800 μ l of 10X buffer II w/o $MgCl_2$
- 50 μ l of AmpliTaq DNA polymerase (5 U/ μ l)

25 μ l of the lower reaction mix and 50 μ l of the upper one were pipetted into a new 96-well plate and 5 μ l of cDNA were added to each well.

The amplification program consisted of:

- 1 cycle of denaturation at 95°C for 10 minutes,
 annealing at 50°C for 30sec
 extension at 72°C for 1 min 30, followed by
- 34 cycles of denaturation at 94°C for 1min,
 annealing at 50°C for 30 sec,
 extension at 72°C for 1 min 30,
- 1 cycle of denaturation at 94°C for 1 min
 annealing at 50°C for 30 sec,
 extension at 72°C for 5 min

3.3.2.2. Internal amplification round

3.3.2.2.1. Internal amplification for Kappa rearrangements

The reaction mixes were prepared as followed:

Lower reaction mix (for 1 plate):

- 1120 μ l of $MgCl_2$ (25 mM)
- 160 μ l of dNTPs (10 mM each)
- 40 μ l of internal V_{κ} primer (100 μ M)
- 40 μ l of each internal J_{κ} primer (100 μ M)
- 1100 μ l of H_2O

Upper reaction mix (for 1 plate):

- 4150 μ l of H_2O
- 800 μ l of 10X buffer II w/o $MgCl_2$
- 50 μ l of AmpliTaq DNA polymerase (5U/ μ l)

25 μ l of the lower reaction mix and 50 μ l of the upper one were pipetted into a new 96-well plate and 5 μ l of cDNA were added to each well.

The amplification program consisted of:

- 1 cycle of denaturation at 95°C for 7 minutes,
 annealing at 65°C for 1 min
 extension at 72°C for 1 min 30, followed by
- 34 cycles of denaturation at 94°C for 1min,
 annealing at 65°C for 30 sec,
 extension at 72°C for 1 min 30,
- 1 cycle of denaturation at 94°C for 1 min
 annealing at 65°C for 30 sec,
 extension at 72°C for 5 min

3.3.2.2. Internal amplification for Lambda rearrangements

The reaction mixes were prepared as followed.

Lower reaction mix (for 1 plate):

- 640 μ l of $MgCl_2$ (25 mM)
- 160 μ l of dNTP (10 mM each)
- 40 μ l of internal $V\lambda$ primer (100 μ M)
- 40 μ l of each internal $J\lambda$ primer (100 μ M)
- 1580 μ l of H_2O

Upper reaction mix (for 1 plate):

- 4150 μ l of H_2O
- 800 μ l of 10X buffer II w/o $MgCl_2$
- 50 μ l of AmpliTaq DNA polymerase (5 U/ μ l)

25 μ l of the lower reaction mix and 50 μ l of the upper one were pipetted into a new 96-well plate and 5 μ l of cDNA were added to each well.

The amplification program consisted of:

- 1 cycle of denaturation at 95°C for 7 minutes,
annealing at 63°C for 30sec
extension at 72°C for 1 min 30, followed by
- 34 cycles of denaturation at 94°C for 1min,
annealing at 63°C for 30 sec,
extension at 72°C for 1 min 30,
- 1 cycle of denaturation at 94°C for 1 min
annealing at 63°C for 30 sec,
extension at 72°C for 5 min

4. Visualisation of PCR products and DNA recovery from agarose gel

All PCR products were separated by electrophoresis through 1,5% Ultra pure agarose electrophoresis grade (GIBCO, BRL) and visualised with ethidium bromide (0.5 µg/ml, Sigma) under UV light (254 nm).

Positive bands (around 350 bp) were cut from agarose and purified using the MinElute Gel Extraction Kit (Qiagen) according to manufacturer's instructions.

Principle: The MinElute system combines the convenience of a spin-column technology with the selective binding properties of a silica-gel membrane. DNA absorbs to the silica-membrane in the presence of high salt while contaminants pass through the column. Impurities are efficiently washed away, and the pure DNA is eluted in water.

Procedure: This kit works in few steps: dissolving of agarose, binding of DNA to the silica-membrane, washing steps using different buffers and elution in 10 µl water.

5. Polishing

Purified PCR products were polished using the PCR polishing kit from Stratagene, in order to create blunt-ended DNA fragments, by removing the 3'-overhang extensions generated by the AmpliTaq DNA polymerase.

The polishing reaction was performed according to manufacturer's instructions and was composed by:

- 1 µl of dNTP mix (10 mM)
- 1.3 µl of 10X polishing buffer
- 1 µl of cloned *Pfu* DNA polymerase (2.5 U/µl)
- 10 µl of purified PCR products

The incubation was done at 72°C for 30 minutes.

6. Subcloning and transformation

The subcloning step was performed using the Zero Blunt-PCR cloning kit (Invitrogen, Life Technologies).

Principle: This kit is designed to clone blunt PCR fragments with a low background of non-recombinants. The pCR-Blunt vector (Fig. 9) allows direct selection of recombinants via disruption of a lethal *E. coli* gene, *ccdB*. The cloning vector, pCR-Blunt, contains the *ccdB* gene fused to the C-terminus of LacZα. The vector is supplied linearized and blunt-ended at a unique

site in the polylinker. Ligation of a blunt PCR fragment disrupts expression of the *lacZα-ccdB* gene fusion permitting growth of only positive recombinants upon transformation. Cells that contain non-recombinant vector are killed when the transformation mixture is plated. The vector also contains both the kanamycin and Zeocin resistance genes for selection in *E. coli*, a versatile multiple cloning site with 12 unique sites, the T7 RNA promoter/priming site for *in vitro* transcription and all M13 universal primer sites for sequencing.

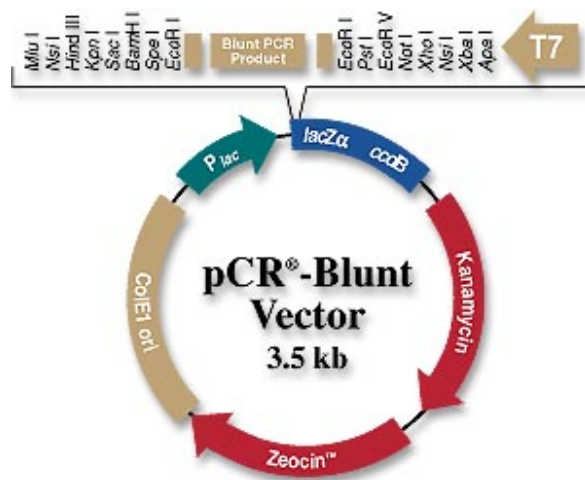


Fig. 9. pCR-blunt vector

Procedure: The blunt-ended generated, polished, DNA fragment is ligated into the pCR-Blunt vector and transformed into One Shot TOP 10 competent cells. Transformants are selected on kanamycin. Positive clones are chosen and their plasmids are purified for further characterization.

6.1. Ligation into pCR-Blunt vector

To obtain high cloning efficiency, blunt-end ligations require high insert to vector ratios. Actually a 5:1 insert to vector ratio was used.

The concentration of the polished fragment was estimated on an agarose plate where a scale of different concentrations of DNA was previously prepared.

After polishing, the usual concentration of the insert was less than 10 ng/μl.

Calculation of picomole ends per microgramme of DNA:

$$\text{pmol ends}/\mu\text{g DNA} = 2.10^6 / (\text{size of DNA -in bp-} \times 660 \text{ Da})$$

The insert is 350 bp. It corresponds to 8.658 pmol ends/ μg DNA.

The pCR-blunt vector is 3512 bp. It corresponds to 0.862 pmol ends/ μg DNA. The concentration of the vector is 25 ng/ μl and 1 μl is used in the ligation reaction; that means 0.0216 pmol ends.

Because the ratio used is 5:1, the insert should have 0.108 pmol ends, which corresponds to 12.5 ng DNA.

So, the ligation protocol was as follows:

- 1 μl (25 ng) of linearized pCR-blunt vector,
- 1 to 5 μl (12.5 ng) of blunt insert,
- 1 μl of 10X ligation buffer
- 1 μl of T4 DNA ligase (4 U/ μl)
- up to 10 μl of H_2O .

The ligation reaction was then incubated at 16°C for 1 hour.

6.2. Transformation into One Shot TOP 10 competent cells

The transformation was performed as described in the subcloning kit. Briefly, 5 μl of the ligation reaction were pipetted into 50 μl of One Shot TOP 10 cells. The vial was incubated 30 minutes on ice and shocked at 42°C for exactly 45 seconds. 250 μl of SOC medium were added and the vial was shaken at 37°C for 1 hour at 225 rpm.

80 μl of the transformation reaction were spread on LB agar plate containing 50 $\mu\text{g}/\text{ml}$ kanamycin, and the plate was finally incubated at 37°C overnight.

7. Analysis of the transformants

Antibiotic resistant transformants were picked, inoculated into 2 ml LB containing 50 $\mu\text{g}/\text{ml}$ kanamycin and grown overnight at 37°C in a shaking incubator at 250 rpm.

Plasmids DNA were isolated using the Wizard Plus SV Minipreps DNA Purification System kit (Promega).

Different procedures were used to check the presence of inserts: restriction digest using the enzyme EcoR1, or PCRs (on plasmid or on bacteria) using the M13 Forward and M13 Reverse universal primers

7.1. Restriction digest

In a 20 μ l-reaction, 0.5 to 1 μ g of DNA were mixed to 3 to 5 units of EcoR1 (New England BioLabs) and 2 μ l of 10X buffer, and incubated at 37°C for 1 hour. The presence of insert was checked by electrophoresis on 1.5% agarose gel.

7.2. PCR on plasmid or on bacteria

Sequences of the primers:

M13 Forward (-20): 5' - GTA AAA CGA CGG CCA G - 3'

M13 Reverse: 5' - CAG GAA ACA GCT ATG AC - 3'

The 25 μ l-reaction mix was composed of:

- 1 μ l (100ng) of plasmid DNA
- 0.5 μ l of dNTPs (10mM each)
- 0.5 μ l of M13F primer (10 μ M)
- 0.5 μ l of M13R primer (10 μ M)
- 2 μ l of MgCl₂ (25mM, Applied Biosystems)
- 2.5 μ l of 10X buffer II w/o MgCl₂ (Applied Biosystems)
- 0.25 μ l of AmpliTaq DNA polymerase (5U/ μ l, Applied Biosystems)
- 17.75 μ l of H₂O

Concerning the PCR on bacteria, the protocol was the same, except for the template that was bacteria picked on a plate instead of plasmid DNA.

The cycling parameters were composed of:

an initial denaturation at 94°C for 2 minutes, followed by

- 25 cycles of denaturation at 94°C for 1 min,
- annealing at 56°C for 1 min,
- extension at 72°C for 1 min,

and a final extension of 10 min at 72°C.

The PCR products were analysed by gel electrophoresis in a 1.5% agarose gel and visualised by ethidium bromide.

8. Sequencing

The sequencing reactions were performed using ABI PRISM[®] BigDye[™] Terminator Cycle Sequencing Ready Reaction kit (Applied Biosystems).

Principle : In the Ready Reaction format, the dye terminators, deoxynucleoside triphosphates, AmpliTaq DNA Polymerase, FS, *rTth* pyrophosphatase (a component in AmpliTaq DNA Polymerase, FS), magnesium chloride, and buffer are premixed into a single tube of Ready Reaction Mix and are ready to use. These reagents are suitable for performing fluorescence-based cycle sequencing reactions.

8.1. Reaction components

- 4 µl of ABI Prism[®] BigDye[™] Terminator
- 0.5 µl of sequencing primer (10 pmol/µl)
- 500 ng of template DNA
- up to 20 µl of H₂O

In the case of plasmid DNA, the sequencing primer was the M13 Forward or M13 Reverse universal primer.

In the case of PCR products from single cell, the sequencing reaction was performed directly after gel extraction and purification, with the 5' (V) primer used to generate the PCR products.

8.2. Cycling parameters

The cycling parameters were:

- an initial denaturation at 95°C for 3 min, followed by
- 25 cycles of
 - denaturation at 95°C for 30 sec,
 - annealing at 50°C for 1 min,
 - elongation at 60°C for 3 min, and
- a final elongation at 72°C for 5 min.

8.3. Purification and precipitation of the PCR products

The PCR products were purified and precipitated by 75% isopropanol. 80µl of 75% isopropanol were added to the 20µl PCR products. In the case of the products from single cell, AutoSeq G-50 columns (Amersham) were previously used before addition of the isopropanol. After 15 min-incubation at room temperature, the samples were centrifuged at maximum speed for 20 min. The supernatants were removed and the pellets washed by 250µl of 75% isopropanol, followed by a centrifugation at maximum speed for 5 min. After removal of the supernatants, the pellets were air-dried. The DNAs were suspended into 18µl of Template Suppression Reagent (Applied Biosystems), denaturated 3 min at 95°C and placed on ice until sequencing.

The sequencing was performed on an ABI PRISM 310 Genetic Analyser (Applied Biosystems).

9. Analysis of the sequences

9.1. Databases

V_H and V_L gene sequences were analysed using the DNAsis software (Hitachi). Germline immunoglobulin V genes were identified using blast search from several databases:

- Vbase: <http://www.mrc-cpe.cam.ac.uk/DNAPLOT.php?menu=901>
- Igbblast: <http://www.ncbi.nlm.nih.gov/igblast/>
- ImMunoGeneTics database:
<http://imgt.cines.fr:8104/cgi-bin/IMGtdnap.jv?livret=0&Option=humanIg>

V BASE is a comprehensive directory of all human germline variable region sequences compiled from over a thousand published sequences, including those in the current releases of the Genbank and EMBL data libraries. The database has been developed over several years at the MRC Centre for Protein Engineering (Cambridge, UK) as an extension of their work on the sequencing and mapping of human antibody genes.

IgBLAST was developed at NCBI to facilitate analysis of immunoglobulin sequences in GenBank. It is based on the [BLAST](#) program also developed at NCBI.

IMGT, the international ImMunoGeneTics database, was created in 1989 by Marie-Paule Lefranc (Université Montpellier II, CNRS, Montpellier, France). It is the first, and so far, the only

integrated system in immunogenetics, specialising in the Immunoglobulins (Ig), T cell receptors (TCR) and Major Histocompatibility Complex (MHC) molecules of the immune system of human and other vertebrate species. The IMGT server provides a common data access to all immunogenetics data.

9.2. Sequence analysis

Three regions of particular variability are identified in both heavy and light chains. They constitute the binding site for antigen and determine specificity by forming a surface complementary to the antigen. These regions are termed complementary-determining regions (CDRs). In light chains, they are located roughly from residues 24 to 34, from 50 to 56, and from 89 to 97 (Fig. 10B-C). In heavy chains, they are located from residues 31 to 35, from 50 to 65, and from 95 to 102 (Fig. 10A). The CDR3 region is the most hypervariable region since it is generated by the recombination of the different gene segments, variable (V), joining (J), and diversity (D) in the case of heavy chains. The diversity of CDR1 and CDR2 is germline encoded (V segment only). The rest of the V domain shows less variability and the regions between the hypervariable regions, which are relatively invariant, are termed framework regions (FRs).

To analyse the sequences, four parameters were taken into consideration:

1. V segment:

- determination of the V gene segment
- mutations: determination by comparing the germline sequence, location
- exonuclease activity: number of nucleotides removed at the 3' end of the V segment
- size of the V segment

2. J segment:

- determination of the J gene segment
- exonuclease activity: number of nucleotides removed at the 5' end of the J segment

3. D segment (in the case of heavy chain only):

- determination of the D segment
- determination of the reading frame
- size of the D segment

4. CDR3 region:

- CDR3 length
- determination is the rearrangement is productive or not (stop codon or out of frame rearrangement)
- determination of n or p nucleotides

Examples of sequences for heavy and light chains are shown in figures 10A-C.

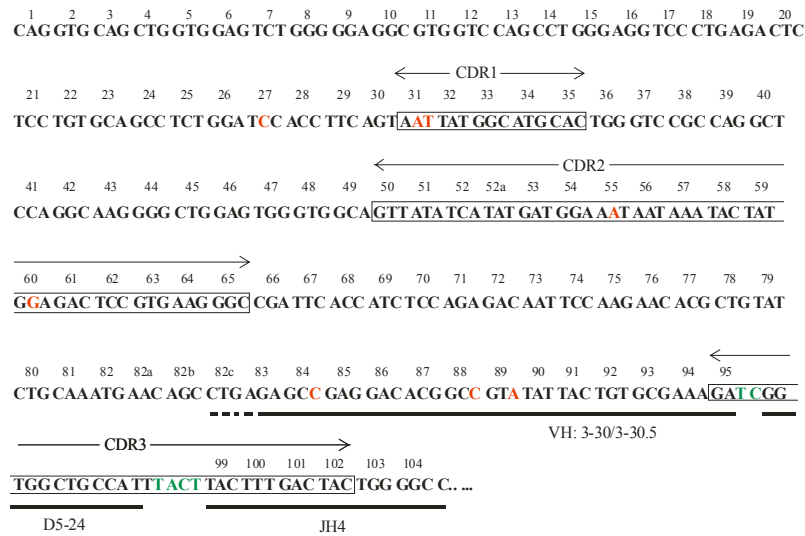


Fig. 10A. Heavy chain sequence. CDRs are shown in boxes. The number of residues is indicated. Mutations are represented in red. N nucleotides are in green.

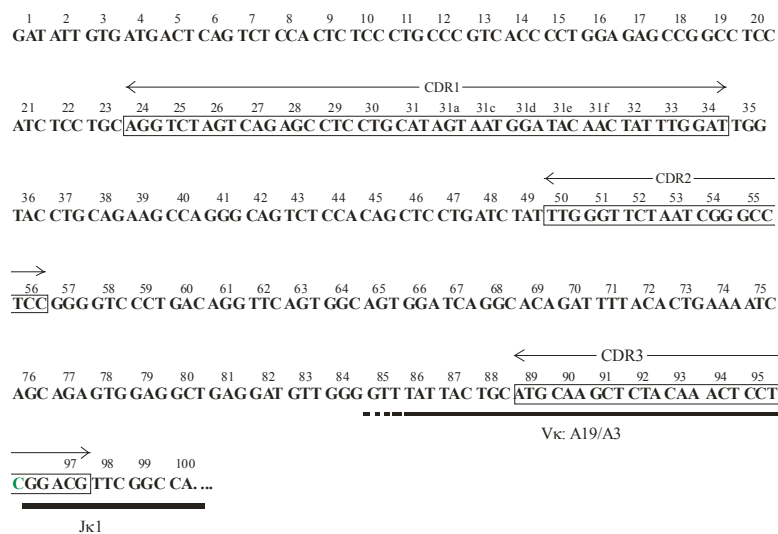


Fig. 10B. κ light chain.

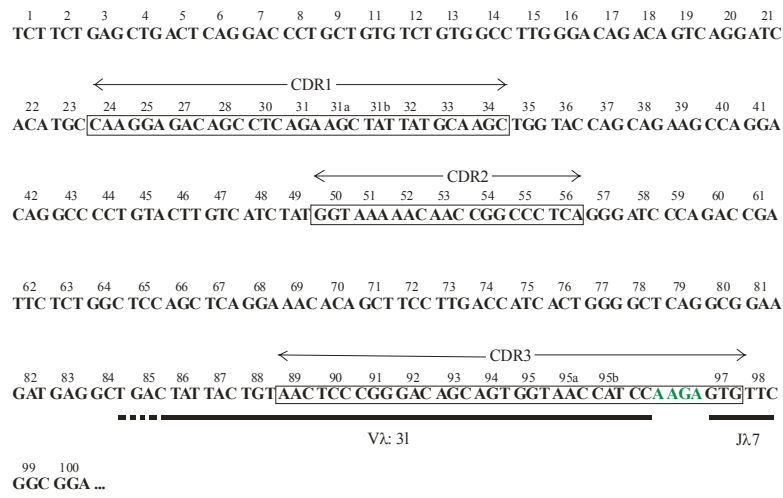


Fig. 10C. λ light chain.

10. Statistical analyses

Statistical analyses were performed using the GraphPad software: <http://www.graphpad.com/>.

Sequences were analysed by the Fisher's exact test to compare the differences in the distribution of particular gene segments. The average lengths of CDR3 as well as the number of nucleotides added (N nucleotides) or removed (exonuclease activity) were studied by the unpaired *t* test. The chi-square test was used to compare the mutational frequencies.

11. Materials

11.1. Buffers

TAE electrophoresis buffer (50X)	242 g Tris base
	57.1 ml glacial acetic acid
	37.2 g Na ₂ EDTA.2H ₂ O
	up to 1 l H ₂ O
6X loading dye	0.25% bromophenol blue
	0.25% xylen cyanol
	30% glycerol in water
TE (10 mM Tris, 1 mM EDTA)	100 μ l EDTA 0.5 M pH 8.0
	500 μ l Tris 1M
	up to 50 ml H ₂ O

LoTE (3 mM Tris, 0.2 mM EDTA) 20 µl EDTA 0.5 M pH 8.0
150 µl Tris 1 M
up to 50 ml H₂O

11.2. Agarose gel

1.5% Agarose UltraPure (Gibco BRL)
1X TAE
0.5 µg/ml ethidium bromide

11.3. Media

HBSS (Gibco BRL)
RPMI (Sigma)
Penicillin-streptomycin (Biochrom AG)
L-glutamine (Gibco BRL)
LB Broth Base (Gibco BRL)
LB Agar (Gibco BRL)
Kanamycin (USB Corporation)

RESULTS

1. Heavy chains

1.1. Clinical data

Figure 11 shows the clinical response of the RA patient H during two treatment periods with rituximab. A rapid B-cell depletion occurred after each therapy and lasted 7 and 10 months respectively. Before therapy, the patient had an active disease as indicated by high CRP level and DAS28 clinical activity index. The disease activity declined continuously after rituximab therapy. The patient had a good clinical response starting from 3 months and lasting over a year. About 13 months after the first therapy, a deterioration of the clinical parameters was observed. Therefore the patient received a second treatment with rituximab at 17 months. Again, he presented a clinical improvement following B-cell depletion. The arrows point out the time points where the B-cell repertoire was studied.

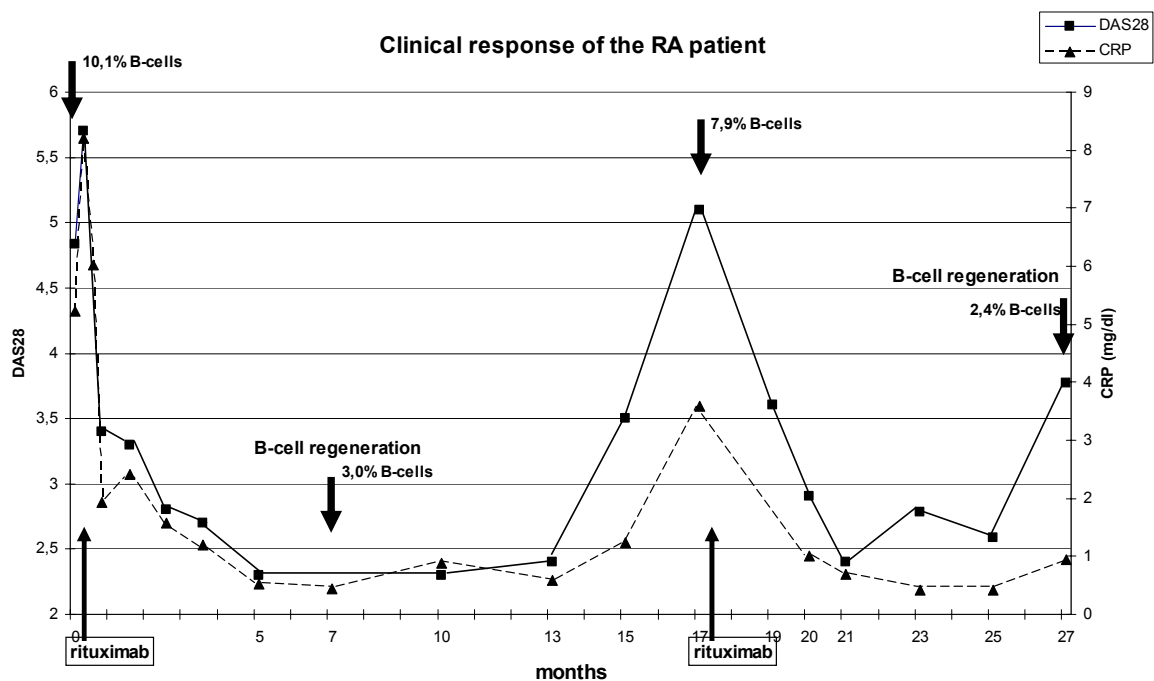


Fig. 11. DAS28 index (squares) and CRP levels (triangles) of the RA patient H who was treated twice with rituximab (at 0 and 17 months). Arrows indicate the percentage of B-cells detected in peripheral blood for the 4 time points analysed (0, 7, 17 and 27 months)

1.2. Detection of peripheral B-cells by PCR

To determine the presence of B-cells in peripheral blood, we amplified the Ig-V_H genes using genomic DNA from PBMCs at different time points as template (Fig. 12). Before therapy (time point 0), B-cells were amplified by PCR. After B-cell depletion induced by rituximab, 7 months was the earliest time point where B-cells could be detected.

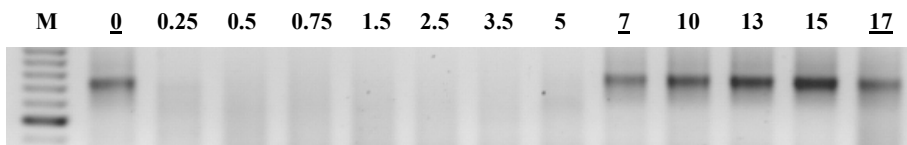


Fig. 12. Amplification of the V_H1 family at different time points (in months). The time points where the repertoire was further analysed are underlined. M, 50 bp ladder. The strongest band corresponds to 250 bp. Successful amplifications are identified as bands corresponding to a product of approximately 350 bp.

1.3. Distribution of V_H genes

Immunoglobulin V_H gene rearrangements from peripheral blood B-cells were analysed using a nested PCR approach, followed by subcloning and sequencing at the time points indicated in figure 11. A total of 687 clones was analysed: 179 clones before treatment, 199 clones during the first phase of B-cell regeneration (7 months after the first therapy), 149 clones after 17 months and 160 clones after 27 months (at the time of the second B-cell regeneration). Only the productive rearrangements were taken into consideration.

Table 4. Number of sequences analysed for each time point within every family

	Before	7 months	17 months	27 months	
V_H1	28	25	22	29	182
V_H2	22	24	15	12	73
V_H3	45	47	38	41	171
V_H4	34	38	33	40	145
V_H5	40	37	29	31	137
V_H6	9	27	8	6	50
V_H7	1	1	4	1	7
	179	199	149	160	765

V_H1 family (Fig.13A)

Before therapy, V_H1-69 and V_H1-18 were the most frequently used V_H1 family members comprising 68% of the sequences analysed in this family. Seven months after therapy, significant changes in the V_H1 distribution were observed. V_H1-02 was significantly increased and became the predominant gene (36% versus 4%; $p=0.0038$), whereas V_H1-69 was decreased (12% versus 36%; $p=0.0594$). Seventeen months after therapy (ten months after B-cell regeneration), the V_H1 gene distribution was largely comparable to that before treatment, i.e. V_H1-18 and V_H1-69 were the most often used genes. Notably, V_H1-03 was shown to be increased and was then the third most frequent gene (18%). After 27 months, the distribution of the V_H1 genes was quite stable with no significant differences to the previous time point, except for V_H1-03 that was not found anymore.

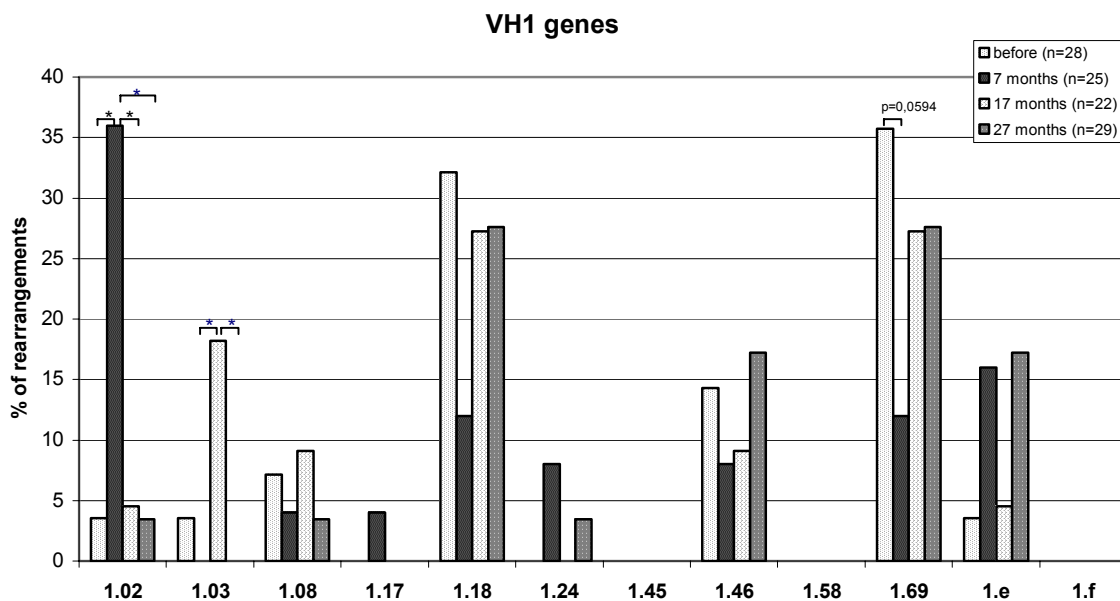


Fig. 13A. V_H1 gene distribution in peripheral blood at the different time points (0, 7, 17 and 27 months). The results are presented as the percentage of rearrangements expressing one particular gene segment within V_H1 family.

* $p < 0.05$ using Fisher's exact test

V_H2 family (Fig. 13B)

In the V_H2 family, before treatment, the gene V_H2-05 was slightly predominant. Seven months after therapy, the distribution was completely shifted toward the usage of V_H2-05 (96% versus 59%; p=0.0041), which shifted back, 10 months later, to the rearrangement frequency found before therapy. At the time point 27 months, during the second regeneration phase, the frequencies of the V_H2 genes were similar to those observed during the regeneration phase following the first treatment (7 months after therapy).

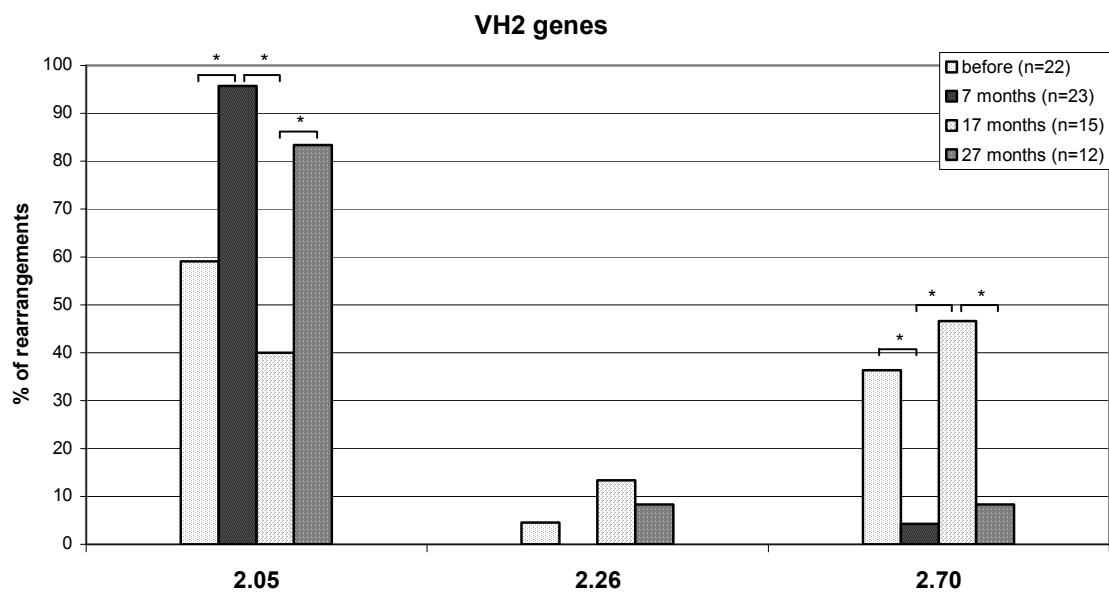


Fig. 13B. V_H2 gene distribution in peripheral blood at the different time points

V_H3 family (Fig. 13C)

The V_H3 family is the largest family comprising 22 members. Before treatment, ten family members were found, two of them accounting for 45% of all V_H3 rearrangements (V_H3-23, 29%; V_H3-30/3-30.5, 16%). Seven months after therapy, the newly regenerated B-cells used a greater variety of genes (16 different V_H3 gene segments could be observed). The overall distribution was similar to the first time point, except for V_H3-07, which was then overrepresented (15% versus 2%; $p=0.059$). Seventeen months after therapy, the gene V_H3-23 was significantly increased when compared with the previous time point (37% versus 17%; $p=0.0481$). It was the most often represented gene, followed by V_H3-09 (16% of all V_H3 rearrangements). No significant alterations in V_H3 gene distribution could be observed in the last time point, despite the tendency for V_H3-23 to decrease to its level found at the time point 7 months.

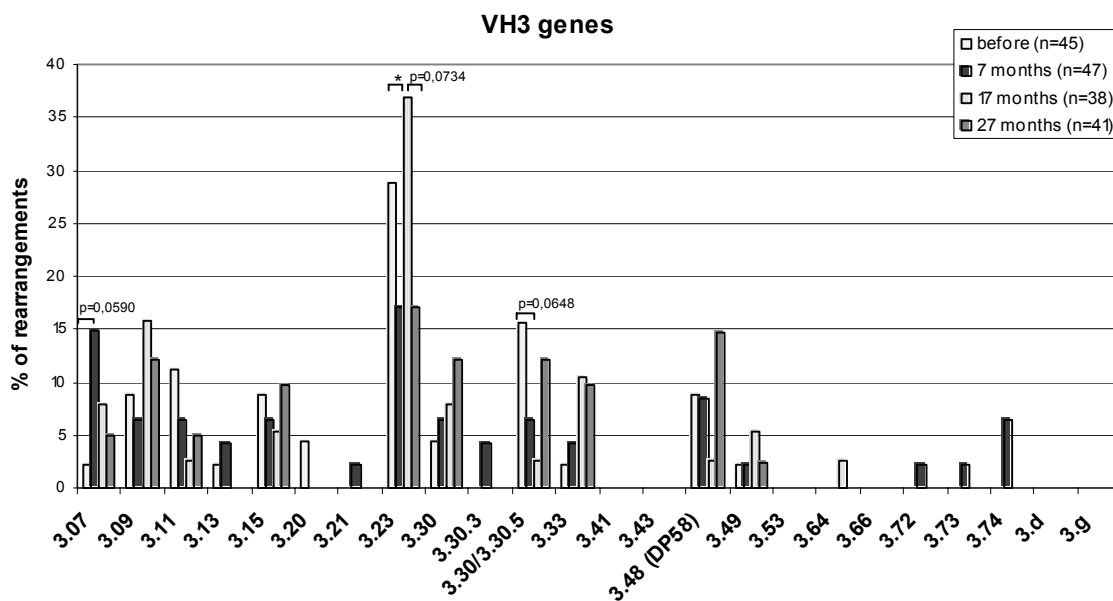


Fig. 13C. V_H3 gene distribution in peripheral blood at the different time points

V_H4 family (Fig. 13D)

In the V_H4 family, one single gene, V_H4-34, was over-expressed before therapy, accounting for more than 40% of all V_H4 rearrangements. The therapy induced some significant changes in the distribution of the V_H4 genes. The frequency of V_H4-34 decreased (16% versus 41%; p=0.0198), whereas V_H4-04 increased (21% versus 3%; p=0.0302). V_H4-59 was also shown to be increased and became the most frequently rearranged gene (39% of the V_H4 sequences after therapy). As described for the V_H3 family, there was also a greater variety of genes used in the V_H4 rearrangements after therapy. Seven different gene segments were used before treatment, whereas nine were found after. At the time point 17 months, the overall rearrangement frequency of the different genes was comparable to that observed before therapy, except for certain genes like V_H4-34 that remained at the level seen directly after therapy. Significant changes could be described between the points 7 and 17 months after therapy. An increased frequency of the genes V_H4-39 and V_H4-30.1/4-31 (18% versus 3%; p=0.0443 and 24% versus 5%; p=0.0372 respectively) was observed, as well as a decreased use of the genes V_H4-59 and V_H4-04 (12% versus 39%; p=0.0146 and 6% versus 21%; p=0.0931 respectively). This distribution was then quite stable up to 27 months in the study.

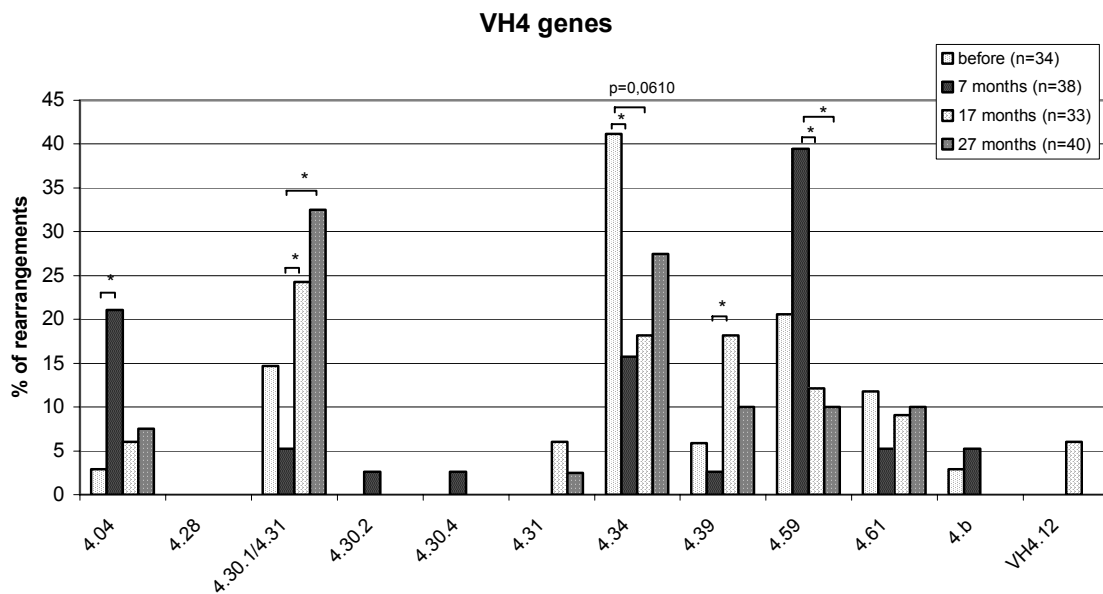


Fig. 13D. V_H4 gene distribution in peripheral blood at the different time points

V_H5 family (Fig. 13E)

Within the two-member V_H5 family, V_H5-51 was the predominant gene at all four time points analysed. It was significantly increased after the first therapy (86% versus 65%; p=0.036), with a further tendency to fall to the pre-treatment level.

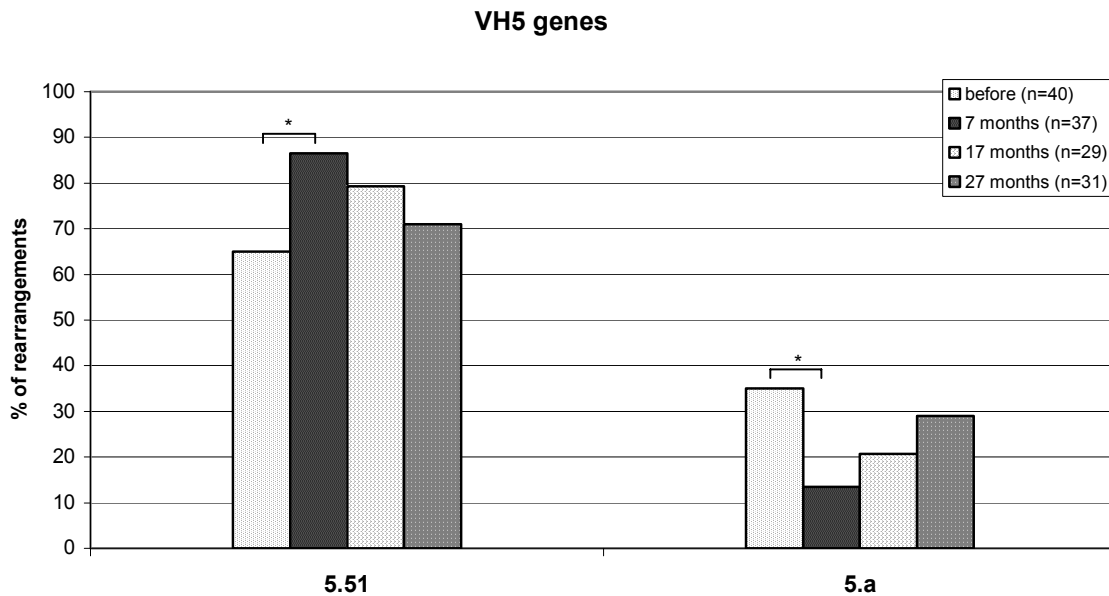


Fig. 13E. V_H5 gene distribution in peripheral blood at the different time points.

Two B-cell clones were found in the repertoire before therapy (Fig. 14 and 15). The first clone comprised 6 clonally related sequences with a number of shared mutations varying between 0 and 6. The 33-nucleotide CDR3 involved V_H5-51 rearranged to D6-6 and J_H5 (Fig. 15). The second clone consisted of 7 clonally related sequences (from which 3 were non productive – one mutation generated a stop codon). The CDR3 was 30 nucleotides long. It was composed by V_H5-a rearranged to D4-14 and J_H4 and had between 0 and 4 mutations. Both B-cell clones disappeared after the first anti-CD20 therapy (at the time point 7 months); their rearrangements were not observed anymore and no other B-cell clones could be detected during follow-up.

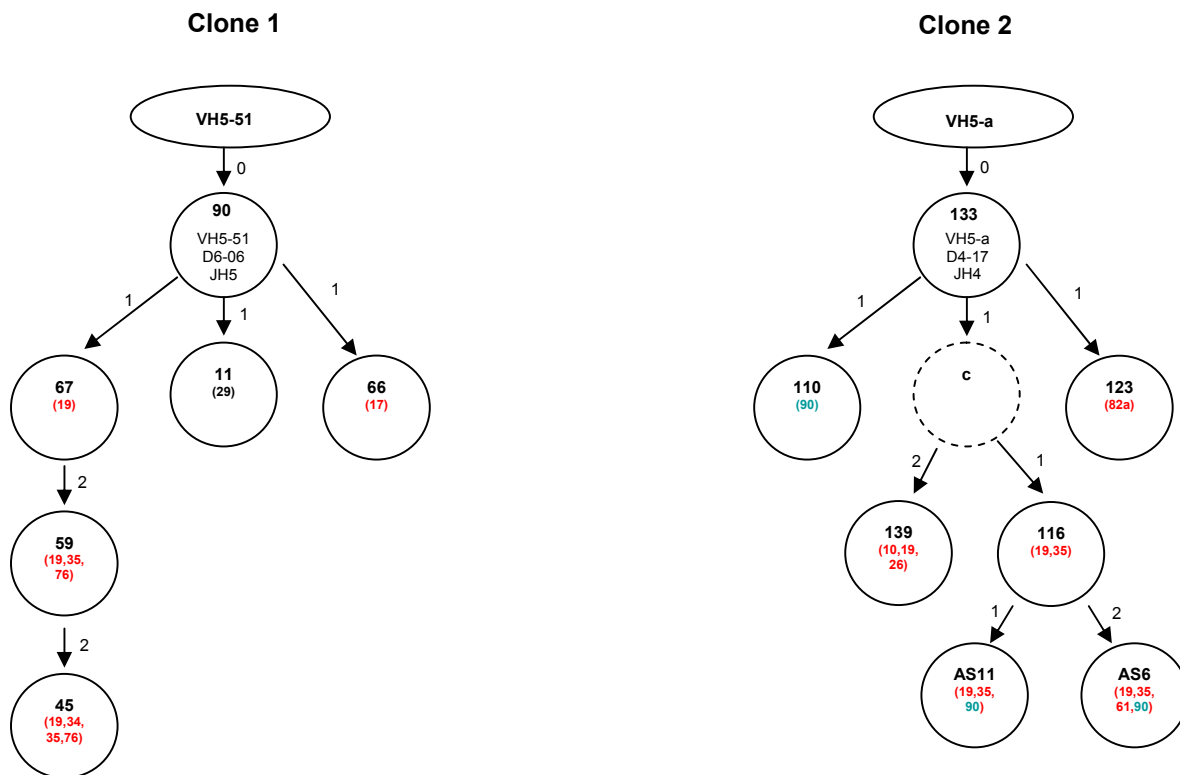


Fig. 14. Genealogical trees of B-cell clones found before therapy in V_H5 family

The best matching germline V_H gene segments are shown in the ellipses. The numbers in the circles refer to individual sequences. Deduced intermediates are shown as dotted circles. The numbers alongside the arrows represent the number of mutations between the different sequences. In brackets: mutated codons. In red: replacement mutations. In green: mutation to stop codon.

		1	2	3	4	5	6	7	8	9	10	11	12	13	14	15	16	17			
5.51 DP-73		GAG	GTG	CAG	CTG	GTG	CAG	TCT	GGA	GCA	GAG	GTG	AAA	AAG	CCC	GGG	GAG	TCT			
90		ATT	CAG	C--	----	----	----	----	----	----	----	----	----	----	----	----	----	----			
66		ATT	CAG	C--	----	----	----	----	----	----	----	----	----	----	----	----	----	C--			
11		ATT	CAG	C--	----	----	----	----	----	----	----	----	----	----	----	----	----	----			
67		ATT	CAG	C--	----	----	----	----	----	----	----	----	----	----	----	----	----	----			
59		ATT	CAG	C--	----	----	----	----	----	----	----	----	----	----	----	----	----	----			
45		ATT	CAG	C--	----	----	----	----	----	----	----	----	----	----	----	----	----	----			
		18	19	20	21	22	23	24	25	26	27	28	29	30	31	32	33	34	35	36	
		CTG	AAG	ATC	TCC	TGT	AAG	GGT	TCT	GGA	TAC	AGC	TTT	ACC	AGC	TAC	TGG	ATC	GGC	TGG	
90		----	----	----	----	----	----	----	----	----	----	----	----	----	----	----	----	----	----	----	
66		----	----	----	----	----	----	----	----	----	----	----	----	----	----	----	----	----	----	----	
11		----	----	----	----	----	----	----	----	----	----	----	----	----	----	----	----	----	----	----	
67		----	----	----	----	----	----	----	----	----	----	----	----	----	----	----	----	----	----	----	
59		----	-G-	----	----	----	----	----	----	----	----	----	----	----	----	----	----	----	----	----	
45		----	-G-	----	----	----	----	----	----	----	----	----	----	----	----	----	----	----	----	----	
		37	38	39	40	41	42	43	44	45	46	47	48	49	50	51	52	52a	53	54	
		GTG	CGC	CAG	ATG	CCC	GGG	AAA	GGC	CTG	GAG	TGG	ATG	GGG	ATC	ATC	TAT	CCT	GGT	GAC	
90		----	----	----	----	----	----	----	----	----	----	----	----	----	----	----	----	----	----	----	
66		----	----	----	----	----	----	----	----	----	----	----	----	----	----	----	----	----	----	----	
11		----	----	----	----	----	----	----	----	----	----	----	----	----	----	----	----	----	----	----	
67		----	----	----	----	----	----	----	----	----	----	----	----	----	----	----	----	----	----	----	
59		----	----	----	----	----	----	----	----	----	----	----	----	----	----	----	----	----	----	----	
45		----	----	----	----	----	----	----	----	----	----	----	----	----	----	----	----	----	----	----	
		55	56	57	58	59	60	61	62	63	64	65	66	67	68	69	70	71	72	73	
		TCT	GAT	ACC	AGA	TAC	AGC	CCG	TCC	TTC	CAA	GGC	CAG	GTC	ACC	ATC	TCA	GCC	GAC	AAG	
90		----	----	----	----	----	----	----	----	----	----	----	----	----	----	----	----	----	----	----	
66		----	----	----	----	----	----	----	----	----	----	----	----	----	----	----	----	----	----	----	
11		----	----	----	----	----	----	----	----	----	----	----	----	----	----	----	----	----	----	----	
67		----	----	----	----	----	----	----	----	----	----	----	----	----	----	----	----	----	----	----	
59		----	----	----	----	----	----	----	----	----	----	----	----	----	----	----	----	----	----	----	
45		----	----	GT-	----	----	----	----	----	----	----	----	----	----	----	----	----	----	----	----	
		74	75	76	77	78	79	80	81	82	82a	82b	82c	83	84	85	86	87	88	89	
		TCC	ATC	AGC	ACC	GCC	TAC	CTG	CAG	TGG	AGC	AGC	CTG	AAG	GCC	TCG	GAC	ACC	GCC	ATG	
90		----	----	----	----	----	----	----	----	----	----	----	----	----	----	----	----	----	----	----	
66		----	----	----	----	----	----	----	----	----	----	----	----	----	----	----	----	----	----	----	
11		----	----	----	----	----	----	----	----	----	----	----	----	----	----	----	----	----	----	----	
67		----	----	----	----	----	----	----	----	----	----	----	----	----	----	----	----	----	----	----	
59		----	----	-A-	----	----	----	----	----	----	----	----	----	----	----	----	----	----	----	----	
45		----	----	-A-	----	----	----	----	----	----	----	----	----	----	----	----	----	----	----	----	
		90	91	92	93	94	95	<u>D6.06</u>					<u>JH5b</u>								
		TAT	TAC	TGT	GCG	AGA	CAT	GAG	CCA	<u>GAT</u>	<u>AGC</u>	<u>AGC</u>	<u>TTT</u>	<u>GTG</u>	<u>TTC</u>	<u>GAC</u>	<u>CCC</u>	<u>TGG</u>	<u>GGC</u>	<u>CAG</u>	
90		----	----	----	----	----	----	----	----	----	----	----	----	----	----	----	----	----	----	----	----
66		----	----	----	----	----	----	----	----	----	----	----	----	----	----	----	----	----	----	----	----
11		----	----	----	----	----	----	----	----	----	----	----	----	----	----	----	----	----	----	----	----
67		----	----	----	----	----	----	----	----	----	----	----	----	----	----	----	----	----	----	----	----
59		----	----	----	----	----	----	----	----	----	----	----	----	----	----	----	----	----	----	----	----
45		----	----	----	----	----	----	----	----	----	----	----	----	----	----	----	----	----	----	----	----

Fig. 15. Complete nucleotide sequences of the clone 1 in comparison with the germline genes V_H5-51, D6-06 and J_H5 (underlined). The amino acid positions are marked and the CDRs are shown in dark blue. Dashes indicate identity to the corresponding character on top. Mutations are shown, in red for replacement, in dark for silent.

1.4. Use of D segments

In 83% of all rearrangements, a D segment could be assigned (87% before and 17 months after therapy, 71% 7 months after therapy, 86% 27 months after therapy). All D gene families could be detected in the sequences analysed. The majority of rearrangements (80%) contained 1 D segment, whereas a minority of sequences (1%) had 2 D segments (data not shown). Before treatment, the 4-member D1 family was under-represented compared with its representation in the genome (3% versus 16% expected). On the contrary, the D6 family that comprises only three members was over-represented (31% versus 15%). After therapy, a significant increase of the D1 family members was observed, bringing the frequency to its expected level. Its use decreased continuously until 27 months. In parallel, D3 became the most frequently used family starting from 17 months after therapy (Fig. 16).

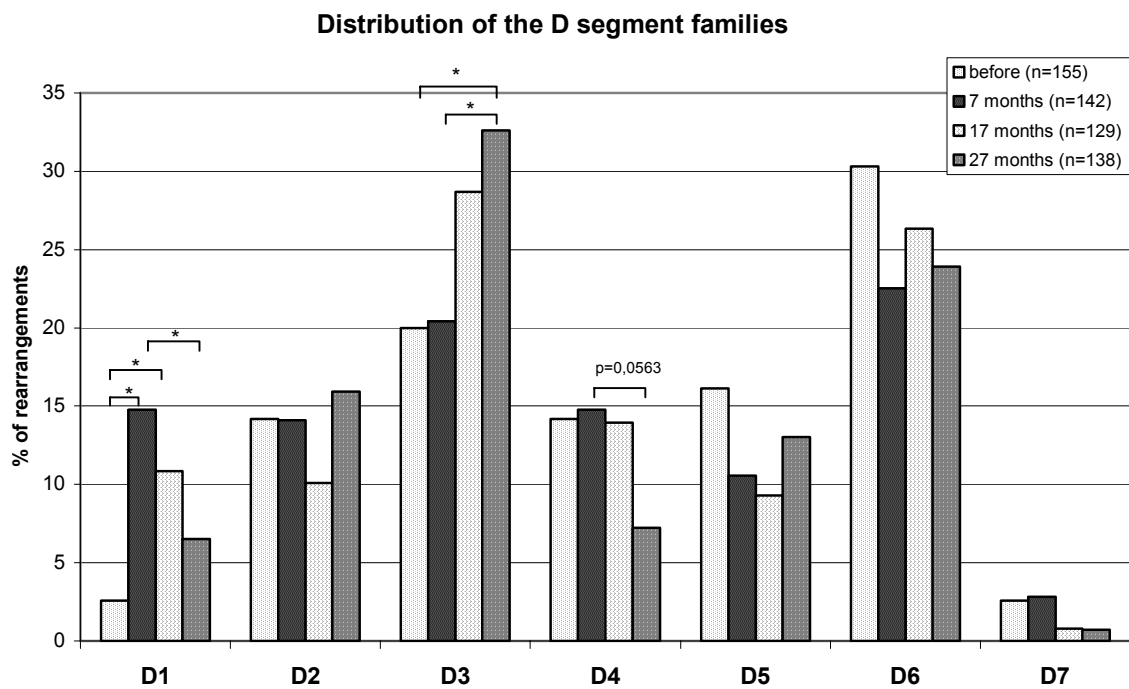


Fig. 16. Distribution of the D segment families at the different time points (0, 7, 17 and 27 months).

* $p < 0.05$ using Fisher's exact test

1.5. Distribution of J_H gene segments

The analysis of the J_H segments indicated that the overall distribution of these components did not vary with the treatment (Fig. 17). J_H4 was represented most frequently (accounting for 50% or more of all rearrangements), followed by J_H6 (between 20 and 30% of all rearrangements). The other genes were less frequently used. After the first B-cell depletion, a significant reduction of the J_H6 use (20% versus 30%; p=0.0223) as well as a significant increase of J_H2 (7% versus 1%; p=0.0069) were observed. The rearrangement frequency of these two gene segments returned to the pre-treatment level at 17 months. In the other families no significant changes were observed.

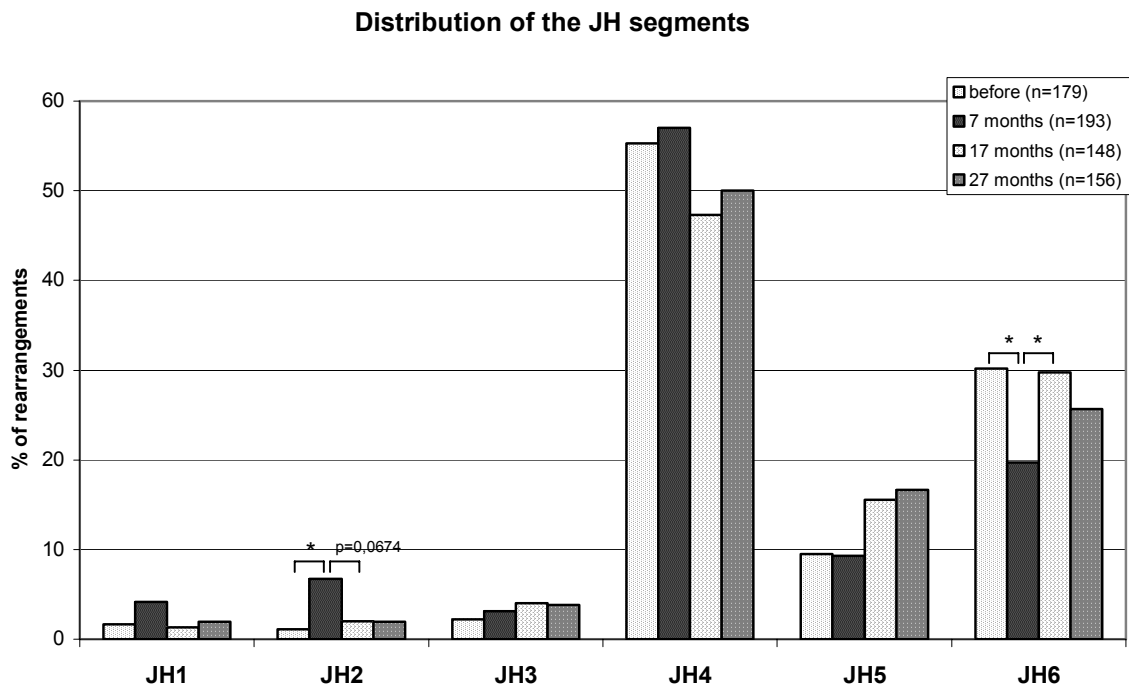


Fig. 17. Distribution of the J_H gene segments at the different time points (0, 7, 17 and 27 months). The results are presented as the percentage of rearrangements expressing one J_H gene segment.

* p<0.05 using Fisher's exact test

1.6. CDR3 length

The CDR3 length was calculated by determining the number of nucleotides from residues 95 through 102. Before therapy, the average length of CDR3 was 38.0 nucleotides (± 11.0), ranging from 9 to 75 nucleotides (Fig. 18). After the first anti-CD20 treatment (7 months after therapy), it was 36.9 nucleotides (± 9.4), ranging from 15 to 69, 17 months after therapy it was 42.6 nucleotides (± 12.1), ranging from 15 to 78 nucleotides and at the time point 27 months it was 42.3 nucleotides (± 10.7), ranging from 18 to 75 nucleotides. Before therapy, the mean size of CDR3 in V_H5 family was significantly lower compared to the other families. Just after the first B-cell regeneration (7 months after therapy), the general tendency was a decrease of the CDR3 size, except for the V_H5 family where it was significantly increased. When the data corresponding to the V_H5 family were excluded, we observed an overall decrease of the mean size of CDR3 (36.9 ± 9.4 versus 39.3 ± 11.9 ; $p=0.0414$). Twenty seven months after therapy, the CDR3 lengths were comparable to those described at the time point 17 months.

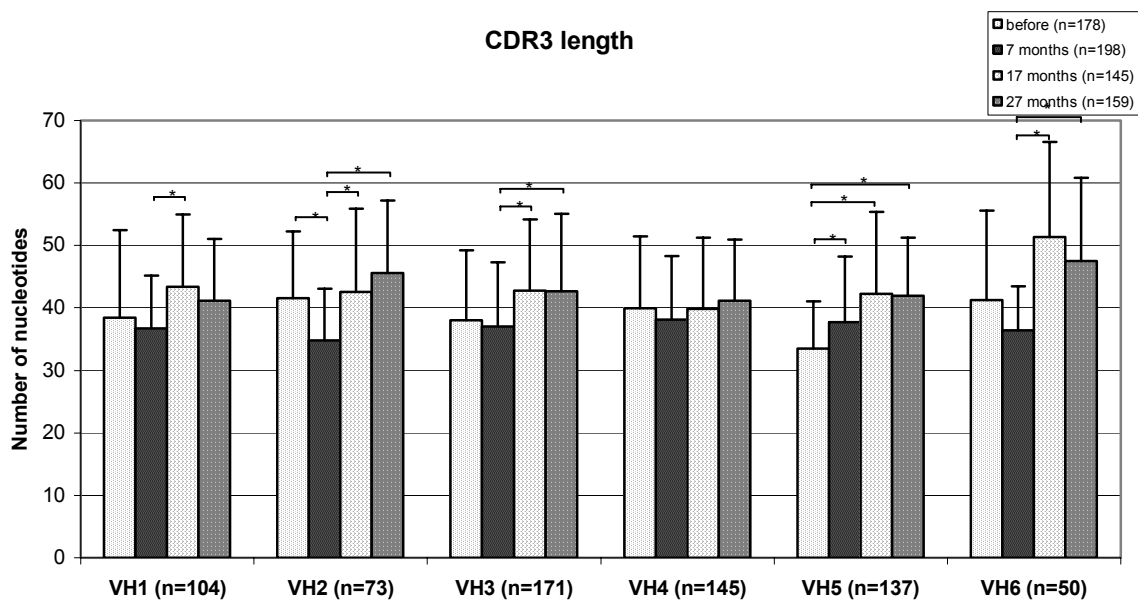


Fig. 18. CDR3 lengths of the rearrangements at the four time points. The average of CDR3 lengths (in nucleotides) is presented for each family.

* $p < 0.05$ using unpaired t test

1.7. Mutational frequencies in V_H rearrangements

1.7.1. Overall mutational frequencies of V_H rearrangements amplified by PCR from bulk DNA

Figure 19 shows the mutational frequencies in V_H rearrangements at the four time points for each family. At the beginning of the study, the overall mutational frequency in the V_H genes was 1.4% (681 mutations/48,891 bp). The mutational frequencies varied from 9 mutations/2,448 bp (0.4%) for the V_H6 family to 278 mutations/12,390 bp (2.2%) for the V_H3 family. During the first B-cell regeneration phase (7 months after therapy), the mutational frequencies varied from 383 mutations/6,940 bp (5.5%) for the V_H2 family to 638 mutations/6,542 bp (9.8%) for the V_H1 family. The overall mutational frequency was highly and significantly increased at this time point (4,032 mutations/54,720 bp (7.4%) versus 681 mutations/48,891 bp (1.4%) before therapy; $p < 0.0001$). At the time point 17 months, the frequency of mutations was decreased to the level found before treatment (519 mutations/39,307 bp (1.4%)). The overall mutational frequency stayed in the same low range at the later time point up to 27 months (725 mutations/44,037 bp (1.6%)).

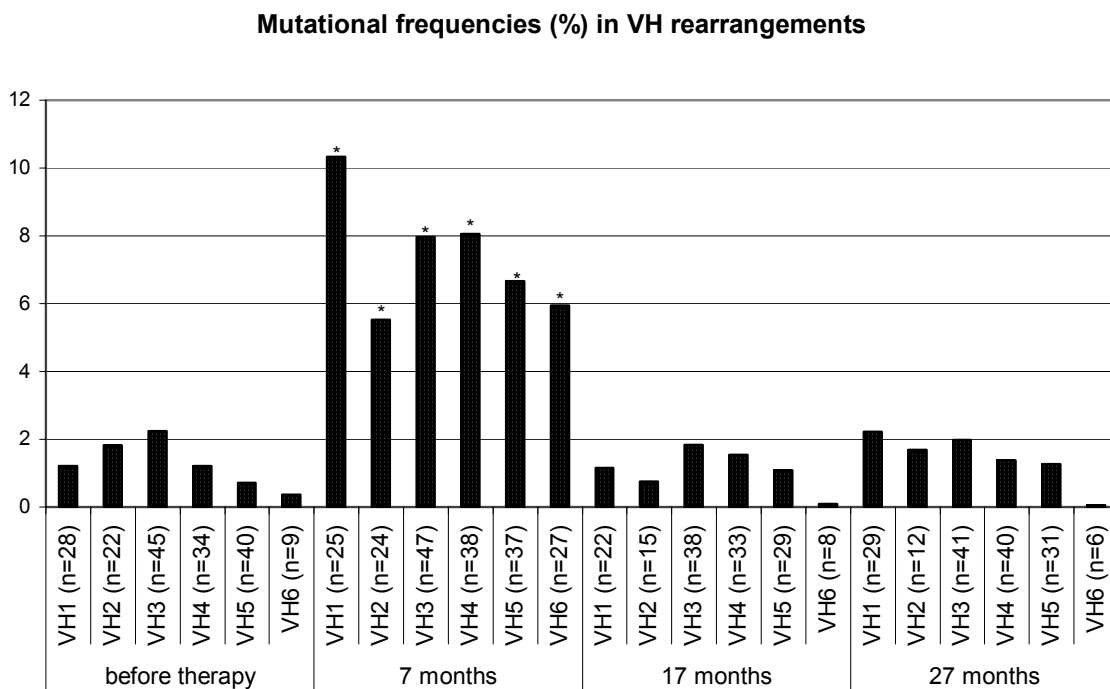


Fig. 19. Mutational frequencies in V_H rearrangements at the four time points for each family

* $p < 0.0001$ using chi-square test

Figures 20A-D represent the number of mutations per rearrangement in the different families. Before therapy (Fig. 20A), the majority of the clones (113 out of 178) contained 2 mutations or less per rearrangement and this distribution was found in all the families. At the time point 7 months (Fig. 20B), almost 90% of the sequences analysed (175 out of 198) had more than 10 mutations per sequence. All the rearrangements amplified were mutated. The time point 17 months showed the same profile as the one before therapy (Fig. 20C): 92 sequences out of 145 contained 2 mutations or less per rearrangement. Only at the time point 27 months the distribution of the mutations per rearrangement was somewhat distinct (Fig. 20D), since 24 out of 159 sequences (15.1%) contained more than 10 mutations (versus 10.1% and 9.7%; before and 17 months after therapy, respectively).

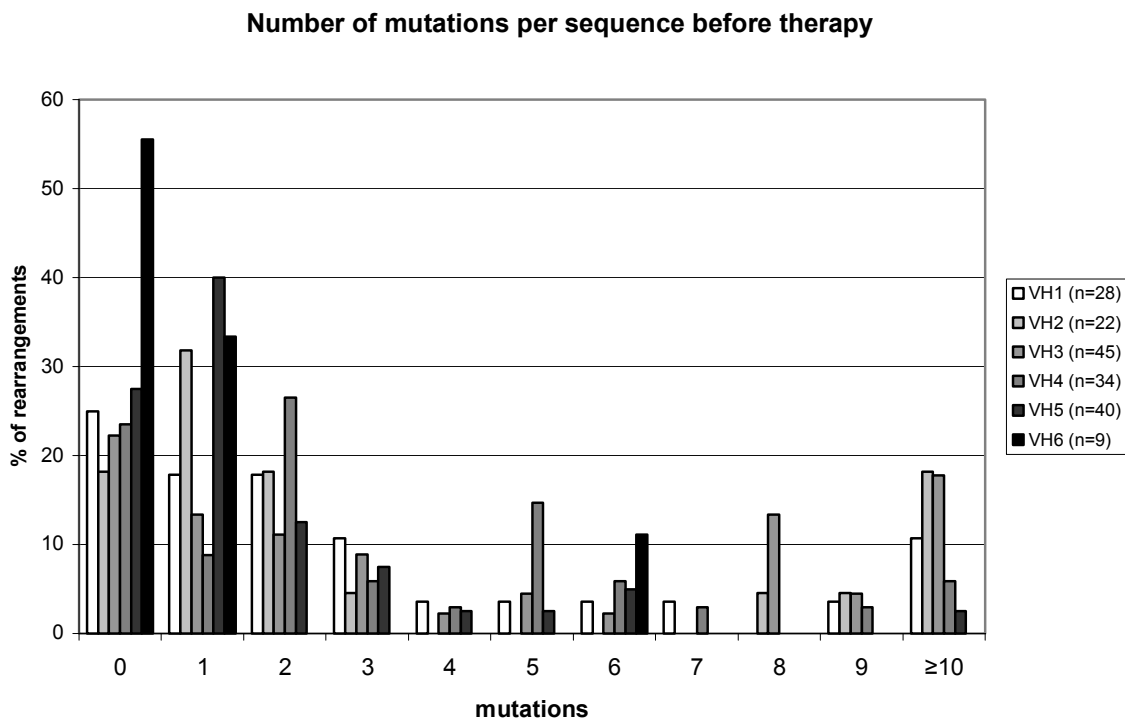


Fig. 20A. Number of mutations per sequence before therapy

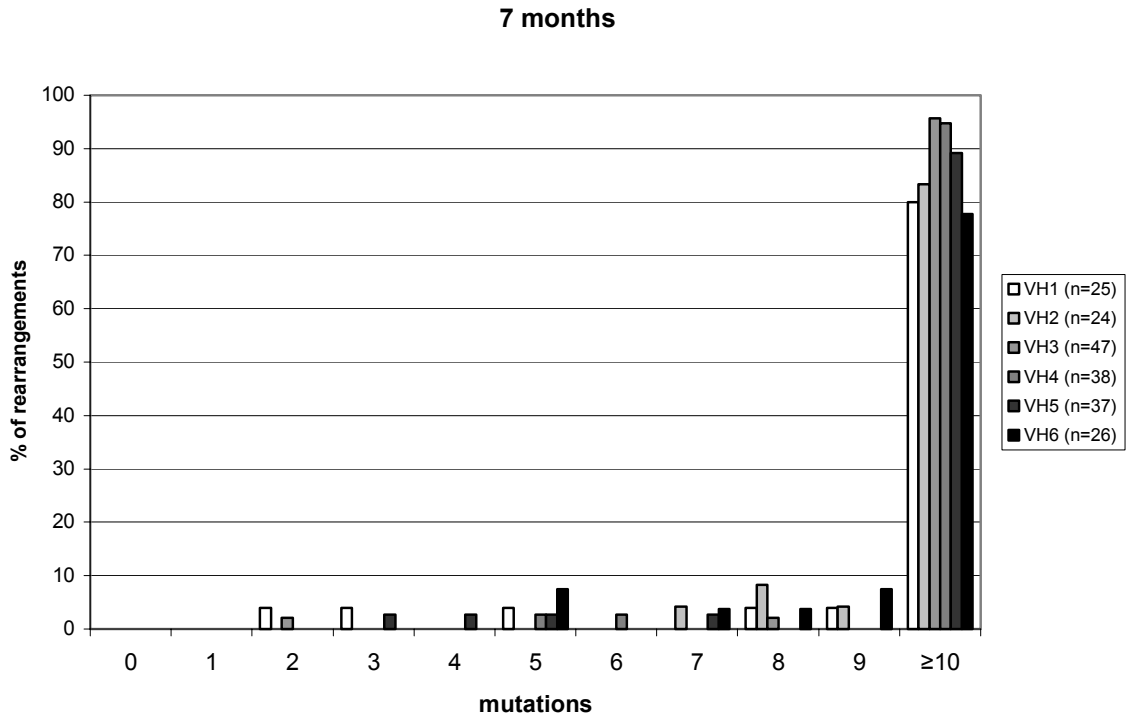


Fig. 20B. Number of mutations per sequence 7 months after therapy

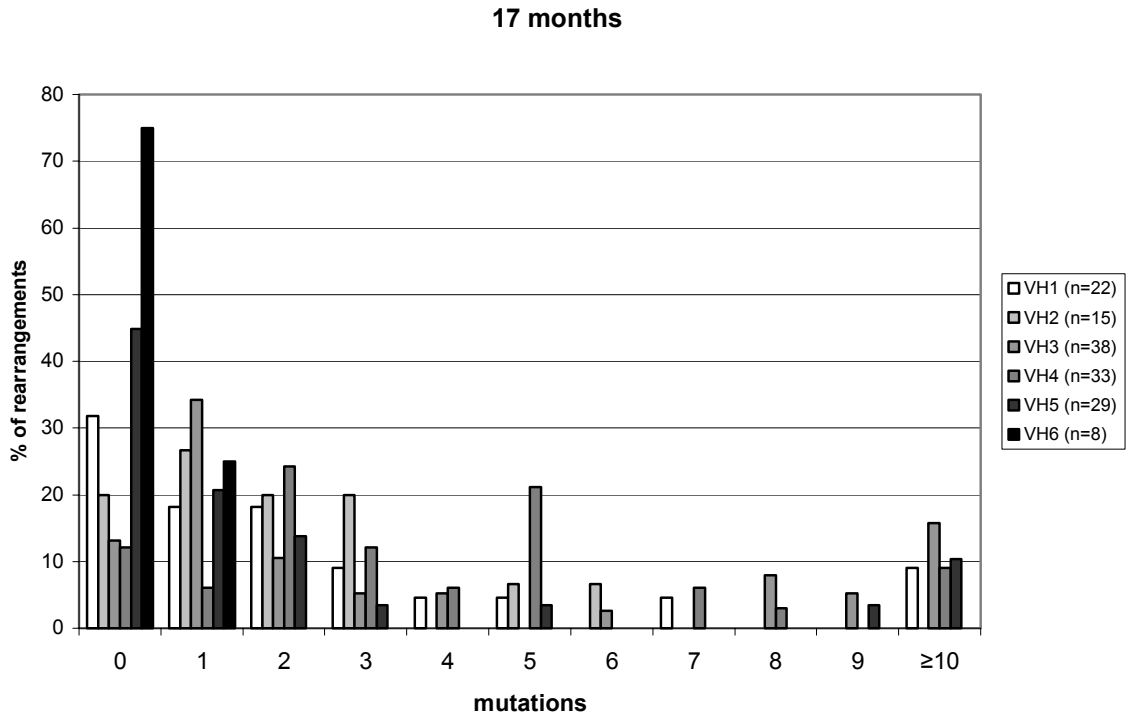


Fig. 20C. Number of mutations per sequence 17 months after therapy

27 months

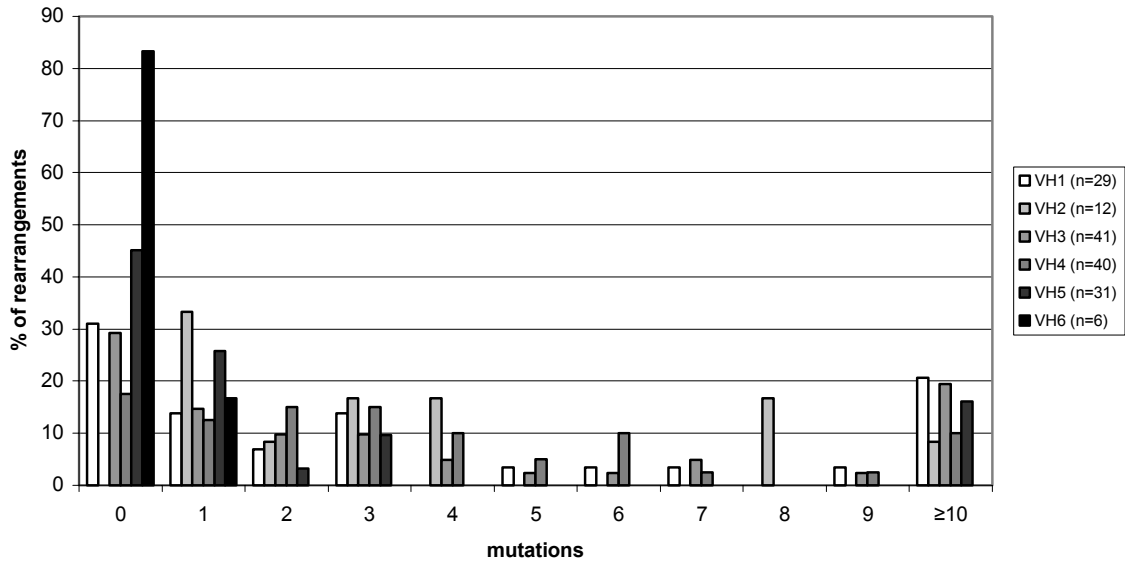


Fig. 20D. Number of mutations per sequence 27 months after therapy

1.7.2. Overall mutational frequencies of V_H rearrangements amplified by PCR from single CD19+ cells

In order to substantiate the unexpected high mutation rate 7 months after the first B-cell depletion, PBMCs were sorted in single CD19+ cells, which were either CD27 positive or negative. This different approach also revealed very high mutational frequencies in both B-cell populations (Table 5). The overall mutational frequencies of CD19+ CD27- single cells were 0.62 and 5.31%, before and 7 months after therapy, respectively. The mutational frequency of CD19+ CD27+ single cells was 8.30% 7 months after therapy.

Table 5. Comparison of the overall mutational frequencies of V_H rearrangements obtained from individual peripheral CD19+ (CD27- or CD27+) B-cells of the RA patient before and 7 months after therapy.

	Before therapy				7 months after therapy			
	n	mut (n)	total bp	mutational frequency (%)	n	mut (n)	total bp	mutational frequency (%)
CD19+ CD27-	18	27	4,349	0.62	15	183	3,443	5.31 *
CD19+ CD27+	not determined				22	477	5,745	8.30

* p<0.0001 versus before therapy by chi-square test.

1.7.3. Overall mutational frequencies of V_H rearrangements amplified by RT-PCR on total RNA at the time point 7 months

To determine the heavy chain class distribution, we performed RT-PCR on total RNA from the time point 7 months (Fig. 21). The IgM population was low mutated as expected (1.7%), but the IgG (9.0%) and IgA (8.9%) populations were highly mutated, in the same range as the genes amplified from genomic DNA (7.4%).

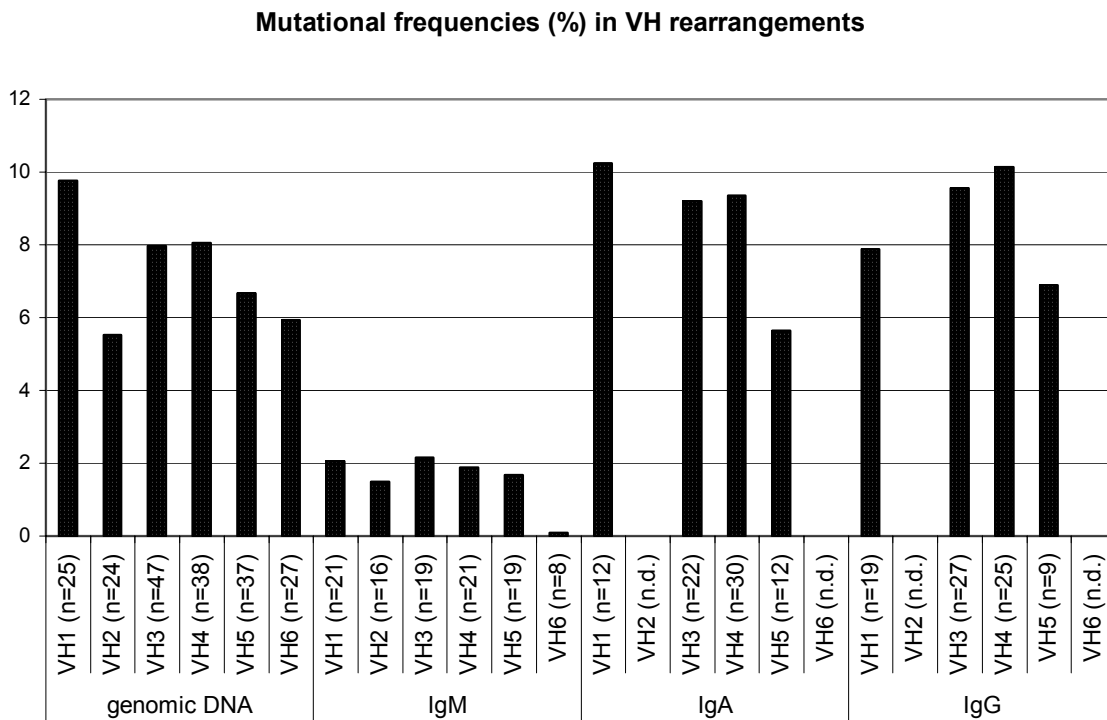


Fig. 21. Mutational frequencies in V_H rearrangements, at the time point 7 months, in total B-cells (PCR) and in IgM, IgA and IgG subpopulations (RT-PCR)

2. Light chains

2.1. Clinical data

The light chain repertoire was analysed in a second RA patient (patient L) who was also treated with rituximab. B-cell depletion occurred rapidly after the treatment and lasted approximately 10 months. Figure 22 shows the clinical data of the patient L. At the beginning of the study, the disease activity of the patient was elevated with a DAS 28 score of 5. However, serological inflammatory parameters, such as CRP, were quite low at this time. After rituximab therapy, the disease activity score (DAS28) showed a significant reduction and the CRP level stayed low. The arrows point out the time points where the B-cell repertoire was studied.

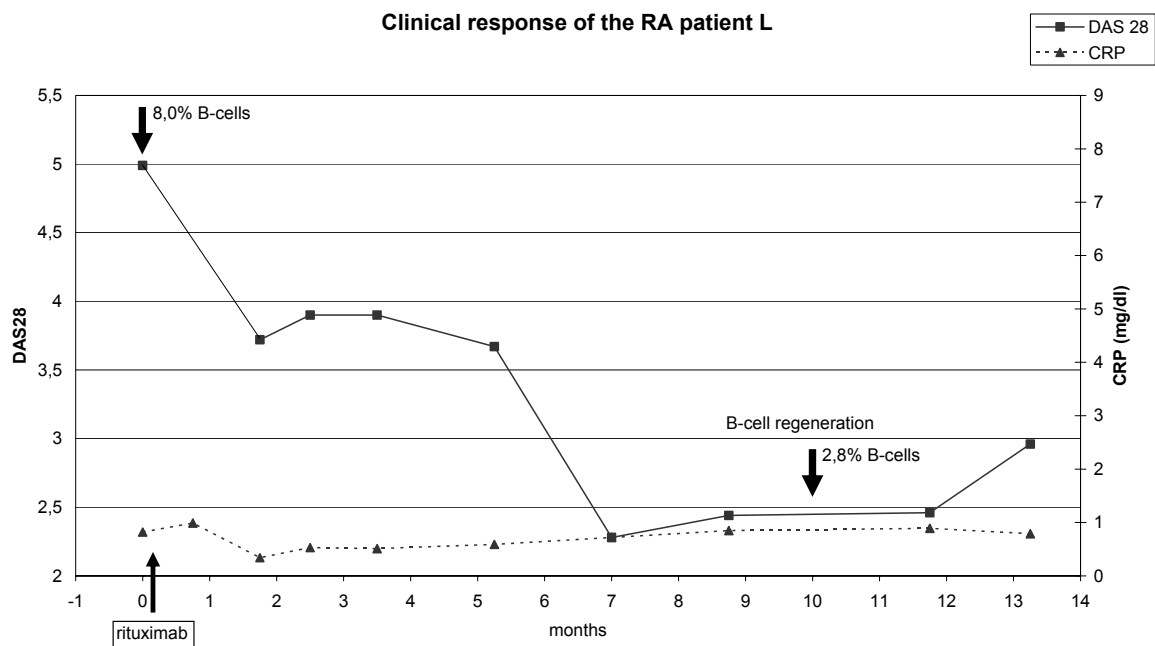


Fig. 22. DAS28 index (squares) and CRP levels (triangles) of the RA patient L who was treated by rituximab. Arrows indicate the percentage of B-cells detected in peripheral blood for the 2 time points analysed (0 and 10 months).

2.2. Amplification of light chain genes from individual B-cells

Individual CD19⁺ B-cells were sorted into CD27⁻ (naive) and CD27⁺ (memory) populations and immunoglobulin V_L gene rearrangements were analysed. 192 individual B-cells were sorted, 96 before therapy and 96 after therapy. In both cases, B-cells were separated into CD27⁻ (48 cells) and CD27⁺ (48 cells).

The majority of individual CD19⁺CD27⁻ or CD27⁺ B-cells contained either one or two rearranged light chain genes (Table 6). A rearrangement was considered productive if the VJ junction maintained the reading frame into the J segment. Rearrangements that involved pseudogenes were considered as nonproductive, as well as those that introduced stop codons and those that were rearranged out of frame. Of the 192 individual B-cells that were sorted, 97 yielded at least one productive rearranged light chain (κ or λ) genes. Before therapy, the overall efficiency was 60.4%. Ten months after therapy, it was 40.6% because of the low sorting efficiency (25.0%) for the CD27⁺ memory B-cells. This is probably due to the small percentage of this memory population in peripheral blood after B-cell regeneration.

The majority of the cells contained one productive rearrangement only: 32 out of 35 V κ genes, 22 out of 23 V λ genes, before therapy; 29 out of 30 V κ genes, 9 out of 9 V λ genes, after therapy. The other wells contained two rearrangements: 1 non productive κ and 1 productive κ or 1 non productive κ and 1 productive λ , before therapy; 2 productive κ , after therapy.

Table 6. Single-cell PCR amplification of V κ J κ and V λ J λ rearrangements from individual CD27⁻ (naive) and CD27⁺ (memory) B-cells before and after anti-CD20 antibody treatment in one RA patient

	Before			10 months after therapy		
	No. wells (%)	Naive pop (%)	Memory pop (%)	No. wells (%)	Naive pop (%)	Memory pop (%)
Total analysed	96	48	48	96	48	48
Total with rearranged VL products	63	30	33	43	29	14
Total with productive VL products	58 (60.4)	30 (62.5)	28 (58.3)	39 (40.6)	27 (56.3)	12 (25.0)
Total with p V κ	35 (60.3)	18 (60.0)	17 (60.7)	30 (76.9)	24 (88.9)	6 (50.0)
Total with p V λ	23 (39.7)	12 (40.0)	11 (39.3)	9 (23.1)	3 (11.1)	6 (50.0)
1 p κ	32	18	14	29	23	6
1 np κ	4	0	4	2	1	1
1 np κ + 1 p κ	3	0	3	0	0	0
2 p κ	0	0	0	1	1	0
1 np κ + 1 p λ	1	1	0	0	0	0
1 np κ + 1 np λ	0	0	0	1	1	0
1 p λ	22	11	11	9	3	6
1 np λ	1	0	1	1	0	1

p, productive; np, nonproductive

The percentage of wells with a productive V_L product is expressed as a function of the total number of wells analysed.

All other percentages are expressed as a function of the number of wells with productive V_L rearrangement.

2.3. Ratio κ to λ

At the beginning of the study, of the total number of wells in which at least one productive V_L rearrangement was detected (n=58), 35 (60.3%) contained one productive κ rearrangement, whereas 23 (39.7%) contained one productive λ rearrangement (Table 6). This ratio reflects the expected distribution of $V\kappa$ and $V\lambda$ chain in human B-cells (60%:40%). Ten months after therapy, the regenerated B-cells exhibited different patterns (Table 6, Fig. 23). CD27⁻ B-cells expressed mainly $V\kappa$ chain rearrangements. The distribution κ to λ was significantly different from that observed before therapy (89%:11%, p=0.0159 using Fisher's exact test). The κ : λ ratio from CD27⁻ B-cells changed from 3:2 before therapy to 9:1 after therapy. CD27⁺ B-cells also showed a changed ratio κ to λ (from 3:2 before therapy to 1:1 after therapy), but the number of rearrangements was too low to be statistically significant.

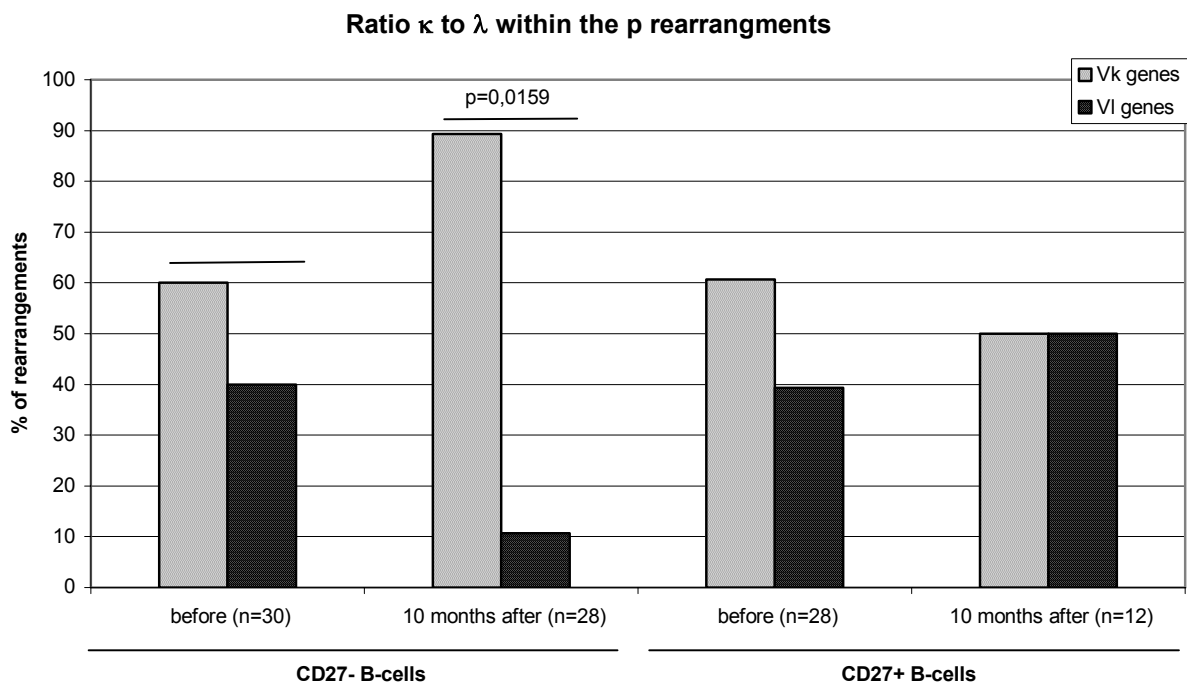


Fig. 23. Ratio of $V\kappa$ to $V\lambda$ rearrangements in naive and memory B-cells before and after anti-CD20 antibody therapy

2.4. V_L family distribution before and after therapy in naive and memory B-cells

2.4.1. V_κ family distribution

Figure 24 compares the distribution of V_κ gene families in CD27⁻ and CD27⁺ B-cells before and 10 months after anti-CD20 therapy. In both naive and memory populations, V_κ1 was the most frequently used V_κ family in the rearrangements, followed by V_κ3 and V_κ2. Naive B-cells used more V_κ3 family members than memory B-cells, whereas memory cells contained mainly V_κ1 members. The therapy did not induce any differences in the distribution of these families. This distribution is comparable to the known distribution based on the presence of the V_κ family members in the genome, and reflects the light chain repertoire reported for normal B-cells (Foster, 1997).

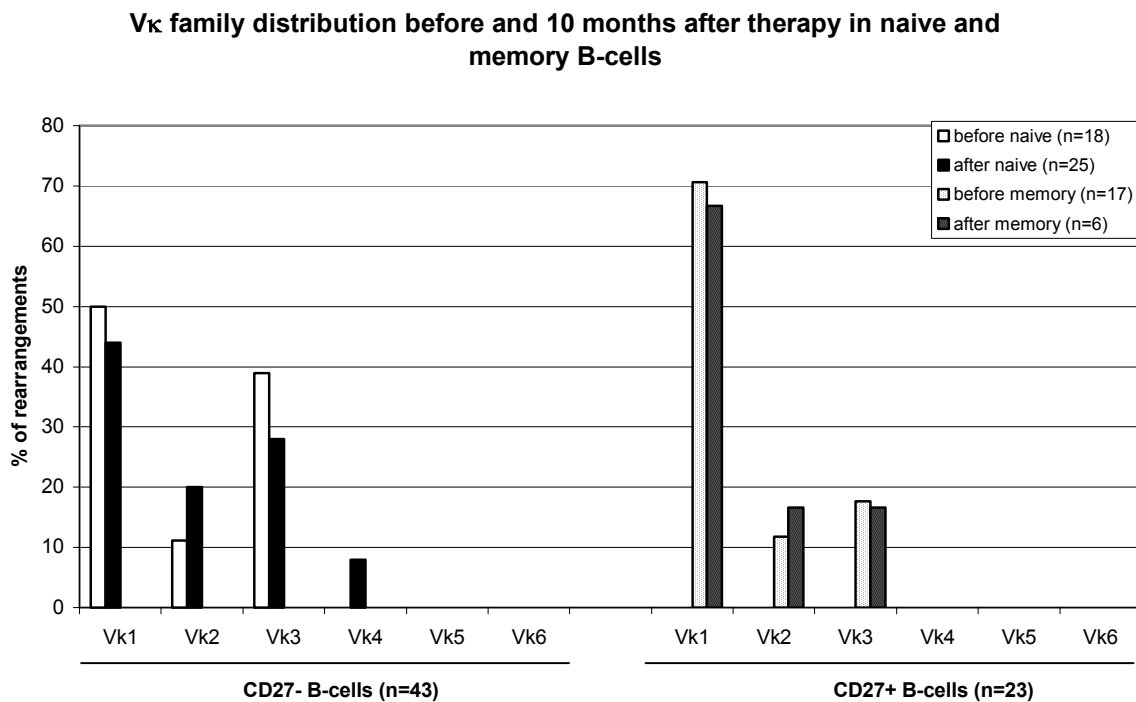


Fig. 24. V_κ family distribution before and 10 months after therapy in naive and memory B-cells

2.4.2. V λ family distribution

V λ light chains are classified into ten families according to sequence homology. Figure 25 shows the distribution of V λ gene families in CD27- and CD27+ B-cells before and 10 months after anti-CD20 therapy. Not all the V λ families were detected. In both naive and memory populations, V λ 1, V λ 2 and V λ 3 families were the most frequently used families. Although the V λ 1 family members were found in a higher proportion in CD27+ B-cells after therapy, this difference was not significant, because of the small number of rearrangements amplified. No significant differences in the distribution of the V λ families were observed before and after therapy.

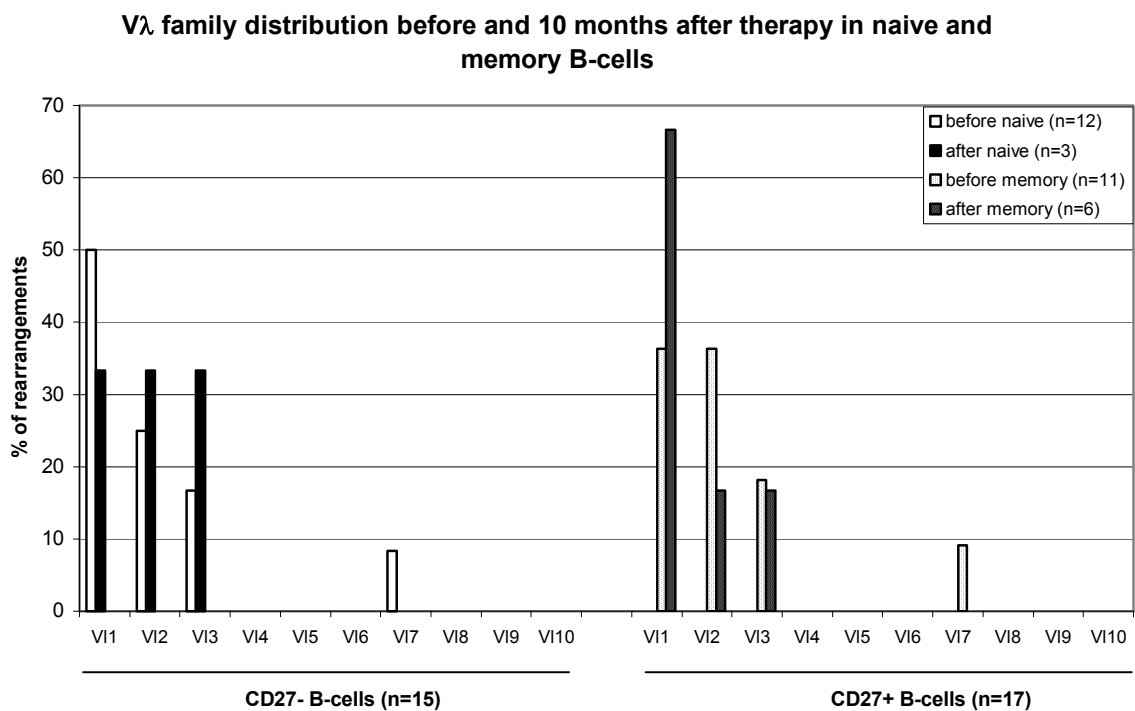


Fig. 25. V λ family distribution before and 10 months after therapy in naive and memory B-cells

2.5. V_L gene distribution before and after therapy in naive and memory B-cells

2.5.1. V_κ rearrangements

2.5.1.1. Distribution of individual V_κ genes

The distribution of individual V_κ genes before and after anti-CD20 therapy is shown in figure 26. The nine most distal V_κ genes (from A7 to L25, see also Fig. 3) are not represented on the graph because in our study no rearrangement used any of these segments. Certain genes, like L6 or L2 were found only in CD27⁻ B-cells, whereas some others, like A17 were found only in CD27⁺ B-cells. The gene L1 was observed only before therapy and the gene A20 only after therapy. The genes A27 and O12/O2 that represent 25% of the productively rearranged repertoire in healthy persons (Foster, 1997) were used in both naive and memory populations before and after therapy. No significant differences in the distribution of the V_κ segment genes were observed after therapy.

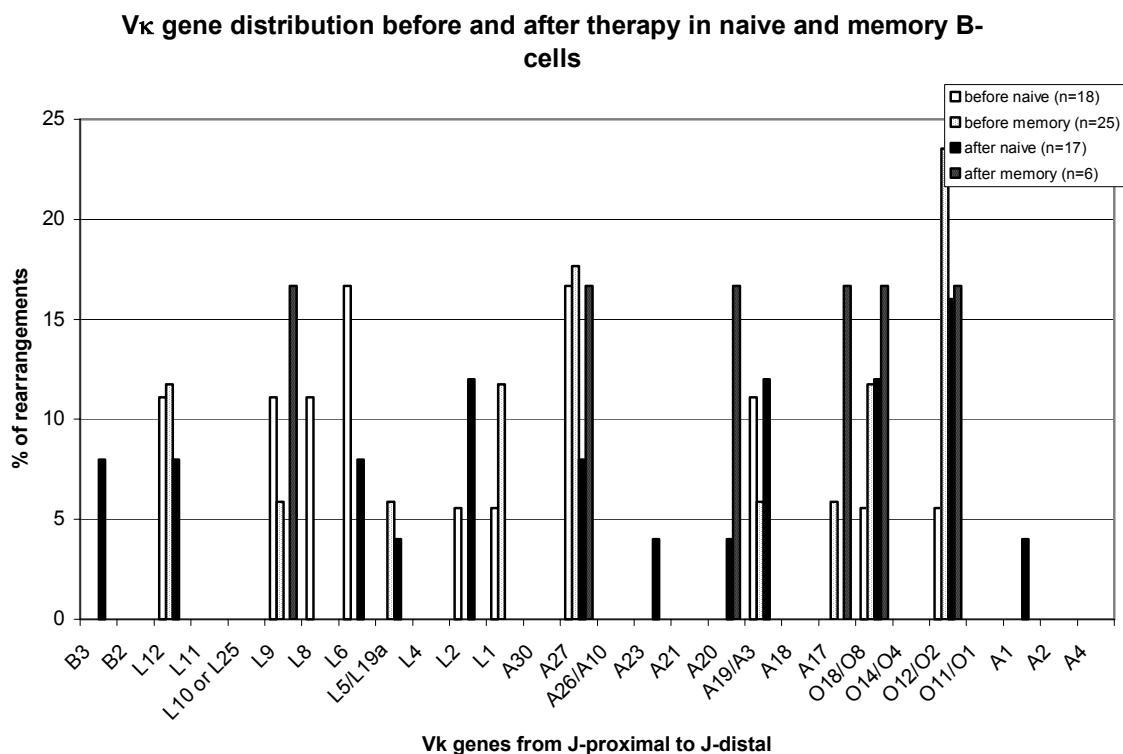


Fig. 26. V_κ gene distribution before and after therapy in naive and memory B-cells

2.5.1.2. Comparison of the usage of the J κ proximal and J κ distal cassettes

The V κ locus is divided into a proximal and a distal cassette. To gain insight into the frequency of usage of individual genes based on their location on the chromosome and their rearrangement with specific J κ segments (as an indirect evidence of receptor editing), we analysed the usage of proximal and distal V κ genes before and after therapy in naive and memory B-cells (Table 7). A18 was chosen as the border of the two cassettes, according to the study from Heimbächer (2001). Before therapy, 89% of the V κ rearrangements in the naive population used V κ genes proximal to A18, whereas they were only 59% in the memory population. This difference was almost significant ($p=0.0599$), indicating that memory B-cells used more frequently V κ distal genes. This is an indication that receptor editing took place. After therapy, the frequency of usage of proximal V κ genes in CD27 $-$ B-cells was decreased to 68%. Although the frequency fell from 89% to 68%, it was not statistically significant ($p=0.1529$). Nevertheless, the results suggests that receptor editing was higher after therapy. In CD27 $+$ B-cells, equal numbers of V κ rearrangements used distal and proximal V κ genes.

Table 7. Comparison of V κ genes proximal or distal to A18 rearranged to J κ 1-4 or J κ 5 gene elements before and 10 months after therapy in naive and memory B-cells

	before				10 months after			
	CD27 $-$		CD27 $+$		CD27 $-$		CD27 $+$	
	prox.	dist.	prox.	dist.	prox.	dist.	prox.	dist.
J κ 1-4	16	1	8	7	15	5	3	2
J κ 5	0	1	2	0	2	3	0	1
Total	18	2	10	7	17	8	3	3
	(89%)	(11%)	(59%)	(41%)	(68%)	(32%)	(50%)	(50%)

2.5.2. V λ gene distribution

The V λ genes are classified into ten families that are themselves divided into three clusters (A, B and C). Cluster A, which is J λ -proximal, contains the V λ 2 and V λ 3 families and the 4c gene from V λ 4 family; cluster B contains the V λ 1, V λ 5, V λ 7 and V λ 9 families; and cluster C, which is J λ -distal, contains the V λ 6, V λ 8 and V λ 10 families, as well as genes 4a and 4b from the V λ 4 family (Fig. 4). Cluster C is not represented in figure 27 since in our study no rearrangement used one of its genes. The frequencies of cluster A and B were comparable in all the populations before and after therapy (Table 8) and did not differ significantly from the expected distribution (cluster A: 46.7%; cluster B: 36.7%) (Farner, 1999). No significant differences in the use of V λ genes were found between naive and memory B-cells. As for V κ genes, not all the V λ genes were detected. Some genes like 3r, 2a2, 2b2, 1c, 1g and 1b were more frequently used and correspond to the genes that are found more often than expected in the productive repertoire of healthy individuals (Farner, 1999). In agreement with the same study, a number of V λ genes were not found at all (4c, 3p, 3a, 2d, 3e, 1a, 5b and 4a). On the other hand, the gene 3l, which is not found in the productive repertoire of healthy persons (Farner, 1999) was used in both naive and memory population before and after therapy in our analysis. Nevertheless, because of the small number of rearrangements, the relevance of this finding is uncertain.

Table 8. Distribution of V λ gene clusters before and 10 months after therapy in naive and memory individual B-cells

	before			10 months after		
	CD27-	CD27+	total	CD27-	CD27+	total
Cluster A	5 (42%)	6 (55%)	11 (48%)	2 (67%)	2 (33%)	4 (44%)
Cluster B	7 (58%)	5 (45%)	12 (52%)	1 (33%)	4 (67%)	5 (56%)
Cluster C	0	0	0	0	0	0
n	12	11	23	3	6	9

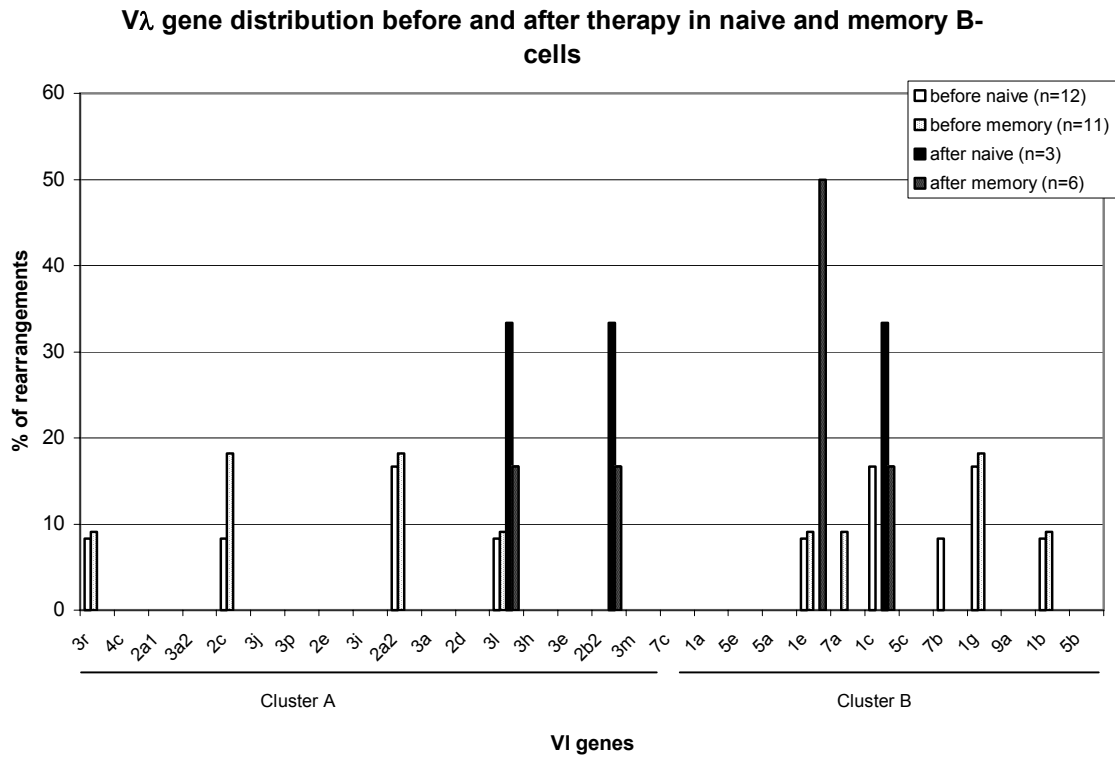


Fig. 27. V λ gene distribution before and after therapy in naive and memory B-cells

2.6. Mutational frequencies in V_L rearrangements

The overall mutational frequencies in V_L rearrangements were as expected, in that CD27⁺ B-cells were more mutated than CD27⁻ B-cells before and after therapy (Fig. 28). Compared to the V_κ rearrangements, significantly more mutations were found in the V_λ rearrangements before therapy in both naive and memory populations. In CD27⁻ B-cells, before therapy, one single V_κ rearrangement contained 17 mutations, whereas the other rearrangements (n=17) had no mutations or less than 2 mutations. The higher mutational frequency in the V_λ rearrangements in the naive population is due to three V_λ rearrangements out of 12 containing more than 6 mutations. In the naive population, the mutational frequencies decreased after therapy (0.8% versus 0.01%; p<0.0001 using chi-square test) whereas in the memory population, no statistically differences were observed.

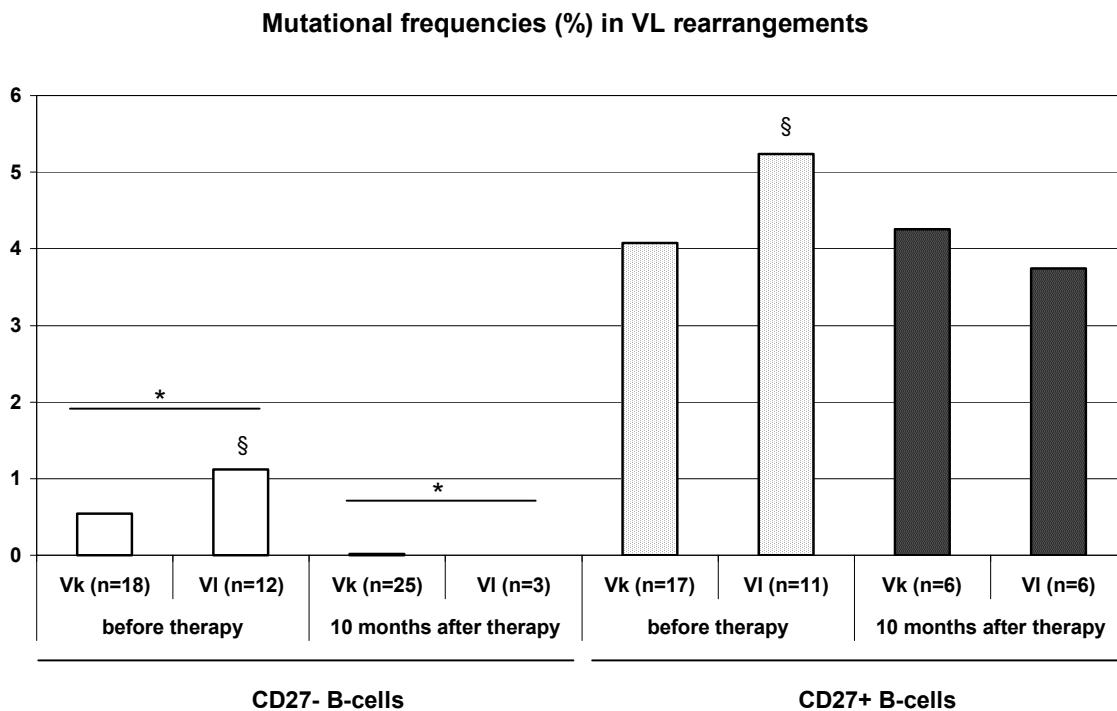


Fig. 28. Mutational frequencies (%) in V_L rearrangements

* p<0.0001 using chi-square test to compare the overall mutational frequencies before and after therapy in CD27⁻ B-cells

§ p<0.05 using chi-square test to compare the mutational frequencies in V_κ and V_λ rearrangements before therapy

2.7. J_L gene distribution before and after therapy in naive and memory B-cells

2.7.1. J_κ gene distribution

All five J_κ gene segments were found (Fig. 29). In both naive and memory populations, before and after therapy, J_κ2 was the most frequently used J_κ segment, whereas J_κ3 was found at the lowest frequency. The gene segment J_κ3 was found only after therapy, whereas J_κ4 was not detected anymore in CD27⁺ B-cells after therapy. The difference after therapy was not statistically different.

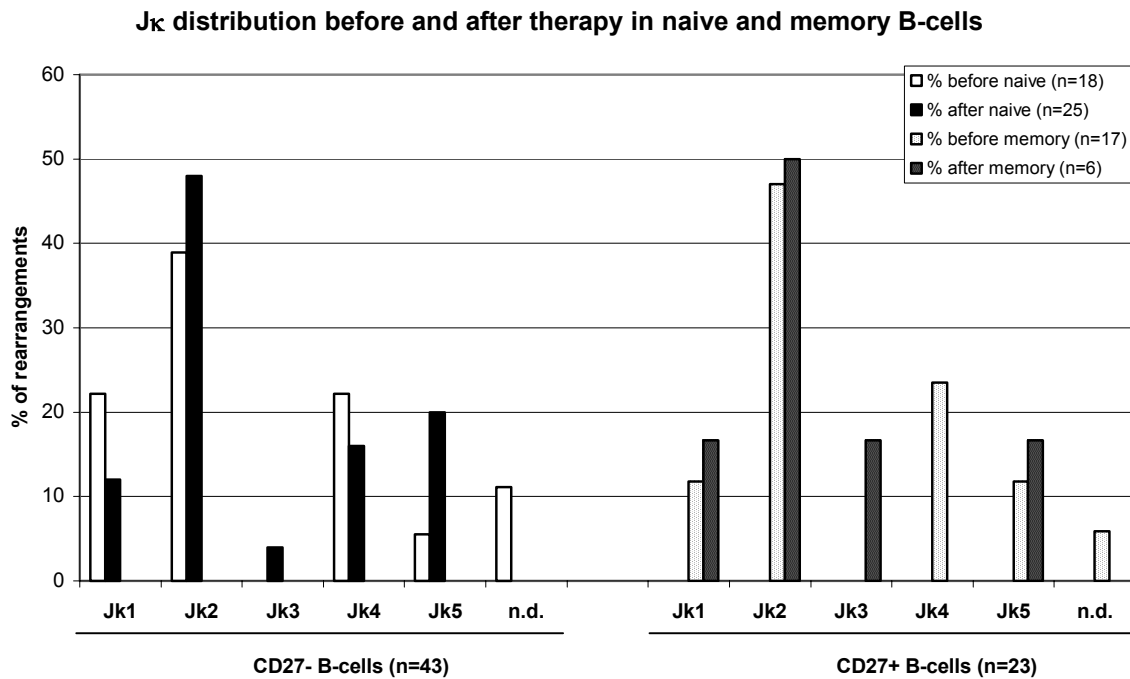


Fig. 29. J_κ distribution before and after therapy in naive and memory B-cells

2.7.2. J λ gene distribution

There are seven J λ segments, of which four (J λ 1, J λ 2, J λ 3 and J λ 7) are considered functional. All functional J λ segments were used in the V λ J λ rearrangements but not in the same populations (Fig. 30). Before therapy, the J λ 2/3 gene segments were the only J λ segments used in the rearrangements. After therapy, J λ 1 was found in CD27⁺ B-cells and J λ 7 was detected in CD27⁻ B-cells. However, these differences were not significant.

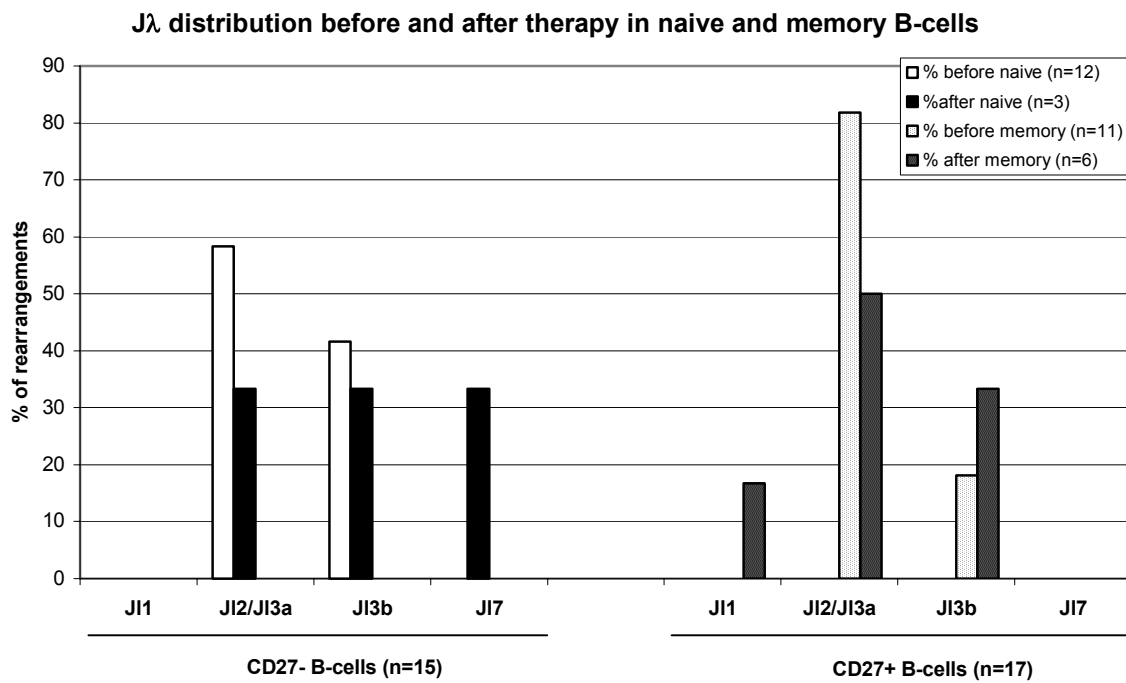


Fig. 30. J λ distribution before and after therapy in naive and memory B-cells

2.8. CDR3 lengths, N nucleotides and exonuclease activity

The sequence diversity in CDR3 is provided by the activities of exonuclease and terminal deoxyribonucleotide transferase (TdT) and by the p-nucleotides formation.

2.8.1. V κ J κ rearrangements

The CDR3 lengths in the V κ J κ rearrangements were very similar (Table 9). The means varied from 27.2 ± 1.7 nucleotides in CD27+ B-cells before therapy to 28.3 ± 2.8 nucleotides in CD27- B-cells before therapy, with a range from 18 to 39 bp. The CDR3 lengths from the naive population were a little longer than the ones from the memory population, but this difference was not significant. The CDR3 means did not differ from the published mean CDR3 length of productive rearrangements (27.2 ± 2.5) (Foster, 1997). The majority of the rearrangements had a CDR3 length of 27. Despite the nearly uniform CDR3 length of V κ J κ rearrangements, no CDR3 were identical. Evidence of N-nucleotides addition and exonuclease activity could be observed in both naive and memory B-cells before and after therapy. The majority of V κ J κ rearrangements had no N nucleotides, except before therapy in CD27- B-cells where the most frequent occurrence was the addition of two N nucleotides. The greatest number of N nucleotides detected was eight before therapy in one rearrangement from the CD27+ B-cells. This rearrangement also showed a high V κ exonuclease activity (11 nucleotides removed). No significant differences in TdT activity were noted before and after therapy, despite the fact that the CDR3 of CD27+ B-cells seemed to contain more N nucleotides compared to before therapy. Evidence of exonuclease activity was detected on both the V κ (5') and J κ (3') sides of the coding join. The most frequent occurrence on the V κ (5') side was the removal of two or three nucleotides by exonuclease. On the J κ (3') side of the join, the most frequent occurrence was removal of none or one nucleotide. No significant differences in exonuclease activity were observed between CD27- and CD27+ B-cells before and after therapy.

Table 9. Single-cell PCR amplification of VκJκ rearrangements from individual CD27- (naive) and CD27+ (memory) B-cells before and 10 months after anti-CD20 antibody treatment

	CD27- B-cells		CD27+ B-cells	
	before	10 months after	before	10 months after
n	18	25	17	6
CDR3 lengths (nucleotides)	28.3 ± 2.8	28.3 ± 2.3	27.2 ± 1.7	27.5 ± 2.3
N nucleotides	1.8 ± 1.2	1.1 ± 1.4	0.5 ± 1.9	2.0 ± 2.1
Exonuclease act. 5' side (V)	-2.4 ± 2.0	-1.6 ± 1.8	-2.8 ± 2.8	-3.3 ± 4.2
Exonuclease act. 3' side (J)	-1.2 ± 1.5 (n=17)	-1.6 ± 2.0	-0.6 ± 1.4 (n=16)	-1.7 ± 1.8

Means ± SD

2.8.2. VλJλ rearrangements

As for the VκJκ rearrangements, the CDR3 lengths in the VλJλ rearrangements were also conserved (Table 10). The length means varied from 30.5 ± 4.0 nucleotides in CD27+ B-cells before therapy to 33.5 ± 3.5 nucleotides in CD27+ B-cells after therapy, with a range from 27 to 39 bp. They did not differ from the published mean CDR3 length of productive rearrangements (30.9 ± 0.2) (Farner). Evidence of TdT activity and exonuclease activity could be observed in both naive and memory B-cells before and after therapy. The majority of VλJλ rearrangements had no N nucleotides. When TdT was active, the rearrangements contained one to four N nucleotides, except for CD27+ B-cells before therapy that contained one to nine N nucleotides. This result explains why, before therapy, by comparing the mean of N nucleotides added, we observed a significant increase of N nucleotides in CD27+ B-cells compared to CD27- B-cells (p=0.036 using impaired *t* test). Exonuclease activity was detected on both the Vλ (5') and Jλ (3') sides of the coding join. On the Vλ (5') side, a range of one to four nucleotides was removed in the majority of the rearrangements, except in the case of memory B-cells before therapy where a broader range was observed (from one to 12 nucleotides). Before therapy the exonuclease activity on Vλ was significantly higher in memory B-cells (p=0.0036 using impaired *t* test) than in naive B-cells. The CDR3 lengths were conserved because the increase of

nucleotides removed was compensated by the addition of N nucleotides. On the J λ (3') side, the majority of the rearrangements had no nucleotides removed. When the exonuclease was active, a range of one to six nucleotides was removed. No significant differences were observed in both subpopulations before and after therapy.

Table 10. Single-cell PCR amplification of V λ J λ rearrangements from individual CD27- (naive) and CD27+ (memory) B-cells before and after anti-CD20 antibody treatment

	CD27- B-cells		CD27+ B-cells	
	before	10 months after	before	10 months after
n	12	3	11	6
CDR3 lengths (nucleotides)	32.0 \pm 2.3	33.0 \pm 3.0	30.5 \pm 4.0	33.5 \pm 3.5
N nucleotides	0.7 \pm 1.2 *	1.3 \pm 2.3	3.1 \pm 3.5 *	1.5 \pm 1.5
Exonuclease act. 5' side (V)	-2.9 \pm 1.3 §	-2.3 \pm 2.1	-6.6 \pm 3.7 §	-1.5 \pm 1.9
Exonuclease act. 3' side (J)	-0.4 \pm 1.2	-1.3 \pm 2.3	-1.1 \pm 1.9	-1.3 \pm 1.4

Means \pm SD

* p=0.036 using unpaired *t* test to compare CD27- and CD27+ B-cells before therapy

§ p=0.0036 using unpaired *t* test to compare CD27- and CD27+ B-cells before therapy

DISCUSSION

Although the role of B-cells in autoimmunity is not completely understood, their importance in the pathogenesis of autoimmune diseases has been more appreciated in the past few years. It is now well known that B-cells are more than just the precursors of (auto) antibody-secreting cells (Jonsson, 2001; Lipsky, 2001; Dörner, 2003; Silverman, 2003b). They are also involved in the regulation of T-cell mediated autoimmune diseases by different mechanisms. In this regard, B-cells are very efficient antigen-presenting cells. Activated B-cells express co-stimulatory molecules, such as CD154, and by this way, contribute to the evolution of T effector cells. They can produce chemokines and cytokines, like lymphotoxin α/β , that are essential for the differentiation of follicular dendritic cells in secondary lymphoid organs and the organisation of effective lymphoid architecture.

The implication of B-cells in the pathogenesis of RA is now well established, but their precise role is still unknown. Numerous studies have shown that B-cell depletion by anti-CD20 therapy can be beneficial for patients suffering from rheumatoid arthritis (De Vita, 2002; Edwards, 2002; Gorman, 2003; Hainsworth, 2003; Oligino, 2003; Kneitz, 2004). Since there is good evidence that the B-cell repertoire is changed in autoimmune diseases, we addressed the question if it can be modulated by transient B-cell depletion. For that we decided to compare the B-cell repertoire of two RA patients before and after effective clinical B-cell depletive therapy by analysing the heavy chain immunoglobulin repertoire in the first patient (H) and the light chain immunoglobulin repertoire in the second patient (L).

1. Heavy chain repertoire

Patient H with active RA was selected for B-cell depletion using rituximab. He showed a good clinical response for over a year after antibody treatment. Eventually the disease relapsed and he got retreated with rituximab. The second B-cell depletive therapy induced again a significant clinical response lasting about 10 months.

At the beginning of the study, the Ig-V_H repertoire of patient H basically resembled the published distributions for healthy people (Brezinschek, 1995 and 1997). Nevertheless certain genes, already described with bias in autoimmune diseases, were used in a different proportion. In particular, the genes V_H1-69 and V_H4-34 were overrepresented. The V_H gene 1-69 that represented 35.7% of the rearrangements for V_H1 family in our study has been found at the frequency of 11.1% in healthy persons (Brezinschek, 1995). The gene V_H4-34 represented 41.2% of the V_H4 genes in our RA patient. Its frequency in healthy people has been described with 14.3% (Brezinschek, 1995) and 15.7% (Brezinschek, 1997). On the other hand, the gene V_H3-07 was found in a smaller proportion (2.2% of the V_H3 genes versus 7.5% (Brezinschek, 1995) and 10.8% (Brezinschek, 1997) in healthy controls). These genes have been shown to exhibit some evidence for (auto) antigen selection, for example for rheumatoid factor activity (Dörner, 2002). In particular, the gene V_H4-34 is often used by anti-DNA antibodies (Stevenson, 1993; van Vollenhoven, 1999) and exclusively used by cold agglutinins (Pascual, 1992). In agreement with Huang's data (1998), the gene V_H3-30 was found less frequently in our RA patient compared to healthy persons. In addition to these genes, the proportion of other variable genes like V_H1-02, 1-18 or 4-04 also differed from the published data of normal controls. Therefore the patient presented a distinct individual pattern of Ig-V_H gene usage, which allowed a longitudinal follow-up during treatment.

The analysis of D segments and J_H genes showed distributions comparable to the ones described in healthy individuals (Brezinschek, 1995 and 1997; Rosner, 2001). D6 represented the predominant D family and J_H4 was the most frequently used J_H segment, followed by J_H6. The only difference we detected before therapy was the underrepresentation of the D1 family.

The CDR3 length average (38.8 ± 11.5 nucleotides) was in agreement with published data (Brezinschek, 1998) where it was 13.3 ± 4.1 amino acids.

These observations suggest that the overall representation of individual V_H genes in peripheral B-cells in this RA patient resembled the repertoire expected in adult but contained characteristic differences in certain genes already seen to be often biased in autoimmune diseases.

B-cell depletive therapy induced two types of changes. The most profound effects were observed during the early regeneration phase, 7 months after the beginning of therapy. The long-term effects were more subtle.

Seven months after the first therapy was the earliest time point when B-cells could be detected either by flow cytometry or by PCR. These early regenerated B-cells presented a distribution of Ig-V_H genes significantly different from the one before therapy. Some V_H genes like V_H1-02 or V_H3-07 were more often used, whereas some others like V_H4-34 were decreased. Also in the distribution of the D segments and J_H genes, significant changes were observed. The most striking differences were the mutational frequencies found in the V_H genes. At this time point, 3% of the peripheral lymphocytes were CD19⁺ B-cells. All the amplified sequences were extensively mutated (mean mutation rate: 7.4%): 88% contained more than 10 mutations per sequence. This was highly significant when compared to the data observed before therapy and at the time point 17 months where only 10% of the rearrangements comprised more than 10 mutations per sequence. This increase of mutations correlated well with the diminution of J_H6 usage and the tendency of lower CDR3 length and argues for the influence of antigen contact and T-cell help (Rosner, 2001; Dörner, 2002).

These cells seemed to be class-switched memory cells, as demonstrated by RT-PCR analyses. To determine the heavy chain class distribution, we performed RT-PCR on total RNA from this time point, using primers specific for IgM, IgG and IgA. The IgM population had a low mutation rate as expected (1.7%), but the IgG (9.0%) and IgA (8.9%) populations were highly mutated, in the same range as the genes amplified from genomic DNA (7.4%).

The unexpected high mutation rates of the B-cells during the first regeneration phase is not likely to be related to selective amplification of specific sequences by our PCR protocol, since high mutation rates were observed in all V_H families amplified with different PCR conditions. Furthermore, the detected repertoire was polyclonal and even presented an extended number of V_H genes. Nevertheless we wanted to substantiate this result using a different approach. Therefore we sorted single cells from this time point in CD27⁺ and CD27⁻ B-cell subpopulations. The increase of mutational frequency was confirmed. Again, the newly recirculating B-cells showed increased mutation rates. This was detectable in both CD27⁺ and CD27⁻ B-cells (8.3% for CD27⁺, 5.3% for CD27⁻ versus 0.6% for CD27⁻ cells before therapy, Table 5). The fact that even the CD27⁻ B-cells were highly mutated was surprising, since CD27 is assumed as a marker for memory B-cells with mutated Ig-receptors (Klein, 1998, Tangye, 1998). However, mutated CD27⁻ B-cells have been described in a study from Hansen et al (2002) in patients with Sjögren's syndrome. Reparon-Schuijt et al (2002) also described in the synovium

of RA patients a population of B lymphocytes that were functionally and phenotypically distinct from classic memory cells. These cells were CD20+, CD38- and CD27- and produced immunoglobulins under induction but had a defective proliferative responsiveness. Although these findings are restricted to one patient, the reappearance of B-cells in the circulation may coincide with distortions of the B-cell memory pool. Under these conditions, CD27 seems not to be a reliable marker for Ig-receptor mutations.

In the regeneration phase following the second anti-CD20 treatment, at the time point 27 months, these highly mutated B-cells were not observed. Their appearance at the time point 7 months could not be explained by an ongoing infection, since no clinical or serological signs of infection were observed. These cells seem to circulate in the periphery only for a distinct time period during early B-cell regeneration, which could have been missed during the second regeneration phase. They show a different composition of the expressed Ig-V_H genes and probably originate from different precursors than the B-cells that composed the peripheral repertoire before and later. Therefore we suggest that these early regenerated B-cells might derive from a pool of class-switched memory cells that are normally not circulating in the periphery.

The general distribution of the V_H gene family repertoire has been shown to be stable for a period of time up to 9 years (Dijk-Hard, 2002). Except for the early regeneration phase 7 months after the first therapy, the emerging repertoire after B-cell depletion was overall also relatively stable. The study was not designed to detect specific disease relevant changes in the repertoire. Nevertheless, there were distinct changes, which paralleled the decrease in clinical activity, for instance the genes of the V_H2 family or the gene V_H3-23. The distribution of the V_H2 family genes was completely shifted toward the use of the gene V_H2-05 during the periods of low disease activity, whereas the frequency of V_H2-70 was very low at these time points. The predominant gene of the V_H3 family, V_H3-23, was found at a high proportion before therapy, it decreased 7 months after, increased again 17 months after therapy, accompanied by a clinical relapse, and decreased again 27 months after the first therapy. For this gene, it is also interesting to note that the use of J_H6 segment in the rearrangements as well as the shorter CDR3s correlated with the disease activity: when the disease was active, the J_H6 segment was found in a higher

frequency accompanied by a shorter CDR3. This suggests that the gene V_H3-23 may be used as an indicator gene.

The V_H gene 4-34 has been described to be frequently used in autoimmune disorders. In our study, V_H4-34 was significantly decreased after therapy and its frequency remained low up to 27 months. Irrespective of the possible pathogenic role of these changes, these results give evidence for a long-term modulation of the V_H gene repertoire induced by anti-CD20 antibody treatment.

Clonal expansion is a characteristic feature of patients suffering from RA. B-cell clones have been found in peripheral blood (Huang, 1998; Itoh, 1999) and in synovial tissue (Itoh, 1999; Kim, 2000). In the present study, we were able to detect 2 clones within the V_H5 family before therapy. The rearrangements used by these 2 clones were not observed anymore after therapy at all studied time points up to 27 months and we were not able to detect any other clonally related sequences. The inducible loss of clonal B-cells is also an indication for the modulation of the B-cell repertoire. Even if their specificity is not known, their relevance in disease activity can be speculated.

Taken together, these results indicate that transient B-cell depletion induces measurable long-term changes in the peripheral heavy chain repertoire.

2. Light chain repertoire

The light chain repertoire was studied in a second patient (L). This patient had a less active disease compared to patient H, in particular the CRP levels were lower. However, similar to patient H, rituximab therapy induced a relevant clinical improvement in patient L, indicated by a decrease of the disease activity score (DAS28). The light chain repertoire was analysed by single cell RT-PCR followed by direct sequencing at two time points: before therapy and during the early phase of B-cell regeneration (time point: 10 months). For the study, CD19⁺ B-cells were sorted into CD27⁻ (naïve) and CD27⁺ (memory) B-cells.

Before therapy, the productive V_κ and V_λ repertoires of patient L were largely comparable to published data of V_L repertoire in healthy donors (Foster, 1997; Farner, 1999). The

overall usage of V κ and J κ genes, as well as the CDR3 characteristics resembled the ones from normal controls. The V κ family distribution, the predominant use of the V κ genes O12/O2 and A27 by the memory CD27⁺ B-cells and the frequent occurrence of J κ 2 in the rearrangements reflected the normal distribution (Foster, 1997).

Although V λ J λ rearrangements presented similarities to the normal productive repertoire (Farner, 1999), some differences were observed. The V λ genes 2a2, 2b2 and 1g, frequently found in healthy people, were also used by our patient. But it was interesting to note that the gene V λ 31, usually not detected in normal donors, was found in both naive and memory populations, before and after therapy as well. This gene has been found in autoimmune diseases, such as in the synovium of a RA patient (Kim, 2000) or in salivary glands infiltrates from Sjögren's syndrome patients (Stott, 1998). Moreover, other genes, like 3p, 3r or 1g, frequently used by antibodies with rheumatoid factor (RF) activity (Elagib, 1999), were also detected in our patient. The J λ usage by the rearrangements was clearly biased toward a greater usage of J λ 2/3 segments compared to normal distribution where rearrangements involving J λ 7 are commonly observed (Farner, 1999). Before therapy, the CDR3 regions of CD27⁻ and CD27⁺ B-cells in V λ J λ rearrangements presented different characteristics. The CDR3 lengths of the memory cells were slightly shorter than the naive cells and the activities of the TdT and exonuclease at the V λ (5') side were greater.

Comparing naive and memory B-cells at the beginning of the study, specific changes could be detected. CD27⁺ memory B-cells were more mutated than CD27⁻ naive B-cells before and after therapy. This was expected since CD27 is a marker of memory cells and its presence usually correlates with mutated Ig-receptors (Klein, 1998). Interestingly, before therapy, the V λ rearrangements harboured more mutations than the V κ rearrangements in the memory but also in the naive population. This could be due to a higher intrinsic mutation rate in the V λ genes. However the lower mutation load of V κ could also result from novel V κ rearrangement in germinal centers B-cells, which have undergone fewer rounds of somatic mutations than the corresponding V λ gene rearrangement. Alternatively, it may be related to the fact that the κ chain usually rearranges before the λ chain. If the κ chain is non productive, the cell has still the possibility to rearrange its λ locus.

Receptor editing, or secondary rearrangement, is achieved by recombination of V genes 5' to the initial VJ rearrangement to 3' J elements and results in biases in association of the most 5' V genes to the most 3' J genes. The V κ locus is divided into a proximal and a distal cassette (Fig. 3). In our study, the V κ gene A18 was chosen as the border of the two cassettes. The rearrangements were then separated in J-proximal and J-distal V κ genes. Before therapy, in the CD27⁻ naive B-cells, the majority of the rearrangements (89%) used J-proximal V κ genes, whereas they were only 59% in the CD27⁺ memory B-cells. This suggests that receptor editing was more frequent in memory than in naive B-cells. The analysis of the J κ usage was consistent with this notion. In CD27⁻ B-cells, the J κ 2 segment was found the most often, followed by J κ 1. In CD27⁺ B-cells, the J κ 1 segment was less frequently used for the benefit of the more V-distal 3' J κ 4 and J κ 5 gene segments.

V λ J λ rearrangements showed evidence of decreased receptor editing compared to normal individuals. No gene belonging to the most distal cluster (cluster C) was found in our study. Distortions toward the usage of J λ 2/3 gene segments were observed, in contrast to healthy controls where the most 3' J λ 7 is used frequently in rearrangements. There was no difference between naive and memory population in regard of this distribution.

Some changes in the V_L repertoire were induced by B-cell depletive therapy. The most striking difference was the shift of the V κ to V λ ratio toward a greater usage of the V κ genes in CD27⁻ B-cells. Before therapy, the ratio κ : λ was 3:2 (as expected in human), whereas 10 months later, in the newly regenerated B-cells, it was 9:1 (Fig. 23). The reason behind this result is not clear, but it might be related to the orderly occurrence of V(D)J recombination during B-cell development, the κ locus being the first to rearrange during ontogeny. Surprisingly, the overall distribution of individual V κ genes was not affected. However, a trend of a lower usage of J-proximal V κ genes by CD27⁻ B-cells was observed after therapy, indicating a more frequent receptor editing in this population. This was not the case in V λ J λ rearrangements: there was no change in the distribution of the V λ and J λ genes. The mechanisms regulating the receptor editing may be different in V κ and V λ genes. Dörner et al. (1999) proposed that the V κ genes edit in the periphery after somatic hypermutation has been initiated, whereas the V λ genes edit centrally in the bone marrow. Consistent with this notion is the fact that, before therapy, the

mutation rates were lower in the V κ genes than in the V λ genes. It can be hypothesised that there is more peripheral receptor editing in the memory population, which takes place in the synovium.

Nevertheless, B-cell depletion induced some changes in the distribution of the V λ genes. The genes 3p, 1g and 3r, which are found in high frequencies in autoantibodies, were not detected anymore after therapy. These genes have been reported to be linked to RF activity. In our patient, the disappearance of these genes correlated to the decrease of the RF. The difference between the CDR3 regions of CD27- and CD27+ B-cells was not noticed anymore after therapy. No difference in the activity of the enzymes TdT and exonuclease was detected anymore. The disappearance of these autoimmune features after therapy may be relevant to the clinical improvement detected in patient L.

After B-cell reconstitution, the mutational frequencies were also changed. There was no more difference between the mutation rates of V κ and V λ chains. However, CD27+ B-cells were more mutated than CD27- B-cells as expected. This differs from the early regeneration phase in patient H, where all the V_H rearrangements were highly mutated. It can be speculated that different mechanisms govern the mutations in heavy and light chains (Boursier, 2003). The V_H chains contain more mutations than the V κ ones (Monson, 2001b). But, since all the V_H rearrangements were highly mutated, even in CD27- B-cells, it seems unlikely that the V_L rearrangements should not contain also mutations. In patient H, 7 months after therapy, the early regenerated B-cells had a repertoire strongly different from the one before therapy. The usage of the V_H and J_H genes, the CDR3 lengths were very different and, mainly, the mutational frequencies were dramatically increased. Moreover, these cells were detected for a short period only: three months later, they were not found anymore. For these reasons, it might be possible that we missed the time point where the highly mutated B-cells may have been detectable in patient L. Furthermore, the analyses of the heavy chain and light chain repertoire were performed in two different patients, using two different methodologies. It can not be excluded that each patient has some particular characteristics in repopulating with peripheral B-cells. Patient H had a more active disease and responded more rapidly to the therapy. Supplementary investigations remain to be done to further investigate B-cell regeneration after B-cell depletion.

Taken together, these results indicate that therapeutic transient B-cell depletion by anti-CD20 antibody therapy modulates the immunoglobulin gene repertoire in the two RA patients studied. Measurable changes were observed in the heavy chain as well as in the light chain repertoire, which may be relevant to the course of the disease. This also supports the notion that the composition of the B-cell repertoire is influenced by the disease and that B-cell depletion can reset some biases that are typically related to autoimmune disorders.

REFERENCES

- Agematsu, K., S. Hokibara, H. Nagumo, and A. Komiyama.** 2000. CD27: a memory B-cell marker. *Immunol.Today* **21**:204-206.
- Berek, C. and C. Milstein.** 1988. The dynamic nature of the antibody repertoire. *Immunol.Rev.* **105**:5-26.
- Boursier, L., W. Su, and J. Spencer.** 2003. Imprint of somatic hypermutation differs in human immunoglobulin heavy and lambda chain variable gene segments. *Mol.Immunol.* **39**:1025-1034.
- Brard, F., M. Shannon, E. L. Prak, S. Litwin, and M. Weigert.** 1999. Somatic mutation and light chain rearrangement generate autoimmunity in anti-single-stranded DNA transgenic MRL/lpr mice. *J.Exp.Med.* **190**:691-704.
- Brezinschek, H. P., R. I. Brezinschek, and P. E. Lipsky.** 1995. Analysis of the heavy chain repertoire of human peripheral B cells using single-cell polymerase chain reaction. *J.Immunol.* **155**:190-202.
- Brezinschek, H. P., S. J. Foster, R. I. Brezinschek, T. Dorner, R. Domiati-Saad, and P. E. Lipsky.** 1997. Analysis of the human VH gene repertoire. Differential effects of selection and somatic hypermutation on human peripheral CD5(+)/IgM+ and CD5(-)/IgM+ B cells. *J.Clin.Invest* **99**:2488-2501.
- Brezinschek, H. P., S. J. Foster, T. Dorner, R. I. Brezinschek, and P. E. Lipsky.** 1998. Pairing of variable heavy and variable kappa chains in individual naive and memory B cells. *J.Immunol.* **160**:4762-4767.
- Bross, L., M. Muramatsu, K. Kinoshita, T. Honjo, and H. Jacobs.** 2002. DNA double-strand breaks: prior to but not sufficient in targeting hypermutation. *J.Exp.Med.* **195**:1187-1192.
- Casellas, R., T. A. Shih, M. Kleinewietfeld, J. Rakonjac, D. Nemazee, K. Rajewsky, and M. C. Nussenzweig.** 2001. Contribution of receptor editing to the antibody repertoire. *Science* **291**:1541-1544.

Cerny, T., B. Borisch, M. Introna, P. Johnson, and A. L. Rose. 2002. Mechanism of action of rituximab. *Anticancer Drugs* **13 Suppl 2**:S3-10.

Chaudhuri, J., M. Tian, C. Khuong, K. Chua, E. Pinaud, and F. W. Alt. 2003. Transcription-targeted DNA deamination by the AID antibody diversification enzyme. *Nature* **422**:726-730.

Cheson, B. D. 2002. Rituximab: clinical development and future directions. *Expert.Opin.Biol.Ther.* **2**:97-110.

de Villartay, J. P., A. Fischer, and A. Durandy. 2003. The mechanisms of immune diversification and their disorders. *Nat.Rev.Immunol.* **3**:962-972.

De Vita, S., F. Zaja, S. Sacco, A. De Candia, R. Fanin, and G. Ferraccioli. 2002. Efficacy of selective B cell blockade in the treatment of rheumatoid arthritis: evidence for a pathogenetic role of B cells. *Arthritis Rheum.* **46**:2029-2033.

de Wildt, R. M., R. M. Hoet, W. J. van Venrooij, I. M. Tomlinson, and G. Winter. 1999. Analysis of heavy and light chain pairings indicates that receptor editing shapes the human antibody repertoire. *J.Mol.Biol.* **285**:895-901.

Dijk-Hard, I. and I. Lundkvist. 2002. Long-term kinetics of adult human antibody repertoires. *Immunology* **107**:136-144.

Dorner, T., N. L. Farner, and P. E. Lipsky. 1999. Ig lambda and heavy chain gene usage in early untreated systemic lupus erythematosus suggests intensive B cell stimulation. *J.Immunol.* **163**:1027-1036.

Dorner, T. and P. E. Lipsky. 2001. Immunoglobulin variable-region gene usage in systemic autoimmune diseases. *Arthritis Rheum.* **44**:2715-2727.

Dorner, T. and P. E. Lipsky. 2002. Abnormalities of B cell phenotype, immunoglobulin gene expression and the emergence of autoimmunity in Sjogren's syndrome. *Arthritis Res* **4**:360-371.

Dorner, T. and G. R. Burmester. 2003. The role of B cells in rheumatoid arthritis: mechanisms and therapeutic targets. *Curr.Opin.Rheumatol.* **15**:246-252.

- Durandy, A.** 2003. Activation-induced cytidine deaminase: a dual role in class-switch recombination and somatic hypermutation. *Eur.J.Immunol.* **33**:2069-2073.
- Edwards, J. C. and G. Cambridge.** 2001. Sustained improvement in rheumatoid arthritis following a protocol designed to deplete B lymphocytes. *Rheumatology.(Oxford)* **40**:205-211.
- Edwards, J. C., M. J. Leandro, and G. Cambridge.** 2002. B-lymphocyte depletion therapy in rheumatoid arthritis and other autoimmune disorders. *Biochem.Soc.Trans.* **30**:824-828.
- Eisenberg, R.** 2003. SLE – Rituximab in lupus. *Arthritis Res Ther* **5**:157-159.
- Elagib, K. E., M. Borretzen, K. M. Thompson, and J. B. Natvig.** 1999. Light chain variable (VL) sequences of rheumatoid factors (RF) in patients with primary Sjogren's syndrome (pSS): moderate contribution of somatic hypermutation. *Scand.J.Immunol.* **50**:492-498.
- Farner, N. L., T. Dorner, and P. E. Lipsky.** 1999. Molecular mechanisms and selection influence the generation of the human V lambda J lambda repertoire. *J.Immunol.* **162**:2137-2145.
- Feeney, A. J., A. Tang, and K. M. Ogwaro.** 2000a. B-cell repertoire formation: role of the recombination signal sequence in non-random V segment utilization. *Immunol.Rev.* **175**:59-69.
- Feeney, A. J.** 2000b. Factors that influence formation of B cell repertoire. *Immunol.Res* **21**:195-202.
- Foster, S. J., H. P. Brezinschek, R. I. Brezinschek, and P. E. Lipsky.** 1997. Molecular mechanisms and selective influences that shape the kappa gene repertoire of IgM+ B cells. *J.Clin.Invest* **99**:1614-1627.
- Frippiat, J. P., S. C. Williams, I. M. Tomlinson, G. P. Cook, D. Cherif, D. Le Paslier, J. E. Collins, I. Dunham, G. Winter, and M. P. Lefranc.** 1995. Organization of the human immunoglobulin lambda light-chain locus on chromosome 22q11.2. *Hum.Mol.Genet.* **4**:983-991.
- Gallo, M. L., V. E. Ivanov, A. Jakobovits, and C. G. Davis.** 2000. The human immunoglobulin loci introduced into mice: V (D) and J gene segment usage similar to that of adult humans. *Eur.J.Immunol.* **30**:534-540.

Gorman, C., M. Leandro, and D. Isenberg. 2003. B cell depletion in autoimmune disease. *Arthritis Res Ther* **5**:S17-S21.

Hainsworth, J. 2003. Safety of rituximab in the treatment of B cell malignancies: implications for rheumatoid arthritis. *Arthritis Res Ther* **5**:S12-S16.

Hansen, A., M. Odendahl, K. Reiter, A. M. Jacobi, E. Feist, J. Scholze, G. R. Burmester, P. E. Lipsky, and T. Dorner. 2002. Diminished peripheral blood memory B cells and accumulation of memory B cells in the salivary glands of patients with Sjogren's syndrome. *Arthritis Rheum.* **46**:2160-2171.

Heimbacher, C., A. Hansen, A. Pruss, A. Jacobi, K. Reiter, P. E. Lipsky, and T. Dorner. 2001. Immunoglobulin V kappa light chain gene analysis in patients with Sjogren's syndrome. *Arthritis Rheum.* **44**:626-637.

Honjo, T., K. Kinoshita, and M. Muramatsu. 2002. Molecular mechanism of class switch recombination: linkage with somatic hypermutation. *Annu.Rev.Immunol.* **20**:165-196.

Huang, S. C., R. Jiang, W. O. Hufnagle, D. E. Furst, K. R. Wilske, and E. C. Milner. 1998. VH usage and somatic hypermutation in peripheral blood B cells of patients with rheumatoid arthritis (RA). *Clin.Exp.Immunol.* **112**:516-527.

Itoh, K., V. Patki, V. R. A. Furie, E. K. Chartash, R. I. Jain, L. Lane, S. E. Asnis, and N. Chiorazzi. 1999. Clonal expansion is a characteristic feature of the B-cell repertoire of patients with rheumatoid arthritis. *Arthritis Res.* **2**:50-58.

Itoh, K., E. Meffre, E. Albesiano, A. Farber, D. Dines, P. Stein, S. E. Asnis, R. A. Furie, R. I. Jain, and N. Chiorazzi. 2000. Immunoglobulin heavy chain variable region gene replacement As a mechanism for receptor revision in rheumatoid arthritis synovial tissue B lymphocytes. *J.Exp.Med.* **192**:1151-1164.

Jonsson, R., K. A. Brokstad, P. E. Lipsky, and M. Zouali . 2001. B-lymphocyte selection and autoimmunity. *Trends Immunol.* **22**:653-654.

- Kaschner, S., A. Hansen, A. Jacobi, K. Reiter, N. L. Monson, M. Odendahl, G. R. Burmester, P. E. Lipsky, and T. Dorner.** 2001. Immunoglobulin Vlambda light chain gene usage in patients with Sjogren's syndrome. *Arthritis Rheum.* **44**:2620-2632.
- Kim, H. J. and C. Berek.** 2000. B cells in rheumatoid arthritis. *Arthritis Res.* **2**:126-131.
- Klein, U., K. Rajewsky, and R. Kuppers.** 1998. Human immunoglobulin (Ig)M+IgD+ peripheral blood B cells expressing the CD27 cell surface antigen carry somatically mutated variable region genes: CD27 as a general marker for somatically mutated (memory) B cells. *J.Exp.Med.* **188**:1679-1689.
- Klonowski, K. D. and M. Monestier.** 2001. Ig heavy-chain gene revision: leaping towards autoimmunity. *Trends Immunol.* **22**:400-405.
- Kneitz, C., M. Wilhelm, and H. P. Tony.** 2002. Effective B cell depletion with rituximab in the treatment of autoimmune diseases. *Immunobiology* **206**:519-527.
- Kneitz, C., M. Wilhelm, and H. P. Tony.** 2004. Improvement of refractory rheumatoid arthritis after depletion of B cells. *Scand J Rheumatol.* **33**:1-8
- Kuppers, R., M. Zhao, M. L. Hansmann, and K. Rajewsky.** 1993. Tracing B cell development in human germinal centres by molecular analysis of single cells picked from histological sections. *EMBO J.* **12**:4955-4967.
- Kuwata, N., H. Igarashi, T. Ohmura, S. Aizawa, and N. Sakaguchi.** 1999. Cutting edge: absence of expression of RAG1 in peritoneal B-1 cells detected by knocking into RAG1 locus with green fluorescent protein gene. *J.Immunol.* **163**:6355-6359.
- Lee, D. M. and M. E. Weinblatt.** 2001. Rheumatoid arthritis. *Lancet* **358**:903-911.
- Lefranc, M. P.** 2001a. Nomenclature of the human immunoglobulin lambda (IGL) genes. *Exp.Clin.Immunogenet.* **18**:242-254.
- Lefranc, M. P.** 2001b. Nomenclature of the human immunoglobulin kappa (IGK) genes. *Exp.Clin.Immunogenet.* **18**:161-174.

- Lefranc, M. P.** 2001c. Nomenclature of the human immunoglobulin heavy (IGH) genes. *Exp.Clin.Immunogenet.* **18**:100-116.
- Lindenau, S., S. Scholze, M. Odendahl, T. Dorner, A. Radbruch, G. R. Burmester, and C. Berek.** 2003. Aberrant activation of B cells in patients with rheumatoid arthritis. *Ann.N.Y.Acad.Sci.* **987**:246-248.
- Lipsky, P. E.** 2001. Systemic lupus erythematosus: an autoimmune disease of B cell hyperactivity. *Nat.Immunol.* **2**:764-766.
- Maloney, D. G., B. Smith, and A. Rose.** 2002. Rituximab: mechanism of action and resistance. *Semin. Oncol.* **29** (1 Suppl 2):2-9
- Matsuda, F., K. Ishii, P. Bourvagnet, K. Kuma, H. Hayashida, T. Miyata, and T. Honjo.** 1998. The complete nucleotide sequence of the human immunoglobulin heavy chain variable region locus. *J.Exp.Med.* **188**:2151-2162.
- Monroe, R. J., F. Chen, R. Ferrini, L. Davidson, and F. W. Alt.** 1999. RAG2 is regulated differentially in B and T cells by elements 5' of the promoter. *Proc.Natl.Acad.Sci.U.S.A* **96**:12713-12718.
- Monson, N. L., S. J. Foster, H. P. Brezinschek, R. I. Brezinschek, T. Dorner, and P. E. Lipsky.** 2001a. The role of CD40-CD40 ligand (CD154) interactions in immunoglobulin light chain repertoire generation and somatic mutation. *Clin.Immunol.* **100**:71-81.
- Monson, N. L., T. Dorner, and P. E. Lipsky.** 2001b. Targeting and selection of mutations in human V λ rearrangements. *Eur.J.Immunol.* **30**:1597-1605
- Nemazee, D. and M. Weigert.** 2000. Revising B cell receptors. *J.Exp.Med.* **191**:1813-1817.
- Neuberger, M. S. and C. Milstein.** 1995. Somatic hypermutation. *Curr.Opin.Immunol.* **7**:248-254.
- Neuberger, M. S., R. S. Harris, J. Di Noia, and S. K. Petersen-Mahrt.** 2003. Immunity through DNA deamination. *Trends Biochem.Sci.* **28**:305-312.

O'Keefe, T. L., G. T. Williams, S. L. Davies, and M. S. Neuberger. 1998. Mice carrying a CD20 gene disruption. *Immunogenetics* **48**:125-132.

Odendahl, M., A. Jacobi, A. Hansen, E. Feist, F. Hiepe, G. R. Burmester, P. E. Lipsky, A. Radbruch, and T. Dorner. 2000. Disturbed peripheral B lymphocyte homeostasis in systemic lupus erythematosus. *J.Immunol.* **165**:5970-5979.

Oligino, T. and S. Dalrymple. 2003. Targeting B cells for the treatment of rheumatoid arthritis. *Arthritis Res Ther* **5**:S7-S11.

Pascual, V., K. Victor, M. Spellerberg, T. J. Hamblin, F. K. Stevenson, and J. D. Capra. 1992. VH restriction among human cold agglutinins. The VH4-21 gene segment is required to encode anti-I and anti-i specificities. *J.Immunol.* **149**:2337-2344.

Patel, D. D. 2002. B cell-ablative therapy for the treatment of autoimmune diseases. *Arthritis Rheum.* **46**:1984-1985.

Radic, M. Z. and M. Zouali. 1996. Receptor editing, immune diversification, and self-tolerance. *Immunity.* **5**:505-511.

Rao, S. P., J. M. Riggs, D. F. Friedman, M. S. Scully, T. W. LeBien, and L. E. Silberstein. 1999. Biased VH gene usage in early lineage human B cells: evidence for preferential Ig gene rearrangement in the absence of selection. *J.Immunol.* **163**:2732-2740.

Reparon-Schuijt, C. C., W. J. van Esch, C. van Kooten, N. P. Ezendam, E. W. Levarht, F. C. Breedveld, and C. L. Verweij. 2001. Presence of a population of CD20+. *Arthritis Rheum.* **44**:2029-2037.

Rosner, K., D. B. Winter, R. E. Tarone, G. L. Skovgaard, V. A. Bohr, and P. J. Gearhart. 2001. Third complementarity-determining region of mutated VH immunoglobulin genes contains shorter V, D, J, P, and N components than non-mutated genes. *Immunology* **103**:179-187.

Schable, K. F. and H. G. Zachau. 1993. The variable genes of the human immunoglobulin kappa locus. *Biol.Chem.Hoppe Seyler* **374**:1001-1022.

Schlissel, M. S. 2003. Regulating antigen-receptor gene assembly. *Nat.Rev.Immunol.* **3**:890-899.

Seagal, J. and D. Melamed. 2002. Role of receptor revision in forming a B cell repertoire. *Clin.Immunol.* **105**:1-8.

Silverman, G. J. and S. Weisman. 2003a. Rituximab therapy and autoimmune disorders: prospects for anti-B cell therapy. *Arthritis Rheum.* **48**:1484-1492.

Silverman, G. and D. Carson. 2003b. Roles of B cells in rheumatoid arthritis. *Arthritis Res Ther* **5**:S1-S6.

Sims, G. P., H. Shiono, N. Willcox, and D. I. Stott. 2001. Somatic hypermutation and selection of B cells in thymic germinal centers responding to acetylcholine receptor in myasthenia gravis. *J.Immunol.* **167**:1935-1944.

Stahl, H.D., L. Szczepaaski, J. Szechiaski, A. Filipowicz-Sosnowska, J.C.W. Edwards, D.R. Close, R.M. Stevens, and T.M. Shaw. 2003. Rituximab in RA: efficacy and safety from a randomised, controlled trial [abstract] *Ann Rheum Dis*, supp 1:65.

Stevenson, F. K., C. Longhurst, C. J. Chapman, M. Ehrenstein, M. B. Spellerberg, T. J. Hamblin, C. T. Ravirajan, D. Latchman, and D. Isenberg. 1993. Utilization of the VH4-21 gene segment by anti-DNA antibodies from patients with systemic lupus erythematosus. *J.Autoimmun.* **6**:809-825.

Stott, D. I., F. Hiepe, M. Hummel, G. Steinhauser, and C. Berek. 1998. Antigen-driven clonal proliferation of B cells within the target tissue of an autoimmune disease. The salivary glands of patients with Sjogren's syndrome. *J.Clin.Invest* **102**:938-946.

Suzuki, I., L. Pfister, A. Glas, C. Nottenburg, and E. C. Milner. 1995. Representation of rearranged VH gene segments in the human adult antibody repertoire. *J.Immunol.* **154**:3902-3911.

Takemura, S., P. A. Klimiuk, A. Braun, J. J. Goronzy, and C. M. Weyand. 2001. T cell activation in rheumatoid synovium is B cell dependent. *J.Immunol.* **167**:4710-4718.

- Tangye, S. G., Y. J. Liu, G. Aversa, J. H. Phillips, and J. E. de Vries.** 1998. Identification of functional human splenic memory B cells by expression of CD148 and CD27. *J.Exp.Med.* **188**:1691-1703.
- Tomlinson, I.M., S. C. Williams, S. J. Corbett, J. B. L. Cox, and G. Winter.** 1999. V BASE Sequence Directory. Cambridge United Kingdom: MRC Centre for Protein Engineering.
- Tonegawa, S.** 1983. Somatic generation of antibody diversity. *Nature* **302**:575-581.
- van Vollenhoven, R. F., M. M. Bieber, M. J. Powell, P. K. Gupta, N. M. Bhat, K. L. Richards, S. A. Albano, and N. N. Teng.** 1999. VH4-34 encoded antibodies in systemic lupus erythematosus: a specific diagnostic marker that correlates with clinical disease characteristics. *J.Rheumatol.* **26**:1727-1733.
- Vasicek, T. J. and P. Leder.** 1990. Structure and expression of the human immunoglobulin lambda genes. *J.Exp.Med.* **172**:609-620.
- Wardemann, H., S. Yurasov, A. Schaefer, J. W. Young, E. Meffre, and M. C. Nussenzweig.** 2003. Predominant autoantibody production by early human B cell precursors. *Science* **301**:1374-1377.
- Wilson, P. C., K. Wilson, Y. J. Liu, J. Banchereau, V. Pascual, and J. D. Capra.** 2000. Receptor revision of immunoglobulin heavy chain variable region genes in normal human B lymphocytes. *J.Exp.Med.* **191**:1881-1894.
- Yu, W., H. Nagaoka, M. Jankovic, Z. Misulovin, H. Suh, A. Rolink, F. Melchers, E. Meffre, and M. C. Nussenzweig.** 1999. Continued RAG expression in late stages of B cell development and no apparent re-induction after immunization. *Nature* **400**:682-687.
- Zhang, Z., P. D. Burrows, and M. D. Cooper.** 2004. The molecular basis and biological significance of VH replacement. *Immunol.Rev.* **197**:231-242.

SUMMARY

Although the role of B-cells in autoimmunity is not completely understood, their importance in the pathogenesis of autoimmune diseases has been more appreciated in the past few years. It is now well known that they have roles in addition to (auto) antibody production and are involved by different mechanisms in the regulation of T-cell mediated autoimmune disorders. The evolution of an autoimmune disease is a dynamic process, which takes a course of years during which complex immunoregulatory mechanisms shape the immune repertoire until the development of clinical disease. During this course, the B-cell repertoire itself is influenced and a change in the distribution of immunoglobulin heavy and light chain genes can be observed.

B-cell depletive therapies have beneficial effects in patients suffering from rheumatoid arthritis (RA), highlighting also the central role of B-cells in the pathogenesis of this disease. Nevertheless, the mechanism of action is unclear. It has been hypothesised that B-cell depletion is able to reset deviated humoral immunity. Therefore we wanted to investigate if transient B-cell depletion results in changes of the peripheral B-cell receptor repertoire.

To address this issue, expressed immunoglobulin genes of two patients suffering from RA were analysed; one patient for the heavy chain repertoire (patient H), one patient for the light chain repertoire (patient L). Both patients were treated with rituximab, an anti-CD20 monoclonal antibody that selectively depletes peripheral CD20+ B-cells for several months. The B-cell repertoire was studied before therapy and at the earliest time point after B-cell regeneration in both patients. A longer follow-up (up to 27 months) was performed in patient H who was treated a second time with rituximab after 17 months.

Heavy chain gene analysis was carried out by nested-PCR on bulk DNA from peripheral B-cells using family-specific primers, followed by subcloning and sequencing. During the study, patient H received two courses of antibody treatment. B-cell depletion lasted 7 and 10 months, respectively and each time was accompanied by a clinical improvement. Anti-CD20 therapy induced two types of changes in this patient. During the early phase of B-cell regeneration, we noticed the presence of an expanded and recirculating population of highly mutated B-cells. These cells expressed very different immunoglobulin V_H genes compared before therapy. They were class-switched and could be detected for a short period only. The long-term changes were more subtle. Nevertheless, characteristic changes in the V_{H2} family, as well as in specific mini-

genes like V_H3-23 , 4-34 or 1-69 were noticed. Some of these genes have already been reported to be biased in autoimmune diseases. Also in autoimmune diseases, in particular in RA, clonal B-cells have been frequently found in the repertoire. B-cell depletion with anti-CD20 antibody resulted in a long term loss of clonal B-cells in patient H. Thus, temporary B-cell depletion induced significant changes in the heavy chain repertoire.

For the light chain gene analysis, the repertoire changes were analysed separately for naive (CD27-) and memory (CD27+) B-cells. Individual CD19+ B-cells were sorted into CD27- and CD27+ cells and single cell RT-PCR was performed, followed by direct sequencing. During the study, patient L received one course of antibody treatment. B-cell depletion lasted 10 months and the light chain repertoire was studied before and after therapy. Before therapy, some differences in the distribution of V_L and J_L genes were observed between naive and memory B-cells. In particular, the predominant usage of $J\kappa$ -proximal $V\kappa$ genes by the CD27- naive B-cells indicated that the receptor editing was less frequent in this population compared to memory cells. In $V\lambda J\lambda$ rearrangements also, some evidence for decreased receptor editing was noticed, with the overrepresentation of the $J\lambda 2/3$ gene segments. The CDR3 regions of naive and memory cells showed different characteristics: the activity of the terminal deoxynucleotidyl transferase and exonuclease in $V\lambda$ (5') side was greater in memory cells. Also in the light chain repertoire, we observed some changes induced by the B-cell depletive therapy. There was a tendency of a less frequent usage of $J\kappa$ -proximal $V\kappa$ genes in the naive population. Some $V\lambda$ genes, previously described in autoimmune diseases and connected to rheumatoid factor activity, such as 3p, 3r, 1g, were not found after therapy. The different characteristics of the CDR3 regions of $V\lambda J\lambda$ rearrangements were not observed anymore. Very significantly, the ratio $V\kappa$ to $V\lambda$ was shifted toward a greater usage of $V\kappa$ genes in the naive population after therapy.

Taken together, these results indicate that therapeutic transient B-cell depletion by anti-CD20 antibody therapy modulates the immunoglobulin gene repertoire in the two RA patients studied. Measurable changes were observed in the heavy chain as well as in the light chain repertoire, which may be relevant to the course of the disease. This also supports the notion that the composition of the B-cell repertoire is influenced by the disease and that B-cell depletion can reset biases that are typically found in autoimmune diseases.

ZUSAMMENFASSUNG

Obwohl die Rolle der B-Zellen für den Verlauf einer Autoimmunerkrankung noch nicht vollständig klar ist, so hat ihre Bedeutung für die Autoimmunpathogenese in den letzten Jahren zugenommen. Man weiß mittlerweile sehr wohl, dass ihre Rolle über die reine Produktion von (Auto-)antikörpern hinausgeht und sie z.B. an der Regulation T-Zellvermittelter Autoimmunstörungen beteiligt sind. Das B-Zellrepertoire selbst wird im Laufe einer autoimmunen Erkrankung durch solche immunregulatorische Prozesse beeinflusst.

B-Zelldepletive Therapien zeigen vorteilhafte Effekte bei Patienten mit Rheumatoider Arthritis, was wiederum die zentrale Rolle von B-Zellen in der Pathogenese unterstreicht. Nichtsdestotrotz bleibt der genaue Mechanismus unklar. So wird z.B. spekuliert, dass mittels B-Zell-Depletion eine Neugenerierung der humoralen Immunität erreicht wird. Vor diesem Hintergrund untersuchten wir, ob eine vorübergehende B-Zell-Depletion zu Veränderungen im peripheren B-Zellrepertoire führt.

Hierfür wurde das B-Zell-Rezeptorrepertoire von zwei Patienten mit Rheumatoider Arthritis im einen Fall bezüglich der schweren Kette (Patient H) und im anderen Fall bezüglich der leichten Kette (Patient L) analysiert. Beide Patienten wurden mit Rituximab, einem monoklonalen anti-CD20 Antikörper, der zu einer selektiven und über mehrere Monate anhaltenden Depletion peripherer CD20⁺-B-Zellen führt, behandelt. Das B-Zellrepertoire wurde für beide Patienten unmittelbar vor Therapie sowie in der frühen B-Zellregeneration untersucht. Bei Patient H erfolgte eine zweite Behandlung mit Rituximab nach 17 Monaten. Das Follow-up erfolgte in diesem Fall bis Monat 27.

Die Analyse der Schwerketten erfolgte mittels nested-PCR mit DNA aus peripheren B-Zellen unter Verwendung familienspezifischer Primer und anschließendem Subklonieren und Sequenzieren. Während der Studie erhielt Patient H zwei Zyklen der Antikörperbehandlung. Die B-Zell-Depletion hielt 7 bzw. 10 Monate an und war zu jedem Zeitpunkt mit einer klinischen Besserung des Patienten verbunden. Die Anti-CD20 Therapie bewirkte zwei Arten von Veränderungen in diesem Patienten. Während der frühen Phase der B-Zellregeneration konnten wir eine ausgedehnte und rezirkulierende Population hochmutierter B-Zellen nachweisen. Diese Zellen exprimierten verglichen mit dem Zeitpunkt vor Therapie sehr unterschiedliche V_H Gene. Es handelte sich hierbei um „class-switched“ Zellen, welche nur für kurze Zeit nachweisbar

waren. Die Langzeit Veränderungen dagegen waren eher diskret. Nichtsdestotrotz konnten Veränderungen sowohl in der Familie V_{H2} als auch in spezifischen Mini-Genen wie V_{H3-23} , 4-34 oder 1-69 festgestellt werden. Eine Häufung einiger dieser Gene wurde bereits im Zusammenhang mit Autoimmunerkrankungen berichtet. Zusätzlich bewirkte die Rituximabtherapie ein Verschwinden klonaler B-Zellen für die gesamte Periode. Folglich bewirkte die vorübergehende B-Zell-Depletion signifikante Veränderungen im Schwerkettenrepertoire.

Für die Genanalyse der leichten Kette wurden die Veränderungen getrennt für naive ($CD27^-$) und Gedächtnis- ($CD27^+$) B-Zellen untersucht. Einzelne $CD19^+$ B-Zellen wurden in $CD27^-$ und $CD27^+$ -Zellen sortiert und anschließend eine Single-cell-RT-PCR mit direkter Sequenzierung der Produkte durchgeführt. Während der Studie erhielt Patient L eine Behandlung. Die B-Zell-Depletion dauerte 10 Monate und das Leichtkettenrepertoire wurde vor und nach Therapie analysiert. Gewisse Unterschiede bezüglich der Verteilung von V_L und J_L Genen zwischen den Populationen naiver und Gedächtnis-B-Zellen konnten vor Therapie nachgewiesen werden. Insbesondere die bevorzugte Nutzung von V_{κ} Genen J_{κ} -proximal in $CD27^-$ naive B-Zellen spricht für ein vermindertes „receptor editing“ in dieser Population. Ferner fanden sich in $V_{\lambda}J_{\lambda}$ -Rearrangements Hinweise für ein vermindertes „receptor editing“ mit einer Überrepräsentation der $J_{\lambda}2/3$ Gensegmente. Die CDR3-Regionen der naiven und Gedächtnis-B-Lymphozyten zeigten unterschiedliche Eigenschaften: die Aktivität der Terminalen-Deoxynucleotidyl-Transferase und Exonuklease im V_{λ} -Abschnitt (5') war höher als in Gedächtniszellen. Die B-Zelldepletive Therapie führte zu signifikanten Veränderungen. So fand sich die Tendenz einer weniger häufigen Nutzung von J_{κ} -proximal gelegenen V_{κ} Gensegmenten in der naiven B-Zellpopulation. Einige V_{λ} Gene, wie z.B. 3p, 3r oder 1g, welche kürzlich in Verbindung mit Rheumafaktor bei Autoimmunerkrankungen beschrieben wurden, waren nach der Therapie nicht mehr nachweisbar. Ebenso verschwanden die unterschiedlichen Eigenschaften der CDR3-Regionen von $V_{\lambda}J_{\lambda}$ -Rearrangements. Besonders auffällig war das Verhältnis V_{κ} zu V_{λ} zugunsten einer häufigeren Nutzung von V_{κ} Genen in der naiven Population nach Therapie verschoben.

Zusammenfassend zeigen diese Ergebnisse, dass mittels therapeutischer und vorübergehender B-Zell-Depletion durch anti-CD20-Antikörper das Immunglobulinrepertoire in den

beiden untersuchten Patienten moduliert wurde. Messbare Unterschiede fanden sich sowohl im Schwerketten- als auch im Leichtkettenrepertoire. Es erscheint wahrscheinlich, dass diese Veränderungen mit dem beobachteten therapeutischen Ansprechen in Verbindung stehen. Die Ergebnisse stützen die Annahme, dass die Zusammensetzung des B-Zellrepertoires durch die Krankheit beeinflusst wird und für Autoimmunerkrankungen charakteristische Veränderungen mittels B-Zell-Depletion aufgehoben werden können.

ABBREVIATIONS

ACR	american college of rheumatology
AID	activation-induced cytidine deaminase
BCR	B-cell receptor
bp	base pair
C	constant
CDR	complementary determining region
CRP	C reactive protein
cRSS	cryptic recombination signal sequence
CSR	class-switch recombination
dist	distal
D	diversity
DNA	deoxyribonucleic acid
DAS	disease activity score
DMARD	disease-modifying antirheumatic drug
DNA-PK	DNA-dependent protein kinase complex
DNA-PKcs	DNA-dependent protein kinase catalytic subunit
dNTP	deoxyribonucleoside triphosphate
FACS	fluorescence-activated cell sorter
FCS	fetal calf serum
FDC	follicular dendritic cell
FITC	fluorescein isothiocyanate
FR	framework region
GC	germinal center
H	heavy chain
HMG	high mobility group
Ig	immunoglobulin
IgH	immunoglobulin heavy chain
Igk	immunoglobulin kappa chain

IgL	immunoglobulin light chain
Igλ	immunoglobulin lambda chain
IgV	immunoglobulin variable gene
IL	interleukin
J	joining
L	light chain
MHC	major histocompatibility complex
mIg	membrane immunoglobulin
mRNA	messenger RNA
mut	mutations
N nucleotide	non-templated nucleotide
NHEJ	non-homologous end-joining
ORF	open reading frame
prox	proximal
p nucleotide	palindromic nucleotide
PB	peripheral blood
PBMC	peripheral blood mononuclear cells
PCR	polymerase chain reaction
PE	phycoerythrin
R	purine
RA	rheumatoid arthritis
RAG	recombination-activating gene
RNA	ribonucleic acid
RNAse	ribonuclease
RSS	recombination signal sequence
RT-PCR	reverse transcriptase - polymerase chain reaction
S _μ	switch region for immunoglobulin μ chain constant region
SHM	somatic hypermutation
sIg	surface immunoglobulin
SLE	systemic lupus erythematosus
SS	Sjögren's syndrome

TCR	T-cell receptor
TdT	terminal deoxynucleotidyl transferase
TNF α	tumor-necrosis factor α
UNG	uracil N-glycosylase
V	variable
Y	pyrimidine

ACKNOWLEDGEMENTS

I am grateful to Prof. Dr. H.-P. Tony for giving me the opportunity to do my PhD work in his lab, in the Medizinische Poliklinik der Universität Würzburg. I thank him for his prompt help when I needed it, for his support and trust during these years.

I thank Prof. Dr. E. Buchner for accepting to be my tutor at the Faculty of Biology and for his support with the formalities concerning the doctoral thesis.

I thank Dr. T. Dörner for his help and advice for the analysis of the B-cell repertoire; the people in his lab, in the Charité Hospital in Berlin, for their valuable technical support with the single-cell sorting. I thank Prof. Dr. H. Vogt for his help with the statistical analyses.

I thank Dr. M. Goller for having been here at my arrival in Germany; for his help with all the administrative processes; for his guidance during my first days in the lab, for his kindness and interest; for teaching me how to work and think independently and for keeping in touch after his departure from the lab.

I thank Prof. Dr. T. Hünig for the very instructive and stimulating talks during the seminars every Thursday in the Graduate College. I thank all my colleagues from the Graduate College 520 “Immunomodulation” for their interesting discussions (scientific or not!), for their support and for their “internationality”.

I deeply thank Ioana Visan, my friend and former colleague; for her presence (either here or thousands kilometres away), for her help and support; for the discussions and all the other things we share together.

I thank the people of the lab, Arumugam Palanichamy and Kathrin Zehe for their technical help, for their support and good mood, Dr. C. Kneitz for the clinical data. I thank Martin Feuchtenberger and Susanne Eckstein for their help with the thesis and for being my friends.

And finally, I particularly thank my family and my friends for their affection and support during all these years.

CURRICULUM VITAE

Name: Anne-Sophie Denyse Georgette Rouzière

Date of birth: 17th of October 1974

Place of birth: Laval, France

Education:

- 1992** **Baccalauréat série C**
Lycée Douanier Rousseau, Laval, France
- 1996** **D.E.U.G. Sciences, Mention « Sciences de la Vie »**
Université de Rennes 1, France
- 1997** **Licence de Biochimie**
Université de Rennes 1, France
- 1998** **Maîtrise de Biochimie**
Université de Rennes 1, France
- 1998-1999** **Research training** in the laboratory of Physiology of Molecular, Cellular and Energetic Regulations, UMR CNRS 5578, Lyon, France, under the coordination of Dr. D. Desplanches
- 1999** **Diplôme d'Etudes Approfondies « Métabolisme, Endocrinologie, Nutrition »**
Université Claude Bernard, Lyon, France
- Since 2000**
- **PhD student** in the laboratory of Molecular Immunology, Medizinische Poliklinik, Universität Würzburg, under the coordination of Prof. H.-P. Tony
 - **Associated member of the Graduate College 520** "Immunomodulation", Würzburg, coordinator Prof. Th. Hünig

PUBLICATIONS

1. Original articles

- **Feuchtenberger, M., H.-P. Tony, A.-S. Rouzière, A.-M. Jacobi, T. Dörner, C. Kneitz, and P. Starostik.** 2003. Semi-quantitative and qualitative assessment of B-lymphocyte VH repertoire by a fluorescent multiplex PCR. *J. Immunol. Methods.* **276**: 121-127.
- **Rouzière, A.-S., C. Kneitz, T. Dörner, and H.-P. Tony.** B-cell depletion by anti-CD20 antibody treatment modulates the immunoglobulin heavy-chain repertoire in rheumatoid arthritis. Manuscript under submission.
- **Ströbel, P., M. Marino, M. Feuchtenberger, A.-S. Rouzière, H.-P. Tony, U. Wulbrand, R. Förster, A. Zettl, S. Gattenlöhner, N. L. Harris, H. Kreipe, R. H. Laeng, H.-K. Müller-Hermelink, and A. Marx.** Micronodular thymoma: an epithelial tumour setting the stage for lymphoma development. Manuscript under submission.

2. Published abstracts

- **Rouzière, A.-S., M. Feuchtenberger, C. Kneitz, M. Goller, P. Starostik, and H.-P. Tony.** 2001. Analysis of immunoglobulin VH-gene rearrangements in peripheral B cells. *Immunobiology.* **204 (1-2)**: 224.
- **Rouzière, A.-S., M. Goller, C. Kneitz, and H.-P. Tony.** 2003. Modulation of the B-cell repertoire by anti-CD20 antibody therapy. *Immunol. Lett.* **87 (1-3)**: 254.
- **Rouzière, A.-S., C. Kneitz, T. Dörner, and H.-P. Tony.** 2003. Veränderung des B-Zell-Repertoires nach B-Zelldepletion mit anti-CD20 Antikörpern (Rituximab). *Zeitschrift für Rheumatologie.* **62 (1)**: 69.
- **Rouzière, A.-S., C. Kneitz, T. Dörner, and H.-P. Tony.** 2003. B-cell depletion by anti-CD20 antibody treatment in rheumatoid arthritis modulates the B-cell repertoire. *Arthritis and Rheumatism.* **48 (9)**: S138.

3. Poster and oral presentations at congresses and symposia

- **Rouzière, A.-S., M. Feuchtenberger, C. Kneitz, M. Goller, P. Starostik, and H.-P. Tony.** Analysis of immunoglobulin VH-gene rearrangements in peripheral B cells. 32nd Annual Meeting of the German Society of Immunology, September 2001, Dresden, Germany.
- **Rouzière, A.-S., M. Feuchtenberger, C. Kneitz, M. Goller, P. Starostik, and H.-P. Tony.** Analysis of immunoglobulin VH-gene rearrangements in peripheral B cells. Euroconference “Interactions between innate and adaptive immunity in mammalian defence against bacterial infections”, June 2002, Goehren-Lebbin, Germany.
- **Rouzière, A.-S.** Modulation of the B-cell repertoire by an anti-CD20 antibody treatment. 15th European Immunology Congress, June 2003, Rhodes, Greece.
- **Rouzière, A.-S.** Can temporary B-cell depletion modulate the expressed B-cell repertoire? Joint Retreat of the Graduate Colleges 520 and 592, “Immunomodulation meets Lymphocyte Activation”, July 2003, Markt Taschendorf, Germany.
- **Rouzière, A.-S., C. Kneitz, T. Dörner, and H.-P. Tony.** Veränderung des B-Zell-Repertoires nach B-Zelldepletion mit anti-CD20 Antikörpern (Rituximab). 32nd Congress of the German society of Rheumatology, Sept. 2003, Frankfurt/Main, Germany.
- **Rouzière, A.-S., C. Kneitz, T. Dörner, and H.-P. Tony.** B-cell depletion by anti-CD20 antibody treatment in rheumatoid arthritis modulates the B-cell repertoire. 67th Annual Scientific Meeting of the American College of Rheumatology, Oct. 2003, Orlando, USA.

EIDESSTATTLICHE ERKLÄRUNGEN

Hiermit erkläre ich ehrenwörtlich, dass die vorliegende Dissertation „*Modulation of the B-cell repertoire in rheumatoid arthritis by transient B-cell depletion*“ selbständig an der Medizinischen Poliklinik der Universität Würzburg angefertigt wurde und dass ich keine anderen als die angegebenen Quellen und Hilfsmittel benutzt habe.

Weiterhin versichere ich, dass die vorliegende Dissertation weder in gleicher oder ähnlicher Form noch nicht in einem anderen Prüfungsverfahren vorgelegen hat und ich bisher noch keine akademische Grade erworben oder zu erwerben versucht habe.

Hiermit bewerbe ich mich erstmals um den Doktorgrad der Naturwissenschaften der Bayerischen Julius-Maximilians-Universität Würzburg.

Würzburg, 5. April 2004

Anne-Sophie Rouzière